PAUL SCHERRER INSTITUT

PSI

Transform Magnitude

— Zn incorporated
— Zn on strong sites
— Zn on weak sites

R + ΔR(Å)

Progress Report 2010

Laboratory for Waste Management
Nuclear Energy and Safety Research Department

Cover photo

Illustration of Zn incorporated in the montmorillonite clay lattice (Zn1) and Zn complexes located at the broken bond/edge sites (Zn2-Zn5) (M1 indicates trans and M2 cis octahedral Al positions). The Zn surface complexes sorbed onto the amphoteric hydroxyl sites at the edges of montmorillonite were identified by applying polarized extended X-ray absorption fine structure (P-EXAFS) spectroscopy to self-supporting montmorillonite films. The spectroscopic results identified potential crystallographic positions of the strong sites and weak sites (not shown) assumed in the 2 Site Protolysis Non-Electrostatic Surface Complexation and Cation Exchange sorption model.

The insert shows the radial structure functions (RSF) obtained by Fourier transforming P-EXAFS spectra measured under conditions in which the Zn located in the continuity of octahedral sheets is preferentially probed. The X-ray polarization vector is parallel to the montmorillonite film plane. The RSFs of representative samples measured under conditions for incorporated Zn (Zn1), Zn on strong (Zn2-Zn5) and weak sites are shown.

PAUL SCHERRER INSTITUT

PSI

Progress Report 2010

Laboratory for Waste Management

Nuclear Energy and Safety Research Department

Preface

The main task of the Laboratory for Waste Management is to carry out an R&D programme to strengthen the scientific basis for radioactive waste management.

The Laboratory serves an important national role by supporting the Swiss Federal Government and Nagra in their tasks to safely dispose of radioactive wastes from medical, industrial and research applications as well as from nuclear power plants. The activities are in fundamental repository chemistry, chemistry and physics of radionuclides at geological interfaces and radionuclide transport and retardation in geological media and man-made repository barriers. The work performed is a balanced combination of experimental activities in dedicated laboratories for handling radioactive elements, field experiments and theoretical modelling. The work is directed towards repository projects and the results find their application in comprehensive performance assessments carried out by Nagra. In particular, a major priority for LES over the next decade or so will be to contribute to the Sachplan Geologische Tiefenlagerung ("Sectoral Plan").

This report summarises the activities and results achieved in the reporting period. It is organised as an overview followed by individual reports on the six waste management group/sub-programme activities.

We gratefully acknowledge the help of the Institute's management and of Nagra in our work.

Table of Contents

1 OVERVIEW

M.H. Bradbury

1.1 Introduction

The progress made in the Laboratory for Waste Management (LES) over the period from January 1, 2010 to December 31, 2010 is summarised in the first part of the report. The activities carried out in the individual groups are described in chapters 2 to 7 and are either predominantly "experimental" or "modelling" in their nature. However, there are strong interactions between groups and between experimentalists and modellers.

1.2 General

The Swiss site selection process for radioactive waste repositories is defined in the conceptual part of the Sachplan Geologische Tiefenlagerung, SGT (Sectoral Plan) for deep geological repositories within the framework of land planning legislation. The Sectoral Plan was published by the Swiss Federal Office of Energy in April 2008. In accordance with the Sectoral Plan, which foresees three stages for site selection, Nagra proposed six geological siting regions for repositories for high-level waste (HLW) and low- and intermediate-level waste (L/ILW) in October 2008 as input to Stage 1 of the Sectoral Plan. After October 2008 Nagra and their partners have shifted the focus of the technical-scientific work to preparations for Stage 2 of the Sectoral Plan.

Nagra is currently carrying out a series of so called "Provisional Safety Analyses" for the different repository types in the potential regions identified, with a view to proposing at least 2 sites each for L/ILW and HLW radioactive waste repositories. A requirement by ENSI (the Swiss nuclear regulatory authority) is that the information available on all of the sites must be sufficient to allow such safety analyses to be carried out. In particular, the geological data used e.g. extent of the host rock, hydraulic permeability, expected hydraulic gradient, geo-chemical conditions, must be adequate to represent the conditions at the sites, and to take into account the existing uncertainties. In connection with this, Nagra has produced a report entitled "Beurteilung der Unterlagen für die provisorischen Sicherheitsanalysen in SGT Etappe 2" (Evaluation of the Information for the Provisional Safety Analyses in SGT Stage 2). The review of this report by ENSI is expected in February 2011.

The usual balance of work carried out in LES between research and development, and application, has currently shifted to activities related to Stage 2 of the Sectoral Plan.

The Laboratory is involved in four projects in the 7th EU Framework Programme. In ReCosy, "Redox Phenomena Controlling Systems" (start date April 1, 2008, duration 4 years), LES is work package leader; WP4, Redox Reactions of Radionuclides. An EU collaborative project entitled "Processes of Cation Diffusion in Clay Rocks" (CatClay) began on the 1st June 2010 (duration 4 years). LES is work package leader of WP2: Diffusion in Illite. After some negotiation difficulties with the EU, ACTINET-I3 officially started on 1st October 2009 (duration 3 years). The microXAS beamline (in co-operation with LES) is part of the core group of the pooled facilities. LES is also work package leader (WP4, Modelling/Theory/Safety Case) in a new EU programme entitled "Slow Processes in Close-to-Equilibrium Conditions for Radionuclides in Water/Solid Systems of Relevance to Nuclear Waste Management" (SKIN) which is due to start in January 2011 (duration 3 years).

At the beginning of 2009, LES, together with the Health and Environmental Physics Department, (Hungarian Academy of Sciences, KFKI Atomic Energy Research Institute), submitted a proposal for a joint programme of work in connection with the Schweizer Erweiterungsbeitrag DEZA/SECO agreement. After a long administrative procedure, the project started on October 15, 2010 and will last for 3 years.

Multi- and bi-lateral co-operations with external institutions and universities are considered to be of high importance and have continued in 2010. The main ones are summarized in Table 1.1. Of particular note in this context is a recent co-operation agreement signed with the Helmholtz-Zentrum für Umwelt-forschung GmbH, (UFZ), Leipzig, Germany. The co-operation centres on the development and application of the OpenGeoSys-GEMS multi component transport code and includes the possibility of joint PhD students and projects. The principal partner in this co-operation at UFZ is Prof. Olaf Kolditz.

The joint project between JAEA (Japan) and LES, set up to investigate the partitioning of Ra(II) between aqueous solutions, bentonite and argillaceous rocks, in the presence/absence of minor minerals (barite, calcite and witherite), was successfully completed in March 2010.

A new guest scientist from Japan, Dr. Takamitsu Ishidera (Research Scientist at JAEA) began a 1-year sabbatical in March 2010 in the Sorption Mechanisms Group working on the influence of temperature on sorption.

Table 1.1: National and international co-operations.

Co-operations
Nagra
Major financial contribution
Various technical working groups
Multinational
7th FP (ACTINET-I3, ReCosy, CatClay, SKIN)
OECD/NEA (sorption III project)
Mont Terri Project (Diffusion Retardation, Cement Interaction experiments)
Grimsel Test Site (Colloid Formation Migration)
Universities
Bern, Switzerland (mineralogy, petrography, water chemistry)
Surrey, United Kingdom; EPFL, Switzerland (cement systems, molecular modelling)
UC London, United Kingdom (molecular modelling)
Mainz, Germany (cement, montmorillonite)
Strasbourg, France (glass)
Tübingen, Germany (geosphere transport)
ETHZ, Switzerland (GEMS)
Research Centres
CEA*, France (near and far field)
CIEMAT, Spain (colloids)
EAWAG, Switzerland (cement)
EMPA*, Switzerland (cement)
IFR, FZD*, Germany (XAS, TRLFS)
INE, KIT*, Germany (near and far field; TRLFS)
JAEA, Japan (Ra in bentonite/argillaceous rocks)
KFKI, AEKI, Hungary (argilleous rocks)
SCK/CEN, Belgium (clays)
UFZ*, Germany (reactive transport)
*formal co-operation agreements

Current PhD and postdoc projects being carried out in LES are listed below:

L. Aimoz (PhD): "Uptake of iodine (I-) and selenium (SeO_3^{2-}) onto pyrite and LDHs". Started September 2008, (Funding: Virtual Institute (INE)/PSI).

F. Hingerl (PhD): "Simulation of geochemical processes in Enhanced Geothermal Systems (EGS)". Co-operation between LES and the Institut für Isotopengeologie und Mineralische Rohstoffe, ETHZ. Started October 2008, (Funding: Competence Center for Environment and Sustainability).

D. Soltermann (PhD): "The influence of Fe(II) on clay properties, the sorption of Fe(II) on clays and competitive sorption investigations: a combined macroscopic and microscopic study". Started August 2010, (Funding: SNF).

H. Wang (PhD): "A novel Micro Beam Analysis Alliance (MBA2) strategy for micro-heterogeneous systems". Started September 2009, (Funding: SNF) LES participation.

M. Bestel (PhD): "Water dynamics in water-clay systems". Started September 2009, (Funding: SNF). LES participation.

B. Dilnesa (PhD): "The fate of iron during the hydration of cement". Started February 2008, (Funding: SNF). LES participation.

Dr. N. Diaz (postdoc): "Assessment of micro-scale heterogeneities in clays for realistic 3D transport modeling in argillaceous rocks". Started March 2009, (Funding: PSI (FoKo)/CEA).

Dr. M. Hayek (postdoc): "Two-dimensional investigations of reactive transport processes at heterogeneous interfaces: Clogging processes at heterogeneous cement/clay interfaces". Started November 2009, (Funding: NES)

Dr M. Tyagi (postdoc): "Up-scaling modelling molecular diffusion coefficients using mesoscopic transport models; Multi-scale modelling of diffusion in clays – From molecular simulations to the continuum scale". Started July 2010, (Funding: PSI FoKo FK)

Dr. L. Pegado (postdoc): "Thermodynamic equilibrium in CASH phases from molecular modelling". Started November 2010, (Funding: SNF-Sinergia project).

It is perhaps important to note that in the majority of cases the funding for postdocs and PhDs is additional external funding i.e. funding from outside LES and Nagra.

In October 2010 K. Rozov completed his PhD at LES ("Thermodynamic stability and radionuclide binding mechanisms in hydrotalcite-like solid solutions") and will be taking up a postdoc position in the Nuclear Disposal Research Department at the Jülich Research Centre in January 2011. Dr. D. Popov's postdoc position at LES ("Crystallographic analysis of micro-diffraction images from heterogeneous polycrystalline samples") came to an end in May 2010, and he has been working in the High Pressure Collaborative Access Team at the Advanced Photon Source in Chicago since June 2010. Dr. X. Gaona completed his 2-year guest scientist stay at LES in August 2010 and has taken up a postdoc position at INE/KIT. We extend our best wishes to them in their future carreers.

The new redox glove box line, with integrated ultra centrifuge, has been successfully installed and commissioned in the Hot Laboratories at PSI. (This glove box line was fully financed by Nagra.) This box line will be used to measure the uptake of redox sensitive radionuclides on argillaceous rocks and cementitious materials under well defined and controlled reducing conditions.

During 2010 members of LES have been invited to participate in various international technical review groups: "Near surface disposal of category A waste at Dessel" Ondraf/Niras, Belgium; "SARG (SFR extension, Application Review Group)", SKB, Sweden; and "Expert Panel on Radionuclide Migration in Plastic Clay", Ondraf/Niras and SCK-CEN, Belgium.

LES is participating in "Nuclear Environmental Chemistry" at ETH Zurich (lectures and exercises on nuclear waste management) within the MSc courses "Nuclear Energy Systems" and "Landfilling, Nuclear Repositories and Contaminated Sites".

On February 25/26, 2010, the Waste Management Program Committee met for their annual meeting. The work performed within LES and the future plans were discussed, as usual. The focus of this meeting was on reactive transport modelling (AN-44-10-05). The valuable help and input from the members of the committee, both at the meeting, and throughout the year, are appreciated by the whole Laboratory.

1.3 Sachplan Geologische Tiefenlager, SGT ("Sectoral Plan")

LES made numerous contributions to Stage 1 of the Sectoral Plan in which 6 regions for the deep geological disposal of L/ILW, and 3 regions for long-lived intermediate level waste, and HLW in Switzerland were proposed by Nagra. These included

new work such as a generic study on the influences of mineralogy and water chemistry on sorption and a series of generic sorption databases covering the major rock type categories; argillaceous rocks, crystalline and calcareous rocks and the range of associated water chemistries. A comprehensive report on diffusion measurements and data in argillaceous rocks from both the Swiss programme, and other international programmes, was compiled together with evaluations of the transport models used in performance assessment. Other contributions consisted of providing various updated and revised data-bases: thermodynamics, solubility limits (bentonite and cement porewaters), sorption (bentonite, cement, clay host rocks) and an interim report on the interaction of a pH plume with sand/bentonite mixtures.

For Stage 2, in which at least two sites for each repository type will be proposed, more detailed, host-rock specific information and data bases for the so called "Provisional Safety Analyses" are required. The sorption data base (SDB) work carried out for Stage 1, provided the basis for a report setting out the processes for deriving SDBs for argillaceous rocks and bentonite in future performance assessment studies. The proposed procedures were tested by comparing the sorption values predicted by this methodology with those for the Opalinus Clay (OPA) and MX-80 bentonite systems used in the Entsorgungsnachweis. (The results were very positive.) A report summarising the physico-chemical characteristics of MX-80 bentonite, and sorption isotherms measured on nine safety relevant radionuclides, has been prepared as a Nagra NTB.

SDBs (including diffusion) in cementitious materials, bentonite, Opalinus Clay, Effingen Member, "Brauner Dogger" and Helvetic marls will be completed by early 2011. These sorption data bases will be prepared using the new procedures previously developed, and include competitive sorption effects from stable isotopes and materials coming from the waste and taking into account the geochemical evolution of the near fields and adjacent rocks. The predicted sorption values of several radionuclides on Effingen Member are currently being bench marked against new experimental measurements. Solubility limits in the bentonite and cementitious near fields will be derived taking into account the factors given above.

Two major activities focused on the preparation of reports on the chemical evolution of the cementitious L/ILW near field (caverns, surrounding host rock, backfilled access tunnels), and the chemical evolution of the HLW near field (tunnels, bentonite backfill, surrounding host rock). The state of the art reactive

transport code, OpenGeoSys-GEMS, was used to model the geochemical evolution of the repository near fields in the different host rocks with respect to their interactions with cementitious materials.

The influences of iron corrosion, the post closure elevated temperature phase, glass corrosion, and the dissolution of spent fuel and zircaloy cladding, on the properties of MX-80 bentonite were assessed.

Methodologies for modelling the porewater chemistries for compacted bentonite and ESTRED cement (low pH cement) were further developed using the GEMS approach.

A further contribution to Stage 2 included a report on the influence of colloids on radionuclide transport in the host rocks Opalinus Clay, Effingen Member, "Brauner Dogger" and Helvetic marls. Finally, diffusion experiments with HTO, $^{36}Cl^-$ and $^{22}Na^+$ on samples from the Effingen Member were performed with the main aim of checking the validity of the extended Archie's relation for estimating effective diffusion coefficients.

1.4   Foundations of repository chemistry

Powder X-ray diffraction (XRD) and extended X-ray absorption fine structure (EXAFS) spectroscopy were used to obtain a molecular-level understanding of the uptake mechanisms of iodide by Zn-Al and Ca-Al layered double hydroxides (LDHs). The results showed that the uptake mechanisms of iodine in LDHs depend on the nature of the cations in the brucite layer.

Solubility data for hydrotalcite-pyroaurite solid solutions with variable Mg – Al/Fe cationic ratios have been interpreted by developing an ideal multi-site solid solution model based on the 'sublattice' concept. This model can be extended by incorporating other substituting cations and anions, and will be the subject of future experimental studies and developments of model fitting algorithms.

Major advances in thermodynamic sorption modelling in GEMS have been achieved with the development of theoretical conversions of intrinsic adsorption constants between different site densities, 'denticities', and concentration scales. This work has also led to new arguments for the convention on standard states for activities of surface species and sites.

1.5   Repository near field

1.5.1 Clay systems

One of the main features the 2 site protolysis non electrostatic surface complexation and cation

exchange (2SPNE SC/CE) sorption model is that two broad categories of edge sorption sites are assumed; the so called "strong" and "weak" sites. In a combined wet chemistry/sorption modelling/polarised- (P)-EXAFS study of Zn sorption on montmorillonite, it was demonstrated for the first time that two very distinct surface complex types exist in loading regions predicted by the modelling to be dominated by strong sites and weak sites, i.e. essentially confirmation of the strong site/weak site hypothesis. The Zn sorbed on the strong sites had many characteristics in common with the Zn incorporated in the montmorillonite lattice (strong P-EXAFS) whereas the Zn on the weak sites showed little or no structure.

The strong site/weak site hypothesis was subsequently further investigated by combining the P-EXAFS data and density functional theory based calculations to reveal the mechanism of Zn^{2+} uptake on the edges of montmorillonite. The strong sites were explained by cation incorporation into the clay structure. The measured P-EXAFS spectra of Zn on weak surface sites could be explained by mono- and bi-dentate Zn complexes absorbed on the edge of the TOT sheet.

In order to support wet chemistry and modelling results on the uptake of U(VI) by montmorillonite, P-EXAFS was employed to elucidate where inner-sphere complexes formed on the montmorillonite surface. The P-EXAFS data showed no anisotropy, although the self-supporting films were well oriented, indicating that U(VI) is not sorbed on montmorillonite in the continuity of the octahedral sheet as a single surface complex, but rather, there appears to be a series of similar complexes formed.

The influence of sorption competition on the migration of radionuclides through compacted bentonite was modelled using the MCOTAC-sorb code, Ni(II) break through curves were calculated for an 0.8 m thick compacted bentonite buffer with and without considering competitive sorption with an equilibrium Fe(II) background concentration of 5.3×10^{-5} M. Such an Fe(II) concentration is anticipated in real systems because the bentonite porewater is expected to be saturated with siderite. The breakthrough time for Ni(II) decreased from about 1000 years to less than 100 years when taking the Fe(II) sorption competition into account.

Diffusion, at the scale of a single pore, can be modelled by molecular dynamics simulations. However, such molecular simulations are no longer feasible at the cm scale. In order to address the up-scaling problem, a two-step simulation approach has been developed which enables macroscopic diffusion coefficients of water and ions to be derived from pore

scale molecular diffusion coefficients. First, local pore diffusion coefficients are derived in molecular dynamics simulations for specific local environments e.g. interlayer, edge regions of clay particles. These local diffusion coefficients are then assigned to different types of porosity in a model clay structure. The structure-averaged diffusion coefficient of the sample is obtained by random walk simulations for a complex, larger-scale structure. The accuracy of the suggested approach has been demonstrated by comparing the results of direct molecular simulations for a (larger scale) stack of pyrophyllite nano-particles with the two-step up-scaling approach. This up-scaling concept is general, and can be used for up-scaling molecular diffusion coefficients for porous materials with arbitrarily complex structures.

Diffusion measurements of bivalent anions ($^{75}SeO_4^{2-}$ and $^{35}SO_4^{2-}$) in compacted clays showed that both anions exhibited significant retention, unlike $^{36}Cl^-$. A possible explanation could be that the tracer undergoes isotopic exchange with a trace mineral impurity in the compacted clay, or is incorporated into a solid solution. The effective diffusion coefficients for bivalent anions are lower than for the monovalent anions. The diffusion results for $^{134}Cs^+$ showed a larger retention than estimated from batch sorption experiments and unusually high D_e values. These diffusion studies are continuing.

1.5.2 Cement

The cement used for the experimental studies is a sulphate-resisting Portland cement, CEM I 52.5 N HTS (Lafarge, France), which is currently in use for the conditioning of radioactive waste in Switzerland. Calcium silicate hydrate (C-S-H) phases are considered to be the most important constituent of hardened cement paste (HCP) for cation and anion binding, which is the reason complementary studies using C-S-H phases are being carried out.

In 2010 a status report summarising the current knowledge on the speciation of ^{14}C in the cementitious near field was completed. (Small organic molecules containing ^{14}C are thought to be generated during the anaerobic corrosion of steel.) An experimental programme was proposed with the aim of resolving currently existing discrepancies concerning the type of organic compounds formed under relevant near field conditions. A detailed evaluation of the analytical equipment needed was also made. High Performance Ion Exclusion Chromatography (HPIEC), coupled with a suitable detection system (Mass Spectrometry, MS), was evaluated and tested in 2010. Experimental

investigations on the uptake of oxygenated hydrocarbons, started in 2008, were continued in 2010. The retention sequence was: formic acid > acetic acid ~ acetaldehyde > formaldehyde ~ methanol ~ ethanol. A mean R_d value of ~10^{-4} m^3 kg^{-1} was estimated with lower and upper bounds of 10^{-6} m^3 kg^{-1} and 10^{-3} m^3 kg^{-1}, respectively.

Kinetic studies on the Np(IV) uptake by C-S-H phases with different Ca:Si (C:S) mol ratios and Np(IV) precipitation tests, have been carried out in alkali-free solutions and in alkali-rich artificial cement porewater (ACW) at pH = 13.3. Reducing conditions were established either by adding 5×10^{-3} M Na-dithionite to the suspensions, or, in few cases, using a potentiostat. The R_ds for Np(IV) were found to range in value between 10^2 and 10^3 m^3 kg^{-1} in alkali-free solutions, and between 10^3 and 10^4 m^3 kg^{-1} in ACW. EXAFS measurements clearly showed that the C-S-H phase in HCP are responsible for Np(IV) immobilization by incorporation into the C-S-H structure.

An aqueous-solid solution thermodynamic model of U(VI) uptake by C-S-H was developed using the compound energy formalism (CEF) as an extension of the CSH3T model recently developed "in house" for 'pure' C-S-H phase solubility. The sub-lattices proposed in the CSH3T model were occupied with U(VI) species in accordance with the spectroscopic findings. The thermodynamic model allowed the predictive modelling of U(VI) immobilization in a degrading cementitious near field of a repository over the pH range ~10 to ~13.3.

1.6 Repository far field

The diffusive behaviour of strongly sorbing tracers, i.e. tracers that sorb via surface complexation is being investigated in compacted illite and Opalinus Clay. Some preliminary in-diffusion experiments with $^{60}Co(II)$ in Opalinus Clay were performed on small drill cores embedded in an epoxy resin. The tracer profile in the samples was analysed using a modified version of the abrasive peeling technique. The experiment clearly shows that Co(II) diffuses faster than expected. One explanation may be the presence of Fe(II) in the porewater competing with Co(II) for the sorption sites resulting in a smaller apparent diffusion coefficient. Modelling with the reactive transport code MCOTAC-sorb and PHREEQC are ongoing.

Four Cs through-diffusion experiments in clay samples from Mont Terri and Benken under different confining pressures were modelled with MCOTAC.

The pore diffusion coefficients and the site capacities needed to model the diffusion data measured on Mont Terri samples differed by less than 10%. The fitted pore diffusion coefficient for through-diffusion experiments on three samples from Benken under 4, 8 and 12 MPa confining pressure, were between 1 and 2×10^{-10} m^2 s^{-1}, i.e. a factor of at least four lower than for the Mont Terri samples.

Micro-heterogeneity is an inherent and highly relevant characteristic of most natural and engineered (geo-) materials. Laser ablation inductively coupled plasma mass spectrometry and micro X-ray fluorescence are being used to measure shallow diffusion profiles in heterogeneous materials. Cs was in-diffused into an Opalinus Clay sample and the profile analysed. By combining the complementary information content of the images from the two techniques, a chemical image with high spatial resolution and improved quantitative reliability could be obtained.

Natural rocks are far from being homogeneous and isotropic. The effect of spatial mineralogical heterogeneities on Cs diffusion in Opalinus Clay is being investigated by monitoring the in situ Cs transport using a micro tomography technique (SLS-TOMCAT beam line). With such a non-destructive technique, data on both the mineral distribution and the time resolved spatial propagation of Cs in the same sample can be acquired. Transport simulations,

under the same conditions as the diffusion experiment, were performed using an "in-house" random walk code. Both sets of profiles (experimental and simulated) show variations in the diffusion profile concentrations which deviate from the smooth classical shape in a homogeneous porous medium. The spatial Cs distributions showed "fingering" which correlated with the clay fraction domains.

The DR (Diffusion and Retention) experiment in the Mont Terri Rock Laboratory was over cored in January 2010. The experimental setup had two injection intervals with different tracer inventories. HDO, ^{18}O, ^{133}Ba, ^{60}Co, ^{137}Cs, ^{152}Eu, and stable Eu were added to the upper interval, and HTO, ^{18}O, I, Br, ^{22}Na, ^{85}Sr, Cs, ^{75}Se, and stable Se were injected in the lower interval. An intact core of about 2 m length and about 30 cm diameter, including the two injection intervals, was retrieved. The first data analysis indicated that the vertical position of the intervals within the core was slightly displaced upward relative to the reference coordinate system during the over coring. Preliminary comparisons with model predictions based on parameters obtained in previous experiments in the Mont Terri Rock Laboratory show a reasonable agreement with the measurements. More detailed evaluations and interpretations of these data, as well as of those of the sorbing active and the mobile inactive tracer profiles measured at PSI and elsewhere, are still ongoing.

Table 1.2: *LES Organigram*
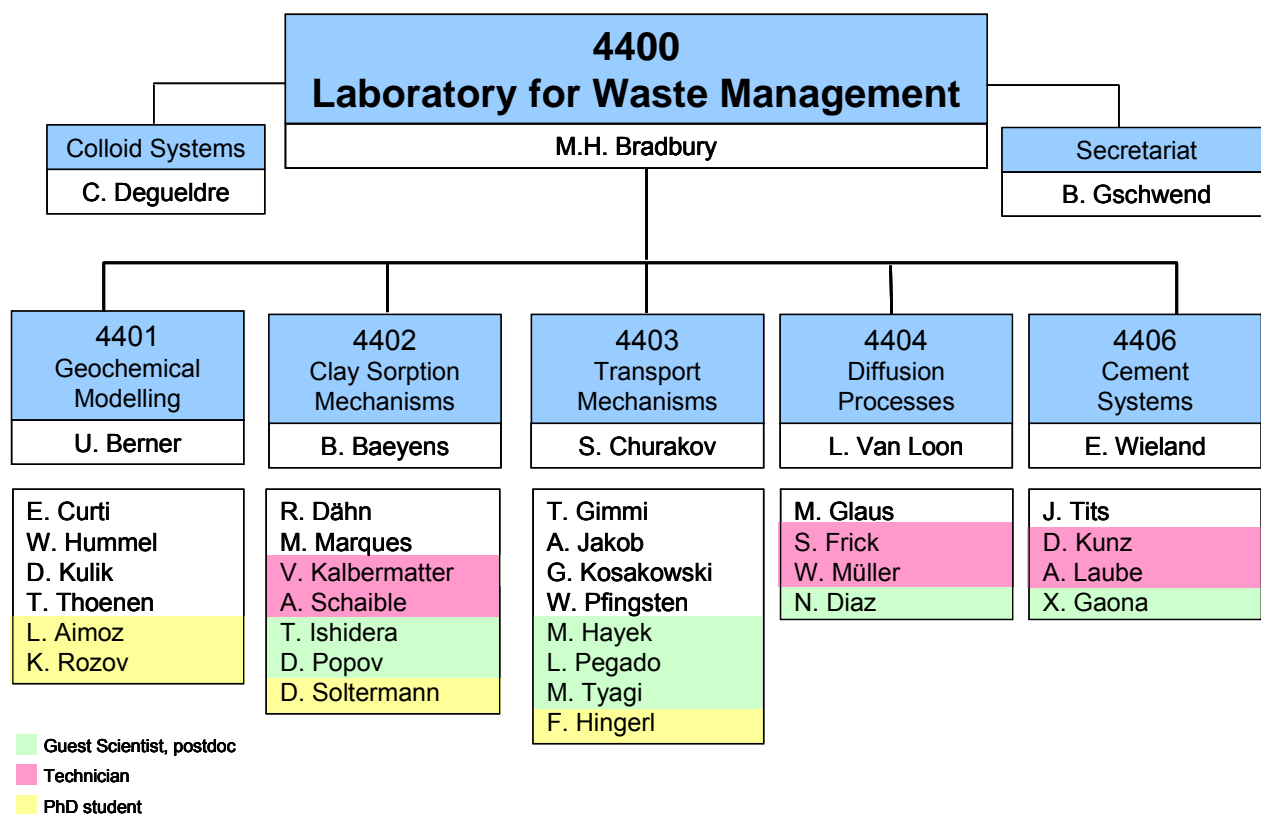
2 GEOCHEMICAL MODELLING

W. Hummel, U. Berner, E. Curti, D. Kulik, T. Thoenen, L. Aimoz (PhD), K. Rozov (PhD)

2.1 Overview

The majority of the Geochemical Modelling Group's work in 2010 was related to the Swiss Sectoral Plan for deep geological disposal. This work comprised of model calculations and extensive literature reviews which contributed to two Nagra Technical Reports on the geochemical evolution of the near-field of planned geological repositories for HLW and L/ILW. Special topics of this work explicitly mentioned here are:

- Reference porewaters at high ionic strengths re-calculated using the specific ion interaction model, SIT.

- Review of experimental data concerning bentonite alteration due to iron corrosion.

- Review of knowledge on the post-closure elevated temperature period.

- New thoughts about "internal reactions" of quartz with cement phases in concrete mixtures.

- Glass corrosion revisited considering bentonite and iron corrosion products.

- Chemical evolution of spent fuel and zircaloy cladding under repository conditions.

Progress on the characterisation and modelling of solid solution systems was made in the framework of two PhD projects (Laure Aimoz and Konstantin Rozov):

- Powder X-ray diffraction and EXAFS spectroscopy were used to obtain a molecular-level understanding of the uptake of iodide by Zn-Al and Ca-Al layered double hydroxides (LDHs).

- Solubility data for hydrotalcite-pyroaurite solid solutions with variable Mg – Al/Fe cationic ratios have been interpreted by developing an ideal multi-site solid solution model based on the 'sublattice' concept.

Advances in thermodynamic sorption modelling with GEMS have been achieved with the development of theoretical conversions of intrinsic adsorption constants between different site densities, 'denticities', and concentration scales.

2.2 Work related to the Sectoral Plan (Sachplan)

2.2.1 Reference porewaters

In the framework of Stage 2 of the Sectoral Plan, a number of reference porewaters were defined by the University of Bern for the Effingen Member, Opalinus Clay, "Brauner Dogger", and for the Helvetic marls. These reference porewaters were derived using the Davies equation for ionic-strength corrections. Several of porewaters had rather high ionic strengths (Effingen Member between 0.7 and 1.3 mol kg^{-1}, high-salinity variants for the Opalinus Clay and the "Brauner Dogger" are 0.8 mol kg^{-1}) which lay well outside the validity range for the Davies equation. (The NEA-TDB guidelines recommend that the Davies equation should not be used at ionic strengths above 0.1 mol kg^{-1}.) In view of this, it was decided to re-calculate the porewaters using the specific ion interaction model, SIT. A database of SIT ion interaction coefficients was prepared which was compatible with the recently updated PSI/Nagra Chemical Thermodynamic Database and comprised of interaction coefficients of cations with Cl$^-$, ClO$_4^-$, and NO$_3^-$ anions with Li$^+$, Na$^+$, and K$^+$. As all of the reference porewaters are dominated by NaCl, this set of interaction coefficients allowed a sufficient approximation of activity coefficients to be calculated.

In the speciations calculated using the Davies equation and the SIT model, differences of up to $\pm\,25\%$ were found. However, these differences are generally smaller than the variations in the data used to define the porewater compositions, e.g. Effingen Member, 0.7 or 1.3 mol kg^{-1} ionic strength.

The SIT model is also currently being used to calculate radionuclide speciation in the revised porewaters in support of the development of the sorption databases.

2.2.2 Iron-bentonite interaction

One of the factors that will influence the geochemical evolution of the near field of the planned Swiss HLW repository is the corrosion of the carbon steel canisters, and other materials containing metallic iron. Initial aerobic and later anaerobic corrosion will release large amounts of Fe^{2+} which may lead to a significant alteration of the surrounding bentonite. An ongoing review of experimental, modelling, and

natural analogue studies aims at identifying the relevant alteration processes and products.

A large number of experiments have shown that iron corrosion may destabilise montmorillonite, thereby reducing the swelling capacity and the sorption capacity of bentonite. The most likely minerals replacing montmorillonite are Fe-rich smectites (e.g. saponite), non-swelling Fe-rich sheet silicates of the serpentine group (e.g. berthierine and odinite), and non-swelling Fe-rich chlorite. While chlorite appears in experiments only at temperatures above 150°C, Fe-rich smectites and Fe-rich members of the serpentine group are formed below 100°C. At the present state of knowledge, the extent of bentonite alteration due to iron corrosion, and the exact type of alteration products produced, cannot be predicted with any confidence. Simple mass balance constraints, however, indicate that enough iron is present in the HLW canisters for a complete alteration of montmorillonite, thus iron-bentonite interactions cannot be neglected on this basis.

2.2.3 Elevated temperature period

For Nagra's project for demonstrating disposal feasibility (*Entsorgungsnachweis*), the evolution of temperature in the near-field of the emplacement tunnels after HLW repository closure has been assessed on the limiting cases of constant high and low water contents of bentonite (JOHNSON et al., 2002). The calculated peak temperatures at the spent fuel canister/buffer interface were 110°C and 160°C, respectively, and the period of time temperatures remained above 100°C was predicted to extend from 100 to 1000 years, depending on the model assumptions.

Later, a more detailed modelling of two-phase flow processes associated with the early closure period was carried out (SENGER & EWING, 2008). In this study of thermal-hydrologic (TH) processes a peak temperature of 132°C was reached at the spent fuel canister surface within about 4 years after tunnel closure, and after 20 years the temperature decreased to about 110°C. This early decrease in temperature explained by the convection of water vapour and subsequent rapid saturation of bentonite.

A number of long-term experiments in rock laboratories have explored the temperature effects on bentonite at temperatures below 100°C. The major part of the bentonite backfill remained intact, and only small alterations of the mineralogical, chemical and mechanical properties were detected in bentonite close to the heaters which represented the steel canisters in

these experiments. At higher temperatures the situation is less clear. In the first years after tunnel closure steep temperature gradients and water vapour convection could, for example, promote disso-lution/precipitation zones of amorphous silica in the backfill. Hence, carefully designed experiments and two-phase flow THMC modelling, explicitly considering chemical (C) effects, seem to be necessary in order to achieve a more detailed understanding of the early post-closure period.

2.2.4 New thoughts on the longevity of high-pH conditions in cementitious materials

The current state-of-the-art view in waste management considers three different stages in the evolution of cementitious structures and their porewaters. At short times, a high-pH stage (pH > 13) determined by the high concentrations of alkali hydroxides, is followed by a portlandite, $Ca(OH)_2$, dominated stage. The duration of this second stage (pH 12.5) may last for quite a long time, depending on the water flow through the cement structure. A third stage is characterized by the absence of portlandite, and the degradation of calcium-silicate-hydrate (C-S-H) phases, from high Ca/Si-ratios to low Ca/Si-ratios. The time scale again depends on the flux of formation water through the system. In the past, all of these considerations were made under the assumption that the concrete aggregates (mainly quartz sand and gravel) are inert.

Recently, coupled chemistry/transport modelling carried out in the framework of the Sectoral Plan has shown that the interface between cementitious and host rock/backfill materials will probably clog due to the precipitation of secondary minerals (KOSAKOWSKI, 2010). Such clogging would have consequences for the different evolution stages of hydrated cements and concretes. Given, in addition, the more realistic assumption that the siliceous aggregates are thermodynamically unstable at elevated pHs, somewhat different concepts on how concretes behave under such conditions need to be developed.

From a thermodynamic point of view the principal reaction

$$Ca(OH)_{2(portlandite)} + SiO_{2(quartz, aggregate)} ---> \text{C-S-H}_{(calcium-silicate-hydrates)} \quad (1)$$
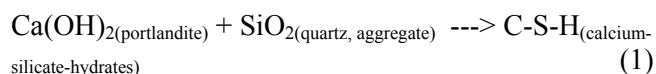
proceeds until portlandite is exhausted, since standard concrete mixtures contain much more quartz than portlandite. If a concrete system is closed by clogging reactions as outlined above, diffusive exchange with

the surroundings ceases. However, the principal reaction (Eq. 1) will proceed internally, and when portlandite is exhausted, the remaining quartz will react with other cement phases. Finally, a system containing mainly clay minerals in the pH range 9 to 10 will be reached. The detailed final stage of the reaction sequence is, at present, difficult to predict because it depends on a number unknown thermodynamic and mass balance constraints.

A key question is the time frame in which this internal reaction with quartz occurs, and particularly also, the comparison with reactions caused by formation waters in the case of non-clogged systems. PALANDRI & KHARAKA (2004) have compiled a "rate parameter database" for application in geochemical modelling. If their rate parameter for the dissolution of quartz at ambient temperature is used, the evolution of a reference concrete system (BERNER, 2009) is accelerated by more than one order of magnitude.

In this first estimate, neither the pH drop due to the formation of alkali-binding C-S-H phases, nor changes in surface areas as a function of ongoing processes, were included. Both processes may slow the rate of quartz dissolution.

Such considerations may have consequences for setting up sorption databases in cementitious environments. The previously assumed long duration of stage 2, could, in fact, be much shorter, independent of the externally driven water flow through the system. Further, the impact of kinetic effects, particularly in reactive systems such as concretes, should not be underestimated.

2.2.5 Glass corrosion: the JSS database

In the time between 1983 and 1988, a broad experimental and theoretical programme focusing on glass corrosion kinetics (JSS) was carried out on behalf of an international consortium (Criepi in Japan, Nagra in Switzerland and SKB in Sweden). Experimental work was conducted in two laboratories (the Hot Labs) at PSI and Studsvik Energiteknik AB in Sweden. A wealth of kinetic data, obtained with both active and inactive glasses, at various temperatures, and partly in the presence of bentonite/Fe-oxide additions, were generated and documented in special reports as well as in publications (e.g. WERME et al., 1990, and references therein).

In view of the renewed interest on the corrosion kinetics of nuclear waste glasses, particularly concerning the effects of alpha irradiation and the

interaction with engineered barrier materials, efforts have been undertaken to re-interpret and systematize the acquired data. In a first step, the leaching data (spread over numerous publications and reports) were entered in a spreadsheet and systematically organized in order to facilitate parametric cross-correlations. Each data point was "labelled" with an identifier that allows the quick determination of the glass used, the reaction time, as well as the physico-chemical conditions under which the experiment was carried out (temperature, surface/water ratio, nature and amounts of additives and type of measurement, e.g. pH, elemental concentration or gravimetric mass loss).

After building up the database, appropriate data were selected in order to identify the effects of alpha self-irradiation and the presence of engineered barrier materials (bentonite and/or Fe corrosion products) on the surface-normalized glass corrosion rate. Fig. 2.1 shows that, over the timescale of the experiments (~ 1 year), the extent of corrosion of the active JSSA glass (red data points) is similar to that of its inactive counterpart (ABS118 glass), both in the presence and absence of the bentonite/magnetite mixture. Because the JSSA glass had been doped with fast-decaying Pu isotopes (in order to simulate advanced levels of structural damage), these data indicate that alpha self-irradiation most probably has no detrimental effect on the glass corrosion kinetics under repository conditions. In contrast, the presence of bentonite and/or magnetite enhances the corrosion kinetics. As indicated by the slope of the data arrays, after 1 year the rate in the presence of the bentonite/magnetite mixture is still considerably larger than for the corresponding experiments in pure water.

Other JSS data (not shown here) for glass corroded in the presence of magnetite or goethite, but without any clay present, confirm the catalyzing effect of canister corrosion products and indicate that this effect increases with the exposed surface area of the magnetite or goethite.

Although the JSS project provided a large body of data, and useful insights into the corrosion behaviour of nuclear waste glasses, the results are not always conclusive due to (a) relatively short reaction times (~ 1-2 year max.); and (b) an experimental setup which is not representative of the conditions in a deep radioactive waste repository (e.g. the use of non-compacted clay directly in contact with the glass). New experimental setups have been proposed in an internal report in order to overcome these shortcomings.

● active glass, with bentonite and magnetite
● inactive glass, with bentonite and magnetite
▲ active glass, no additives
▲ inactive glass, no additives
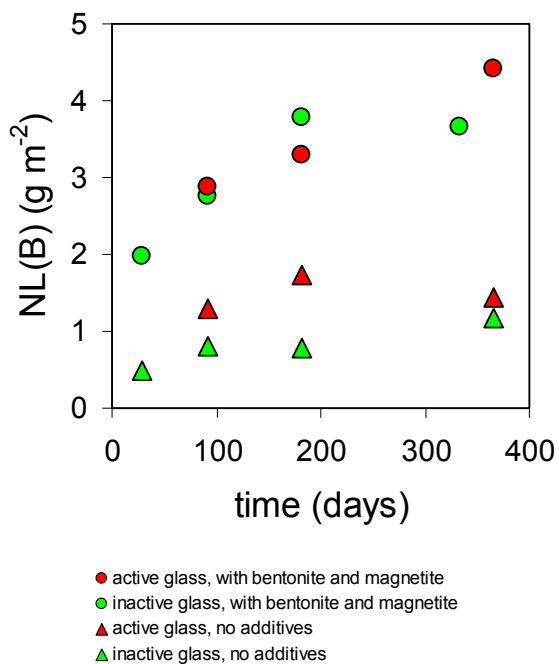
Fig. 2.1: Combined effect of alpha self-irradiation and additions of MX-80 bentonite (133 g L^{-1}) and magnetite powder (33 g L^{-1}) on the corrosion of active and inactive COGEMA glass at 90 ^{o}C. NL(B) indicates the amount of glass corroded per unit surface area as derived from boron concentrations in the aqueous phase.

2.2.6 Spent fuel

Spent Fuel (SF) is a heterogeneous and complex material that continuously evolves during in-reactor irradiation, intermediate storage and aqueous corrosion in a deep geological repository. In a technical report (under review) all three aspects were considered, with particular emphasis on aqueous corrosion after canister failure in a deep geological repository.

A review of published data on SF dissolution kinetics is provided, particularly focusing on the role of hydrogen produced through anaerobic corrosion of a metallic canister. Recent experiments showed that hydrogen, at the expected elevated partial pressures, effectively de-activates dissolved radiolytic oxidants (H_2O_2, O_2) that would otherwise lead to oxidative dissolution of SF. After completion of canister corrosion (~10^5 years after repository closure), and the diffusion of hydrogen, radiolysis will be too weak to cause oxidative dissolution. From these findings, it was concluded that oxidative corrosion will not be a relevant mechanism in the reference scenario. It is argued that SF dissolution will proceed for most of the time at, or close to, thermodynamic equilibrium, and

will be driven by the recrystallization of U(Pu)O$_2$ combined with out-diffusion of U(Pu) species.

The report also includes thermodynamic equilibrium calculations aiming at predicting the chemical composition and radionuclide concentrations in the porewater directly in contact with SF. The calculations were based on detailed chemical and radionuclide inventories of the materials involved (SF, zircaloy and steel) assuming reaction with state-of-the-art bentonite porewater. The results suggest that a number of simple phases, liable to limit the solubility of a number of radionuclides, could precipitate soon after water ingress in the waste form. In view of the lack of experimental data on long-term SF alteration, and adequate thermodynamic data for possible complex solid solutions, these calculations must be considered as tentative.

2.3 Solid solutions

2.3.1 Uptake of iodine by layered double hydroxides

Layered Double Hydroxides (LDHs) are a broad group of minerals capable of fixing anionic species in their interlayers. They may potentially contribute to the retention of long-lived anionic nuclides such as ^{129}I, ^{79}Se and ^{99}Tc during their migration from a deep geological repository. In the context of an ongoing PhD project (Laure Aimoz), Powder X-Ray Diffraction (PXRD) and Extended X-ray Absorption Fine Structure (EXAFS) spectroscopy were used to obtain a molecular-level understanding of the uptake of iodide by Zn-Al LDHs and Ca-Al LDHs (the latter are known as AFm phases in cement chemistry).

Iodine-bearing LDHs were prepared by the co-precipitation technique. Zn-Al,I LDHs were prepared through slow addition of Zn-Al nitrate (Zn/Al= 2, 3, and 4) and NaOH (to maintain constant pH) into a KI solution. Whereas Ca-Al,I LDHs were synthesised through stoichiometric addition of C$_3$A (tricalcium-aluminate) and CaI$_2$ (Ca/Al = 2) and aged for long times (up to 84 days). For both phases, PXRD analyses indicated the formation of pure crystalline LDHs (hexagonal structure) with iodine occupying the interlayer space. A Rietveld structural refinement on the most crystalline Zn-Al,I sample (Zn/Al=4) revealed the presence of stacking faults, a common feature in LDH phases, and the positions of iodine atoms in the interlayer did not show long range ordering, as also reported by PRASANNA et al. (2010). EXAFS studies at the iodine and zinc K-edges were performed at the BM26A beamline of the European

Synchrotron Radiation Facilities (ESRF, Grenoble, France), using a He cryostat. The Zn-K and I-K EXAFS spectra of the synthesized Zn,Al-I LDHs are shown in Fig. 2.2a and 2.3a, respectively, along with the corresponding radial structure functions (RSF) (Fig. 2.2b and 2.3b), and Fourier back-transformed spectra (Fig.2.2c and 2.3c). The k^3-weighted Zn-K spectra (Fig. 2.2a) revealed a distinctive beat pattern at ~8 Å^{-1} < k < ~8.5 Å^{-1}, typical for LDH phases (SCHEINOST & SPARKS, 2010). RSFs at the zinc K-edge showed a local order of the cations within the brucite layer for all samples, with 6-fold coordination by oxygen atoms and Zn/Al neighbours at R+ΔR up to ~9.2 Å (Fig. 2.2b). No Zn-I backscattering pairs were found, indicating a lack of short-range order between Zn in the octahedral layer and I in the interlayer. This result was confirmed by data measured at the iodine K-edge on the same samples, which did not reveal any preferred distance for I-Zn pairs (Fig. 2.3b). In contrast, the EXAFS spectra at the I K-edge of the Ca-Al,I LDH show a well-ordered distribution of iodine atoms in the interlayer, with I-I pairs at R+ΔR up to ~6.0 Å, and I-Ca pairs at ~5.7 Å (Fig. 2.3b).

No preferential arrangement between the interlayer anions and the octahedral sheets was found in the case of Zn-Al LDH, whereas a larger degree of ordering was found in the case of Ca-Al LDH.

These results show that the uptake mechanisms of iodine in LDHs depend on the nature of the cations in the brucite layer. Future work will be devoted to investigating iodide uptake by pure AFm-Cl$_2$, AFm-SO$_4$ and AFm-CO$_3$ and to the determination of the solubility product of AFm-I$_2$.
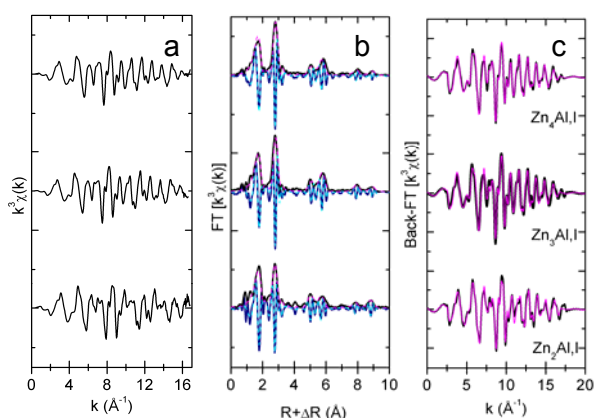
Fig. 2.2: *EXAFS spectra at the zinc K-edge; (a) k^3-weighted spectra (b) experimental and fitted (dotted lines) imaginary and real part RSFs (c) k^3-weighted EXAFS function for the Fourier backtransform spectra obtained from Fig. 2.2b.*
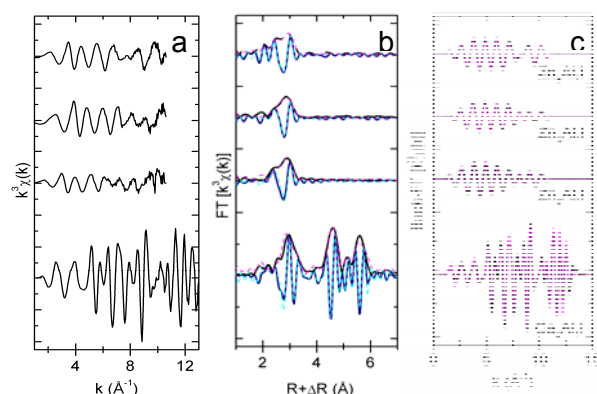
Fig. 2.3: *EXAFS spectra at the iodine K-edge; (a) k^3-weighted spectra (b) experimental and fitted (dotted lines) imaginary and real part RSFs (c) k^3-weighted EXAFS function for the Fourier backtransform spectra obtained from Fig. 2.3b.*

2.3.2 Sublattice model for hydrotalcite-pyroaurite solid solutions with variable cationic ratios

The main part of a now finished PhD project (ROZOV, 2010) on layered double hydroxides (LDH), concerned the synthesis and characterization of a LDH hydrotalcite–pyroaurite solid-solution series (ROZOV et al., 2010) and investigations of the stability/solubility of these hydrotalcite-pyroaurite solid solutions with Mg/(Al+Fe^{III}) cationic ratios (*CR*) close to 3.

In the final part of this PhD project LDH solids Mg$_{1-z}$(Al, Fe)$_z$(OH)$_2$(CO$_3$)$_{z/2}$ · nH$_2$O with cationic ratios $CR = (1-z)/z$ close to 2.75, 2.5, 2.25 and 2.0, and with variable mole fractions of iron (x_{Fe}) at $CR \approx 2.0$, were studied in co-precipitation and long term (153 days) dissolution experiments at pH 11.2, 10.9, 10.6 and 10.3 under ambient conditions. Aqueous concentrations of Na, Al, Fe, Mg and C were determined using ICP-OES, TIC (Total Inorganic Carbon), and (in some samples) LSC (Liquid Scintillation Counting) with ^{55}Fe. Solid products were characterized by PXRD, thermogravimetric analysis, Raman spectroscopy and wet chemical analysis. PXRD data showed that hydrotalcite-pyroaurite solid solutions with the unit-cell parameter $a_o = b_o$ are a linear function of x_{Fe} and, for hydrotalcites, a function of *CR*. This Vegard's-law dependence of a_o and b_o cell parameters indicates complete mixing in both *CR* and x_{Fe} directions.

Thermodynamic interpretation of the solubility data has been performed by developing an ideal multi-site

solid solution (SS) model based on the 'sublattice' concept (e.g. LUKAS et al., 2007).

Sublattices are defined as sets of equivalently coordinated positions (so-called sites) in the crystal structure. Each sublattice site is characterized by the number of substituting ions or vacancies (so-called species). Actually, any crystalline solid can be represented using the sublattice concept. There are situations when one or more sublattices with the substitution of two or more species can be identified in the mineral structure. This is the case for the hydrotalcite-pyroaurite system with variable cationic ratio CR.

To construct a multi-site model, the sublattices and substituting species in them must be defined. Five sublattices a, b, c, d, h with the sublattice stoichiometry $a_8 b_3 c_3 d_1 h_{15}$ were selected by considering the crystal structural features of the hydrotalcite-pyroaurite solid solution system (Fig. 2.4). Sublattice 'a' is occupied only with $Mg(OH)_2$. The 'c' sublattice represents the charged part of the layer occupied with randomly-mixed Al^{III} and Fe^{III} cations. The sites of the 'd' type are occupied either with $Mg(OH)_2$ or with randomly mixed Al^{III} and Fe^{III} composite species. The structural charge created by trivalent cations on 'c' or 'd' sites is compensated by interlayer anions (CO_3^{2-}), either located on 'b' sites or, together with H_2O, in positions connected to 'd' sites. The rest of the interlayer water is assigned to 'h' sites. Expressing the stoichiometry of LDH per 24 cations in order to avoid non-integer stoichiometry coefficients in the chemical formulae, this sublattice scheme can be represented on a sublattice diagram (Fig. 2.4, top). The list of necessary SS end members to produce the full compositional range is then generated by taking one species per site. This leads to six end members, since 'c' includes two species and 'd' three species (Fig. 2.4, bottom). This solid solution model is termed "reciprocal", because it has two end members, $Ht31$ and $Py31$, having $CR = 3.0$, and four end members, $Ht21$, $HtPy21$, $PyHt21$ and $Py21$, having $CR = 2.0$. Reciprocity means that there are more end members than linearly independent compositional components, hence some end members can be expressed through others by so-called 'reciprocal reactions':

$Py31 + Ht21 \leftrightarrow Ht31 + PyHt21$
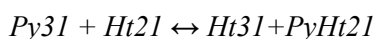
$\Delta G_{rcp}(1) = G^o_{Ht31} + G^o_{PyHt21} - G^o_{Py31} - G^o_{Ht21} = 0$
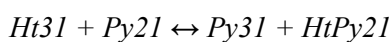
$Ht31 + Py21 \leftrightarrow Py31 + HtPy21$
$\Delta G_{rcp}(2) = G^o_{Py31} + G^o_{HtPy21} - G^o_{Ht31} - G^o_{Py21} = 0$

'a_8'	'b_3'	'c_3'	'd_1'	'h_{15}'
M	C	A F	M ACH FCH	H

Ht21	$M_8C_3A_3(ACH)H_{15}$
PyHt21	$M_8C_3F_3(ACH)H_{15}$
HtPy21	$M_8C_3A_3(FCH)H_{15}$
Py21	$M_8C_3F_3(FCH)H_{15}$
Ht31	$M_8C_3A_3(M)H_{15}$
Pv31	$M_8C_3F_3(M)H_{15}$

Fig. 2.4: *Sublattice stoichiometry diagram (top, abbreviations: M: = $Mg_2(OH)_4$, A: = $Al_2(OH)_4^{2+}$, F: = $Fe_2(OH)_4^{2+}$, C: = CO_3^{2-}, H: = H_2O), and the generated list of SS end members (bottom).*

In this study, the free energy effects of these reactions were assumed to be zero, which allowed the standard molar Gibbs energies G^o of two end members to be calculated from the fitted G^o values of the other four end members.

To fit the sublattice SS model to experimental solubility data, a stepwise approach was used.

(1) The standard molar Gibbs energies, G^o_{298}, of the $Ht31$ and $Py31$ end members were obtained from the G^o_{298} values of $Htlc$ and Pyr end members of the simple binary SS model determined previously (ROZOV, 2010). The G^o_{298} of $Ht31$ and $Py31$ end members were then kept fixed.

(2) The set of experimental co-precipitation and dissolution data for LDH solids with $CR \approx 3$ was used in a pair-wise adjustment of G^o_{298} of ($Ht21$; $PyHt21$) and ($Py21$; $HtPy21$) end members in order to keep the Gibbs energy effects of the reciprocal reactions at zero in accord with the assumptions given above. Small pair-wise changes do not produce visible effects on the calculated total dissolved concentrations $[Mg_{aq}]$, $[Al_{aq}]$ and $[Fe_{aq}]$, but strongly affect the calculated iron partitioning between the 3:1 and 2:1 components of the solid solution. The absence of any data showing preferential iron partitioning thus provides very narrow boundaries for the two fit parameters. This resulted in a good model representation of solubility data with calculated $CR = 2.97$.

(3) Without any further adjustment, the sublattice SS model was then applied to new solubility data for $CR = 2.75$, 2.5, 2.25 and 2.0. As seen from Fig. 2.5, in all cases the modelled total-scale Lippmann solubility products

$\log_{10} \Sigma \Pi_T = \log_{10}([Mg_{aq}]^a \cdot ([Al_{aq}] + [Fe_{aq}])^{(b+c)} \cdot [C_{aq}]^e) + (d - 4 \cdot (b+c)) \cdot (pH-14)$

are between the points for co-precipitation and dissolution experiments, corroborating the internal consistency of the equilibrium aqueous solid solution model. However, the number of experiments was insufficient to deduce any information about the model non-ideality at intermediate x_{Fe} and intermediate *CR* values, or to fine-tune the SS model.

This part of Konstantin Rozov's PhD thesis (ROZOV, 2010) presents, for the first time: (i) internally consistent thermodynamic constants for hydrotalcite

and pyroaurite (with carbonate anions); (ii) the application of total-scale Lippmann diagrams for plotting experimental solubility data and comparing them with the model solidus and solutus curves; and (iii) the development of a multi-site sublattice SS model for LDH phases capable of representing changes in the cationic ratios and Fe^{III} content simultaneously. The model can be further extended by incorporating other substituting cations and anions, which will be subjects for future experimental studies and developments of model fitting algorithms.
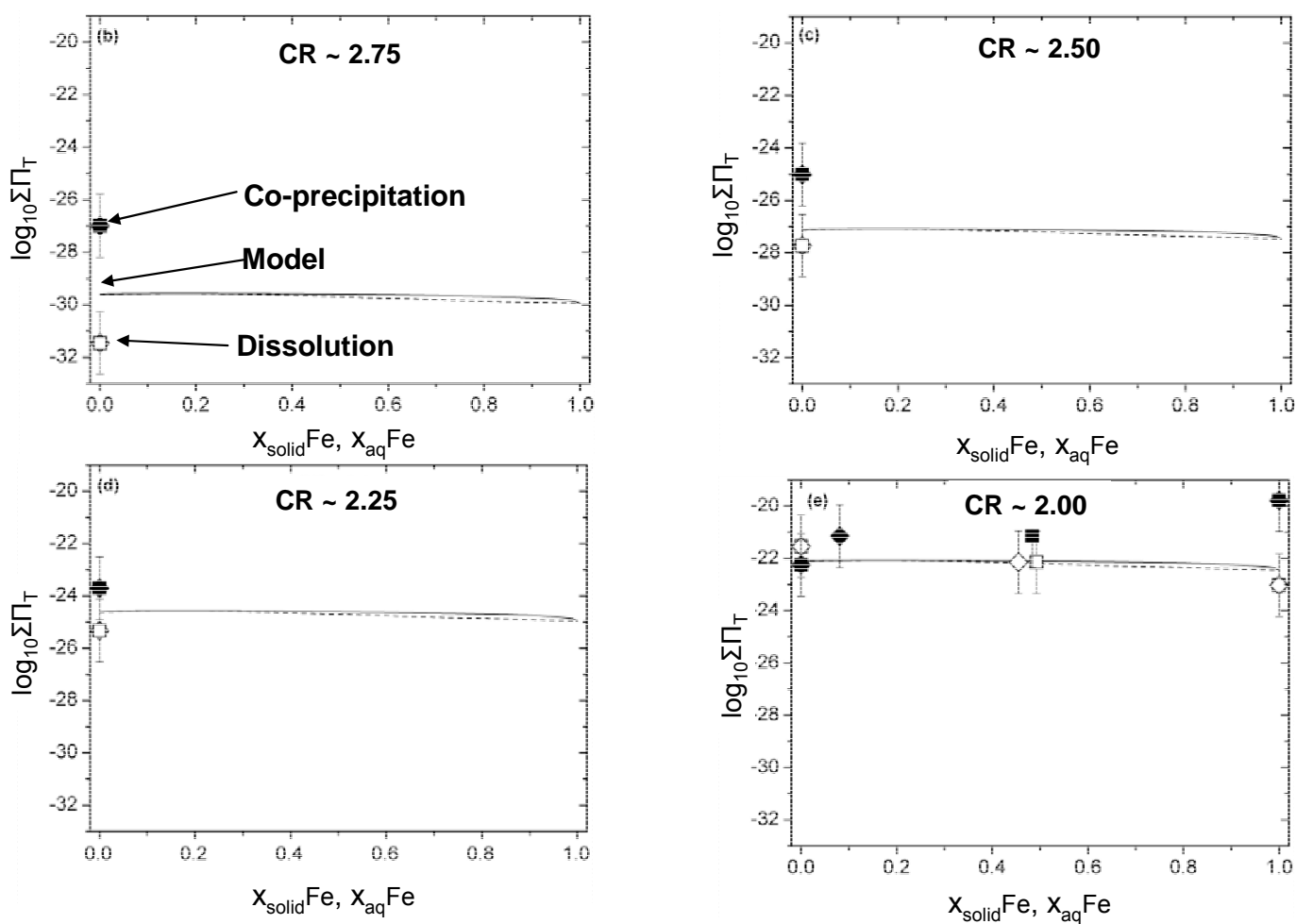
**Fig. 2.5:** *Total-scale Lippmann diagram for LDH with CR < 3. The solidus (upper) and solutus (lower) curves come from the six-end member ideal sublattice SS model (Fig. 2.4). The symbols are results from co-precipitation (filled) and dissolution (open) experiments. Squares correspond to solidus, and diamonds to solutus points. Error bars represent analytical errors on aqueous measurements.*

2.4 Thermodynamic sorption modelling

Major advances in thermodynamic sorption modelling with GEMS have been achieved with the development of theoretical conversions of intrinsic adsorption constants between different site densities, 'denticities', and concentration scales (in collaboration with J. Lützenkirchen (KIT) and T. Payne (ANSTO)). This work (KULIK et al., 2011), completed in September 2010, has also led to new arguments toward a convention on standard states for activities of surface species and sites.

Spectroscopic studies and atomistic simulations of (hydr)oxide surfaces, which show that some aqueous cations bind to two or four surface oxygen atoms, necessitate the incorporation of multi-dentate species into surface complexation models (SCMs).

The core of any SCM consists of a set of intrinsic equilibrium constants K_M^{int} for the formation reactions of surface complexes of a sorbate M. The reference states of K_M^{int} are infinite dilution of adsorbed and aqueous M, and zero surface electrostatic potential. In existing SCMs and codes, surface species may be treated on the concentration scales of molarity or molality, as a dimensionless site coverage fraction, as a relative surface concentration, as a surface mole fraction, as a relative surface density, or as molecular surface density (mol·m^{-2}). In a systematic investigation for a range of binding denticities from 1 to 4, KULIK et al. (2011) have derived the conversions of K_M^{int} values between these different surface concentration scales (Table 2.1).

For mono-dentate binding and a given site density, K_M^{int} has the same numerical value in all concentration scales. However, the use of published K_M^{int} values for multi-dentate adsorption reactions may lead to grossly erroneous results in model calculations if concentration scales are not precisely defined in both the original data fitting, and the subsequent model application. Modelling examples of applying K_M^{int} in

different SCM codes showed the magnitudes of such 'denticity effects' which can be eliminated by applying conversion factors from Table 2.1. For example, the conversion of K_M^{int} for multi-dentate binding from the molarity scale (used e.g. in the FITEQL code) to the relative surface concentration scale (used in the ECOSAT code) involves a factor which can range between 10^{-2} and 10^{-18} for typical adsorption systems.

Because sorption experiments usually yield aqueous and adsorbed concentrations of M at a given solid concentration and specific surface area, the site density and the denticity are often considered as adjustable model parameters. The reported numerical value of K_M^{int} then depends on the chosen value of the site density parameter and, in some concentration scales, on the chosen denticity. The appropriate conversion factors from one chosen site density to another, and between different denticities, are given in Table 2.2.

For future compilations of thermodynamic sorption data bases, an agreement should be reached concerning a convention on standard states for activities of surface complexes and surface sites. KULIK et al. (2011) recommend that the published K_M^{int} values should be made dimensionless and invariant to denticity and site density. Table 2.2 shows that standard states based on molarity, molality or absolute surface density concentration scales depend on both site density and denticity, and thus are inconvenient and should not be used in the future. Of the remaining concentration scales, only relative surface density is independent of both denticity and site density. Therefore, a standard state defined via a relative surface density scale at a common standard surface density Γ_o leads to equilibrium constants that are comparable between various mineral-water interfaces. However, an agreement is still needed on which value should be chosen for Γ_o.

Table 2.1: Conversion factors between intrinsic equilibrium constants $K_M^{int,\delta}$ of formation of δ-dentate surface complex of adsorbate M expressed in various concentration scales.

Scale: to / from	Molarity M, molality m	Site coverage fraction θ_δ	Relative surface concentration θ, surface mole fraction x	Relative surface density Γ/Γ_o	Surface density Γ
M (mol·L⁻¹) m (mol·kg⁻¹)	1	$\delta^1 \cdot [\equiv]_{TOT}^{\delta-1}$	$[\equiv]_{TOT}^{\delta-1}$	$\Gamma_o^{\delta-1}\Gamma_C^{1-\delta} \cdot [\equiv]_{TOT}^{\delta-1}$	$\Gamma_C^{1-\delta} \cdot [\equiv]_{TOT}^{\delta-1}$
θ_δ	$\delta^{-1} \cdot [\equiv]_{TOT}^{1-\delta}$	1	δ^{-1}	$\delta^{-1} \cdot \Gamma_o^{\delta-1}\Gamma_C^{1-\delta}$	$\delta^{-1} \cdot \Gamma_C^{1-\delta}$
θ, x	$[\equiv]_{TOT}^{1-\delta}$	δ^1	1	$\Gamma_o^{\delta-1}\Gamma_C^{1-\delta}$	$\Gamma_C^{1-\delta}$
Γ/Γ_o	$\Gamma_o^{1-\delta}\Gamma_C^{\delta-1} \cdot [\equiv]_{TOT}^{1-\delta}$	$\delta^1 \cdot \Gamma_o^{1-\delta}\Gamma_C^{\delta-1}$	$\Gamma_o^{1-\delta}\Gamma_C^{\delta-1}$	1	$\Gamma_o^{1-\delta}$
Γ (mol·m⁻²)	$\Gamma_C^{\delta-1} \cdot [\equiv]_{TOT}^{1-\delta}$	$\delta^1 \cdot \Gamma_C^{\delta-1}$	$\Gamma_C^{\delta-1}$	$\Gamma_o^{\delta-1}$	1

Notes: Conversions are given for the reaction $\delta \equiv + M = \equiv_\delta M$ representing also surface hydrolysis reactions such as
$\delta >SOH + M^x \leftrightarrow (>SO)_\delta M^{x-\delta} + \delta\, H^+$.
δ is the denticity of binding (1, 2, 3 or 4); $\equiv$ denotes 'free' surface site; $\equiv_\delta M$ is a species in which M occupies δ surface sites.
$K_M^{int,\delta}$ is taken at reference states of infinite dilution of M and $\equiv_\delta M$, and of pure surface (i.e. all sites unoccupied) for the 'free' surface site $\equiv$.
Fixed parameters: aqueous concentration $[M]$ and activity $\{M\}$; surface density Γ_M (mol m⁻²) of adsorbed M; solid concentration c_S (g L⁻¹); specific surface area A_S (m² g⁻¹); site density Γ_C (mol m⁻²) and standard surface density Γ_o (mol m⁻²).
$[\equiv]_{TOT} = c_S A_S \Gamma_C$ is the total site concentration (mol L⁻¹) in the system.
Adapted from KULIK et al. (2010).

Table 2.2: Conversions of $K_M^{int,\delta}$ from site density Γ_{C1} to Γ_{C2} and from 'denticity' $\delta1$ to $\delta2$.

Surface concentration scale	Conversion factor for site density parameter	Conversion factor for denticity
Molarity M (mol·L⁻¹) Molality m (mol·kg⁻¹)	$\left(\Gamma_{C1}/\Gamma_{C2}\right)^\delta$	$[\equiv]_{TOT}^{\delta1-\delta2}$
Surface density Γ (mol·m⁻²)	$\left(\Gamma_{C1}/\Gamma_{C2}\right)^\delta$	$\Gamma_C^{\delta1-\delta2}$
Site coverage fraction θ_δ Relative surface concentration θ Surface mole fraction x	Γ_{C1}/Γ_{C2}	1
Relative surface density Γ/Γ_o	1	1

Notes: Conversions are given for the reaction $\delta \equiv + M = \equiv_\delta M$ assuming that all properties of the system except the site density Γ_C and the denticity δ are kept constant. See also notes to Table 2.1.
Modified from KULIK et al. (2011).

2.5 Teaching activities

Teaching duties of W. Hummel as Privatdozent (PD) for "Nuclear Environmental Chemistry" at ETH Zurich included lectures and exercises on nuclear waste management within the scope of the courses "Nuclear Energy Systems" (Spring Semester 2010) and "Landfilling, nuclear repositories and contaminate sites" (Autumn Semester 2010).

D. Kulik did GEMS teaching at the PhD/postdoc level

- at the joint DMG-DGK-Helmholtz-Virtual-Institute workshop "From atomistic calculations to thermodynamic modelling", Univ. Frankfurt, Germany, 1 - 6 March 2010, see http://www.-kristall.uni-frankfurt.de/workshop/,

- at the EMU-School 2010 "Ion-partitioning in ambient temperature aqueous systems", Oviedo, Spain, 27 - 30 June 2010, see http://www.-geol.uniovi.es/emu/,

- and at the GeoSpec2010 Conference "Geochemical Speciation & Bioavailability of Trace Elements: Progress, Challenges and Future Trends", Univ. Lancaster, UK, 7 - 8 September 2010, see http://www.minersoc-emg.org/events/GeoSpec_2010.php.

2.6 References

BERNER U. (2009)
Modelling hydrated HTS cement and its porewater. PSI Internal Report AN-44-09-10.

JOHNSON L.H., NIEMEYER M., KLUBERTANZ G., SIEGEL P., GRIBI P. (2002)
Calculations of the temperature evolution of a repository for spent fuel, vitrified high-level waste and intermediate level waste in Opalinus Clay. NTB 01-04, Nagra, Wettingen, Switzerland.

KOSAKOWSKI G. (2010)
Scoping reactive transport calculations on the geochemical evolution of interfaces between concrete, Opalinus Clay and tunnel backfill materials. PSI Internal Report AN-44-10-03.

KULIK D.A., LÜTZENKIRCHEN J., PAYNE T.E. (2011)
Consistent thermodynamic treatment of multi-dentate surface complexation reactions: Intrinsic equilibrium constants. (To be submitted to Geochim. Cosmochim. Acta).

LUKAS H.L., FRIES S.G., SUNDMAN B. (2007)
Computational Thermodynamics - The Calphad Method. Cambridge University Press.

PALANDRI L.L., KHARAKA Y.K. (2004)
A compilation of rate parameters of water-mineral interaction kinetics for application to geochemical modeling, U.S Geological Survey, Open File Report 2004-1608.

PRASANNA S.V., VISHNU KAMATH P., SHIVAKUMARA C. (2010)
Interlayer structure of iodide intercalated layered double hydroxides (LDH's). J. Colloid Interface Sci. 344, 508-512.

ROZOV K. (2010)
Stability and solubility of hydrotalcite-pyroaurite solid solutions: synthesis, characterization and thermo-dynamic modeling. Inauguraldissertation der Philosophisch-naturwissenschaftlichen Fakultät der Universität Bern, angenommen den 28. Oktober 2010. 140 p.

ROZOV K., BERNER U., TAVIOT-GUEHO C., LEROUX F., RENAUDIN G., KULIK D., DIAMOND L.W. (2010)
Synthesis and characterization of the LDH hydrotalcite–pyroaurite solid-solution series. Cem. Concr. Res. 40, 1248-1254.

SCHEINOST A., SPARKS D.L. (2010)
Formation of layered single- and double-metal hydroxide precipitates at the mineral/water interface: A multiple-scattering XAFS analysis. J. Colloid Interface Sci. 223, 167-178.

SENGER R., EWING J. (2008)
Evolution of temperature and water content in the bentonite buffer: Detailed modelling of two-phase flow processes associated with the early closure period. NAB 08-32, Nagra, Wettingen, Switzerland.

WERME L, BÖRNER I.C., BART G., ZWICKY H.U., GRAMBOW B., LUTZE W., EWING R.C., MAGRABI C. (1990)
Chemical corrosion of highly radioactive borosilicate nuclear waste glass under simulated repository conditions. J. Mater. Res. 5, 1130-1146.

3 TRANSPORT MECHANISMS

S. Churakov, T. Gimmi, A. Jakob, G. Kosakowski, W. Pfingsten,
M. Hayek (postdoc), M. Tyagi (postdoc), F. Hingerl (PhD)

3.1 Overview

Geochemical and transport phenomena in the near field of HLW and L/ILW repositories are being investigated to provide scientific support for the site selection process being carried out in Stage 2 of the Sectoral Plan. Reactive transport simulations are aimed at predicting the evolution of interfaces in the repository barrier systems, and estimating the effective transport properties of radionuclides under different geochemical conditions in the repository. Inverse modelling of conventional diffusion experiments provides the radionuclide transport parameters needed in performance assessment studies.

The simulations carried out for performance assessment studies span time frames of a million years or more and thus have to be conceptually simple and numerically robust. The appropriateness of such simplified models are tested against field experiments and the assumptions made are checked against calculations performed using a more detailed mechanistic understanding of the radionuclide transport mechanisms. Knowledge on radionuclide transport and retention mechanisms is furthered by taking advantage of the unique analytical infrastructure available at PSI's large scale facilities and state-of-the-art computer simulations. Numerical codes are benchmarked, and the model capabilities extended to maintain the "correctness" of the results and conceptual quality of the system description. The supervision of PhD students and postdocs has become an integral part of the group's activities.

3.2 Activities in support of the Sectoral Plan

3.2.1 Reactive transport modelling of the geochemical evolution of L/ILW and HLW repository near fields

In co-operation with the Geochemical Modeling Group, and in continuation of last year's work, a refined reactive transport code (OpenGeosys-GEMS) was applied to modelling the long term evolution of cement/clay host rock, cement/sand-bentonite backfill and cement/bentonite backfill interfaces. Chemistry and transport are fully coupled in such simulations,

and therefore the modelling results are sensitive to the uncertainties in thermodynamic and kinetic data and relationships between porosity changes and transport parameters. Despite the uncertainties and unknowns in input parameters, these models are valuable tools which allow quantitative comparisons to be made between different scenarios for different host rocks and transport conditions. The results of such simulations, together with simplified mass balance estimations, are documented in two reports on the geochemical evolution of a L/ILW and a HLW repository.

During 2010, a systematic comparison of the evolution of cement/host rock interfaces (Effingen Member, Opalinus Clay, "Brauner Dogger", Helvetic marls) under diffusive and advective transport conditions has been completed. A typical result for a diffusive transport scenario is shown in Fig. 3.1, which illustrates the mineralogical profile over an Opalinus Clay – concrete interface after the pore space has clogged. In all of the diffusive scenarios, the porosity at the interface is reduced strongly by the precipitation of minerals with higher molar volumes. In the case shown in Fig. 3.1, these are mainly zeolites. The spread of the zones with altered mineralogy (clay dissolution in the Opalinus Clay, and portlandite dissolution in the concrete) are only a few centimeters in extent because clogging effectively prevents the diffusion of dissolved species over the interface. As clogging times are highly uncertain due to the unknown relations between porosity change and transport parameters, scenarios with constant transport parameters were investigated to obtain information on the maximum extents of mineralogical and pH changes. For the case of Opalinus Clay – concrete interactions, mineralogical changes and pH increases are limited to a zone of less than 1 meter on either side of the interface in 100000 years. All of the earlier calculations on the extent of mineralogical changes were based on much simpler mass balance estimations (e.g. NEALL, 1994). The current reactive transport models allow the uncertainties on the extent of the changes to be narrowed. By comparing the results obtained for reference and alternative scenarios, the response of the transport model to uncertainties in the model parameters can be estimated.
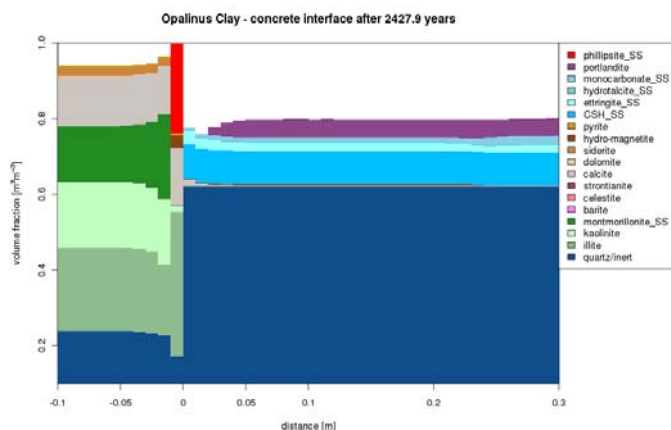
Fig. 3.1: *Mineralogical profile over an Opalinus Clay (left) - concrete (right) interface after clogging. The remaining porosity is shown in white.*
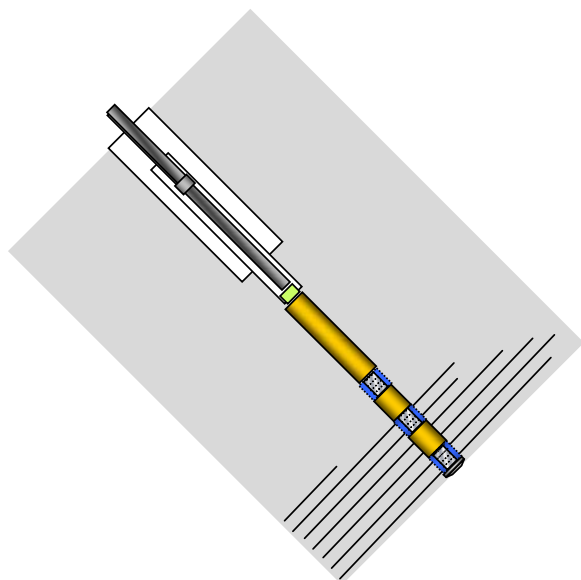

Fig. 3.2: *Sketch of the DR diffusion experiment in the Mont Terri Rock Laboratory. The drilled borehole contains several packers (black in the sketch) separating volumes (blue areas) for releasing the tracers to the surrounding rock (grey area). The borehole is perpendicular to the bedding of the clay which is indicated by parallel lines. The tracer injection volumes are lined with a porous Teflon filter to prevent disintegration of the Opalinus Clay borehole walls.*

3.2.2 Influence of sorption competition on the transport of radionuclides through compacted bentonite

Together with the Clay Sorption Mechanisms Group the influence of sorption competition on the migration of radionuclides through compacted bentonite was investigated. The 2SPNE SC/CE sorption model (BRADBURY & BAEYENS, 1997) was incorporated into the MCOTAC code. The resulting code, MCOTAC-sorb, was used to calculate Ni(II) break through curves in an 0.8 m thick compacted bentonite buffer with and without considering competitive sorption with an equilibrium Fe(II) background concentration of 5.3×10^{-5} M. Such an Fe(II) concentration is expected in real systems because the bentonite porewater is anticipated to be saturated with siderite. A constant Ni(II) input concentration of 10^{-5} M at the bentonite surface was taken. The breakthrough time for Ni(II) decreased from about 1000 years to less than 100 years when taking the Fe(II) sorption competition into account, demonstrating the importance of Fe(II) sorption competition on the migration of Ni(II). This work is part of an ongoing programme to assess the importance of competitive sorption effects in reality-near repository systems.

3.3 Data acquisition and modelling of experiments on the laboratory and field scales

3.3.1 DR experiment in the Mont Terri Rock Laboratory

The DR (Diffusion and Retention) experiment in the Mont Terri Rock Laboratory was over cored in January 2010. The experimental setup had two injection intervals with different tracer inventories. HDO, ^{18}O, ^{133}Ba, ^{60}Co, ^{137}Cs, ^{152}Eu, and stable Eu were added to the upper interval, and HTO, ^{18}O, I, Br, ^{22}Na, ^{85}Sr, Cs, ^{75}Se, and stable Se were injected in the lower interval. The injection borehole was oriented perpendicularly to bedding at an angle of about 40° with respect to the floor of the rock laboratory (Fig. 3.2). An intact core of about 2 m length and about 30 cm diameter, including the two injection intervals, was retrieved. The core was then cut with a pad saw into 4 cm thick disks. In order to limit the number of samples, and thus the effort for sampling and analysis, only one segment per disk in the central and lower part of the lower interval was initially sampled, assuming a radially and vertically symmetric migration of the tracers.
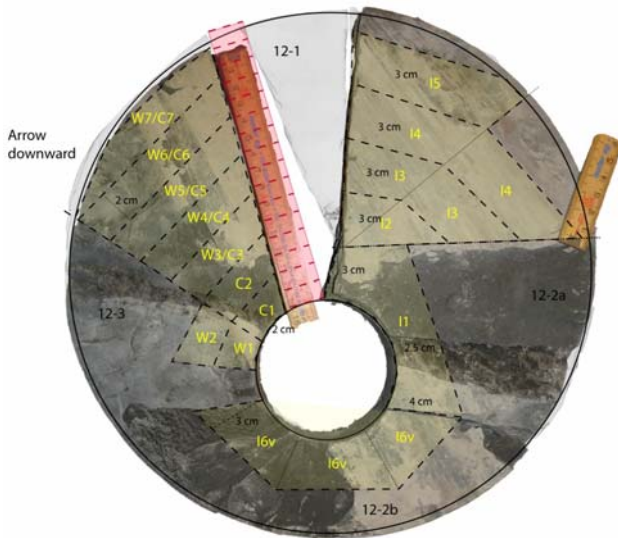
Fig. 3.3: One of the 4-cm thick disk samples from the lower interval of the DR experiment. The red areas show the positions of the 77 centimetre-sized samples for HTO and ^{22}Na determinations in this disk. The yellow areas show the larger samples taken for I and Br.

In the case of the upper interval with more strongly sorbing tracers, only the central part of the interval was sampled. Fig. 3.3 shows the disks from the lower interval from which the subsamples were taken for analysis of the active tracers at PSI (J. Eikenberg) and of some inactive tracers at the University of Bern (RWI, in co-operation with H.N. Waber).

The first data analysis has indicated that the vertical position of the intervals within the core was slightly displaced upward relative to the reference coordinate system during the over coring. The displacement was confirmed by a second sampling of the upper part of the lower interval three months later. As a result, the data do not include the central part of the interval, but extend further into the unaffected background.

Fig. 3.4 shows the HTO distribution around the lower interval obtained from the 77 samples taken. The data evaluation is not yet finished, partly because of the very long counting times required for the low activities. First comparisons with model predictions based on parameters obtained in previous experiments in the Mont Terri Rock Laboratory show a reasonable agreement with the measurements which can be further improved with slight parameter adjustments. More detailed evaluations and interpretations of these data, as well as of those of the sorbing active and the mobile inactive tracers measured at PSI and elsewhere, are still ongoing.
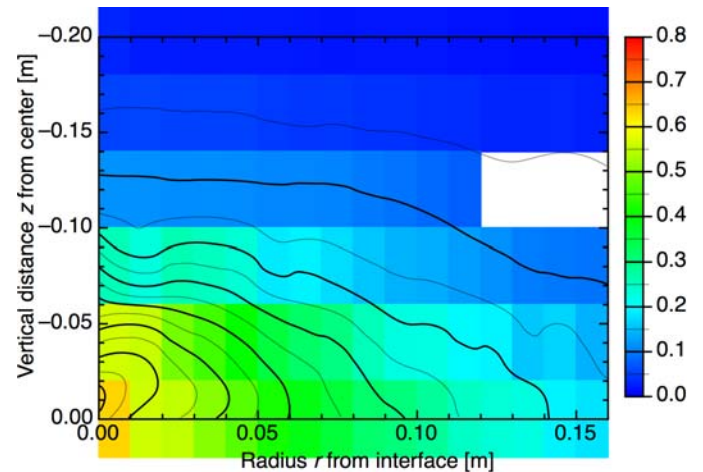

Fig. 3.4: Measured two-dimensional distributions of the mobile tracer HTO around the lower interval, obtained from the several disks of the core.

3.3.2 Estimations of the uncertainty in the modelling of the DR experiment caused by the reduction of the spatial dimensions in the transport model

Argillaceous rocks are inherently heterogeneous with regard to their composition and texture at various scales. Direct consideration of complex sample heterogeneity in transport modelling is often hampered either by a serious lack of data which are needed for a given model, or by large uncertainties in the data itself. Hence, model simplifications are, in most cases, inevitable. Such model simplifications often involve a reduction in the spatial dimensions, because this considerably reduces the simulation time and also simplifies the handling and interpretation of the result.

Considering the experimental layout of the Mont Terri DR experiment (Fig. 3.2), at least 2D axial-symmetric calculations or even a full 3D description have to be applied for an adequate representation of anisotropic solute diffusion. The primary source of the experimental information during the experiment was the tracer concentrations in the borehole. After the over coring, the spatial distribution of some tracers around the injection interval was available as well, but a full sampling of the adjacent rock was not feasible on technical and cost grounds. The concentrations within the borehole were supposed to be homogeneous throughout the injection interval because of the continuous fluid circulation within the interval from the surface tank. In such a case, a 2D axial-symmetric representation would be sufficient.
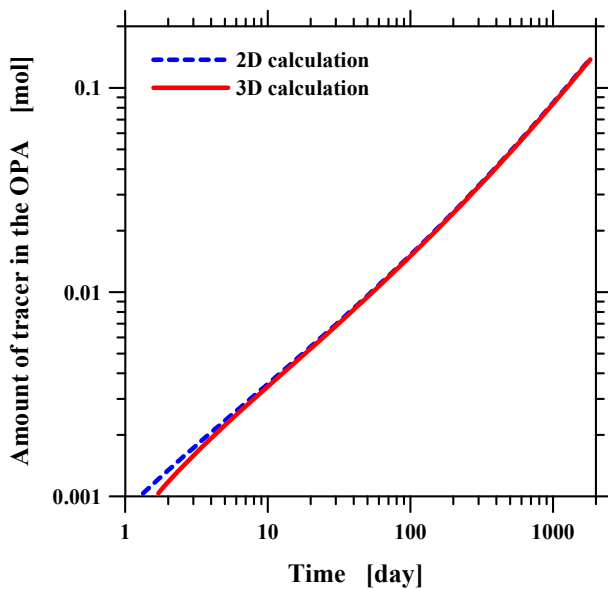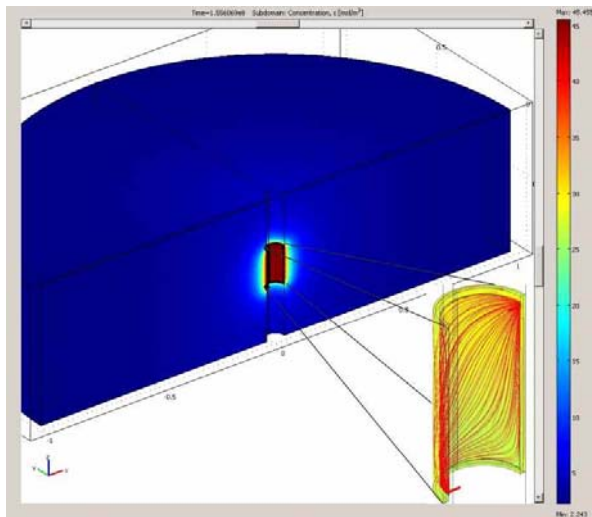
Fig. 3.5: *The upper sub-figure shows the HTO distribution in a cylindrical section of the Opalinus Clay (section radius = 1 m) after five years close to the packered volume obtained from a 3D calculation in the frame of the DR experiment in the Mont Terri Rock Laboratory. The insert shows the streamlines (red) in both void spaces and the porous Teflon filter after reaching steady state hydraulic conditions. Artificial porewater and, subsequently, dissolved tracers are released at the upper right and collected in the lower left tube of a packered section of the borehole.*
The lower sub-figure shows the temporal evolution of the total amount of HTO being accumulated in the OPA applying a 2D- and a 3D-model. Only at early times are there some systematic deviations between the two models.

However, the fluid was injected at a single point and withdrawn from a point on the opposite side of the bore hole, which may, in principle, lead to inhomogeneous concentrations. A full 3D numerical modelling, including the small asymmetries of the injection system, was thus considered as desirable in order to estimate the uncertainties in the tracer concentrations in the borehole and in the rock associated with the simplification of the spatial model dimensions.

For this purpose a series of 3D, 2D and 1D model calculations were performed with carefully chosen parameters. The results of 2D and 3D simulations of the mixing tank in the injection interval, and the time dependent uptake of a conservative tracer (HTO) by the host rock, are shown in Fig. 3.5. The simulations indicate that, except for very early times, a 2D axial-symmetric model is sufficient for the analysis. However, for stronger sorbing radionuclides where tracer uptake by the Opalinus Clay will happen preferentially close to the release point (i.e. right upper tube), such a model simplification might not be justifiable any longer; this issue is presently under investigation.

3.3.3 Inverse modelling of Cs in-diffusion experiments with samples from Mont Terri and Benken under different confining pressures

After the successful application of a coupled multi-species transport model to the Cs through and out-diffusion experiment in a clay sample from Mont Terri (JAKOB et al., 2009), four additional Cs through diffusion experiments in clay samples from Mont Terri and Benken under different confining pressures have been successfully modelled with MCOTAC in co-operation with the Diffusion Processes Group.

To reproduce the through diffusion experiments for the Mont Terri clay sample under 4 MPa confining pressure, only a small modification to the pore diffusion coefficient (from 9.5×10^{-10} $m^2 s^{-1}$ to 8.5×10^{-10} $m^2 s^{-1}$) and an 8% increase of the site capacity with respect to the parameters used to model the Cs diffusion experiment through a Mont Terri clay sample at a confining pressure of 1MPa, were necessary (Fig. 3.6). Such a minor adjustment of the diffusion coefficient is within the error of the diffusion measurements. Similarly, an 8% change in the site capacity is within the uncertainty of the measured illite content in the clay.
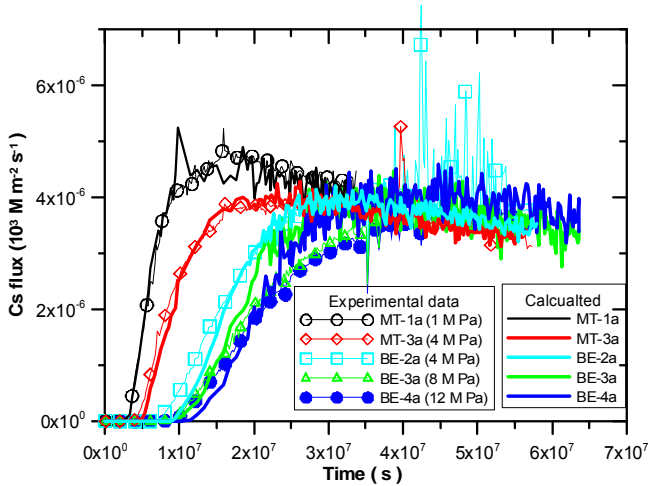
Fig. 3.6: *Calculated Cs breakthrough curves versus experimental data for MT-1a, MT-3a, BE-2a, BE-3a, BE-4a diffusion experiments.*

For the through diffusion experiments with clay samples from Benken under 4, 8 and 12 MPa confining pressure, and adjustments for the Benken clay specific parameters i.e. porosity, illite content and porewater composition, the fitted pore diffusion coefficient for these three samples was between 1 and 2×10^{-10} $m^2 s^{-1}$, i.e. a factor of four lower than for the Mont Terri samples. (Note that the porewater composition had the major influence on the calculated breakthrough curves.) As an additional independent parameter, the Cs mass balance in the reservoir was monitored. Fig. 3.7 illustrates the good agreement between calculated and measured Cs concentrations in the reservoir.
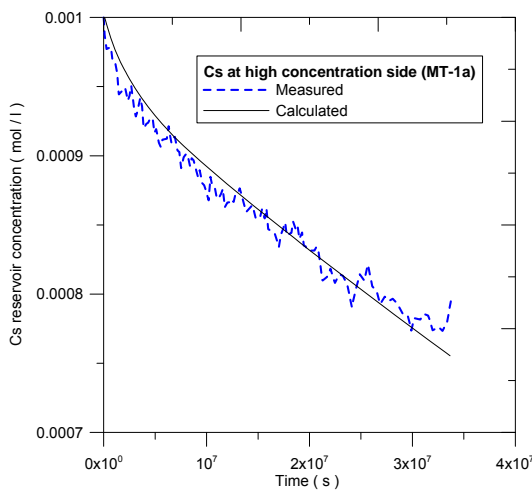

Fig. 3.7: Calculated and measured Cs concentrations in the reservoir for MT-1a experiment.

3.3.4 Diffusion of strongly sorbing radionuclides in OPA: The new filter-free experimental setup and the influence of metal background concentrations

New laboratory in-diffusion experiments with strongly sorbing radionuclides (see Diffusion Processes Group) will be performed using an experimental setup without filters. This setup should avoid the difficulty of quantifying sorption of radionuclides on filters. For such a setup, 1-2 cm long cylindrical clay samples are in contact with a radionuclide tracer solution within a large reservoir; the rest of the cylindrical sample is protected from the solution by an epoxy resin sleave so that one-dimensional radionuclide in-diffusion into the cylinder can be assumed for a nearly constant radiotracer concentration in the solution reservoir. Background concentrations of stable isotopes in the porewater can influence the transport of radionuclides in such experiments (stable carrier is competing with radioisotope for sorption site). All relevant concentrations have to be known for a correct modelling/interpretation of the experimental diffusion data. Unfortunately, in many diffusion experiments these magnitudes remain ill defined. Therefore, the potential effects of "background concentrations" on the diffusion of radionuclides in clay systems has been assessed based on generic calculations.

The calculations were performed for different background concentrations in the porewater and carrier concentrations for the tracer using a multi-site sorption model for Cs, Ni, Co (BRADBURY & BAEYENS, 2005). The simulations indicated faster in-diffusion with increasing background concentration of stable isotopes within the sample (Fig. 3.8). Thus the background isotope concentration in the porewaters needs to be known.
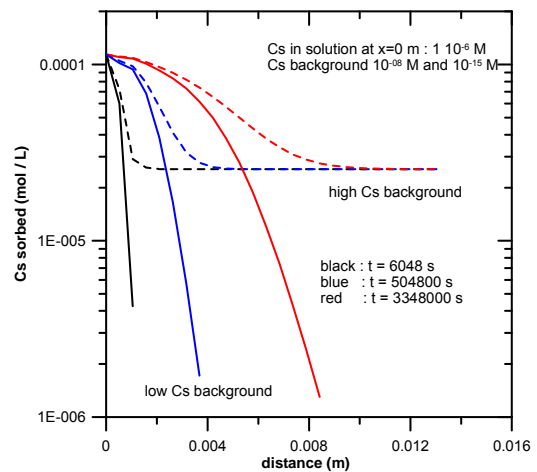

Fig. 3.8: *Cs concentration profiles for different background Cs concentrations in OPA.*

3.4 Understanding radionuclide transport and sorption mechanisms

3.4.1 Effects of heterogeneous mineral distributions on solute transport

Diffusion in natural porous media has so far mainly been studied in laboratory scale experiment assuming that the transporting medium is homogeneous and isotropic. Usually, the diffusion is monitored through the mass flow entering or leaving a sample as a function of time or, in the case of strongly sorbing tracers, by measuring the diffusion profile in the sample. Conventional interpretations of these experiments are based on the classical Fickian laws.

Natural rocks are far from being homogeneous and isotropic. Rather, they are composites of several mineral phases with potentially different transport properties. Nathalie Diaz, a postdoc, has been investigating the effect of spatial mineralogical heterogeneities on Cs diffusion in Opalinus Clay. In this project the Cs transport was monitored in situ using a micro-tomography technique available at the PSI-TOMCAT beam line. With such a non destructive technique, data on both the mineral distribution and the time resolved special propagation of Cs in the same sample can be acquired. Measurements were made on a $692 \times 692 \times 1182$ mesh with 3 μm spatial resolution. Each cell of the mesh was assigned the transport properties corresponding to the mineral phase present. The clay phase was treated as the phase in which caesium diffused while calcite was considered to be an impermeable material. Transport simulations, under the same conditions as the diffusion experiment, were performed on an equivalent $692 \times 692 \times 1182$ mesh using an "in-house" random walk code. The sorption was taken into account by using linear and non-linear sorption isotherms. The transport parameters for the clay fraction were estimated from experimental results. The simulations with the linear sorption isotherm overestimated the penetration of the caesium into the sample. The non linear sorption isotherm gave a sharper profile and allowed the experimental diffusion profile time series to be reproduced fairly well (Fig. 3.9).
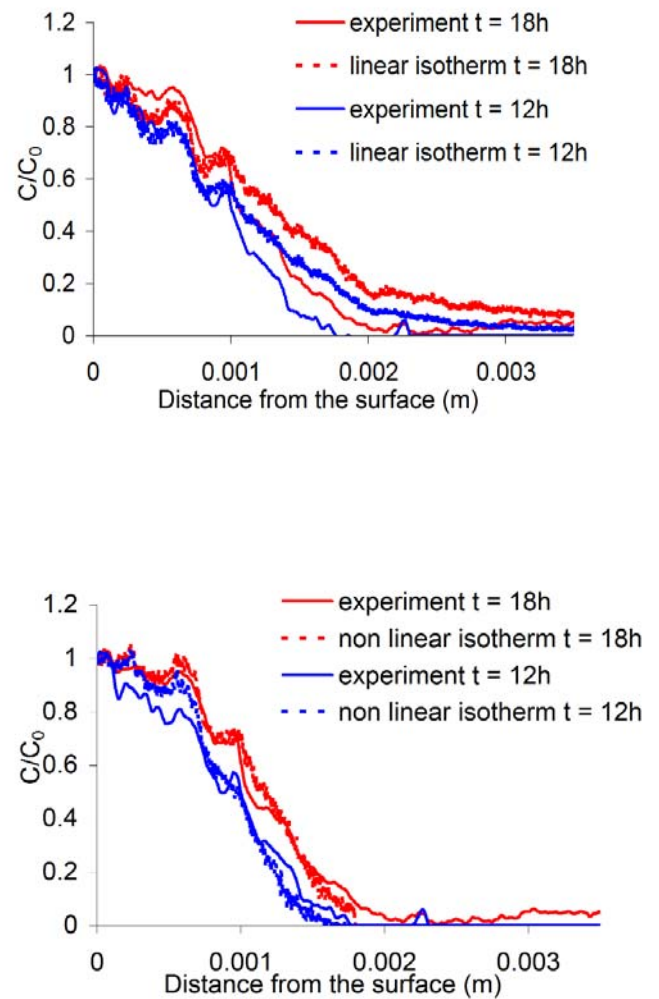
Fig. 3.9: Integral 1D Cs profile in the sample of OPA clay derived from measured 3-D Cs distributions in the sample and the modelling using a 3-D setup with linear (top) and nonlinear sorption (bottom) models. The uncertainties in the measured Cs concentrations are about 20 % of C_0.

Both sets of profiles (experimental and simulated) show variations in the concentrations which deviate from the smooth classical shape of the diffusion profile in a homogeneous porous media. The spatial Cs distributions showed "fingering" which correlated with the clay fraction domains (Fig. 3.10).

The variations were thus related to the spatial mineral distributions, in particular the clay mineral distribution in the sample.

Simulation

Experimental
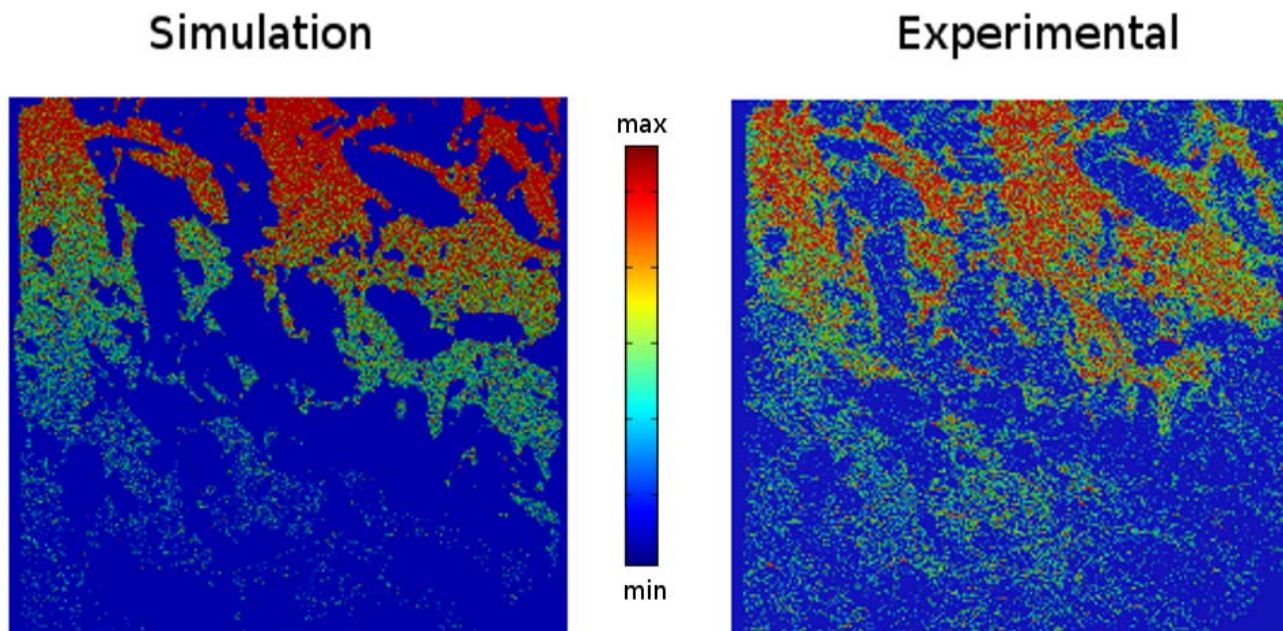
Fig. 3.10: *Comparison of the simulated and measured Cs distributions in 2-D for a radial slice through the sample.*

3.4.2 Influence of clay particle arrangement on molecular diffusion coefficients in clays

The diffusion of dissolved components through clays results from the Brownian motion of molecules and ions in the solution and from their interaction with the surface of the solid medium. At the scale of a single pore, these molecular phenomena can be modelled by molecular dynamics (MD) simulations. At the scale of a few centimeters, which is typically of interest for continuum simulations of the diffusive spreading of contaminants through clay barriers, such molecular simulations are no longer feasible. Instead, the corresponding diffusion coefficients are most often empirically determined from time-consuming experiments. To address the up-scaling problem, a two-step simulation approach has been developed which enables macroscopic diffusion coefficients of water and ions to be derived from pore scale molecular diffusion coefficients. The starting point for the up-scaling procedure are local pore diffusion coefficients derived in molecular dynamics simulations for specific local environments, such as the interlayer or edge regions of clay particles (see Fig. 3.11). These local diffusion coefficients are then assigned to different types of porosity in a model clay structure. The structure-averaged diffusion coefficient of the sample is obtained by random walk simulations for a complex, larger-scale structure (Fig. 3.11).
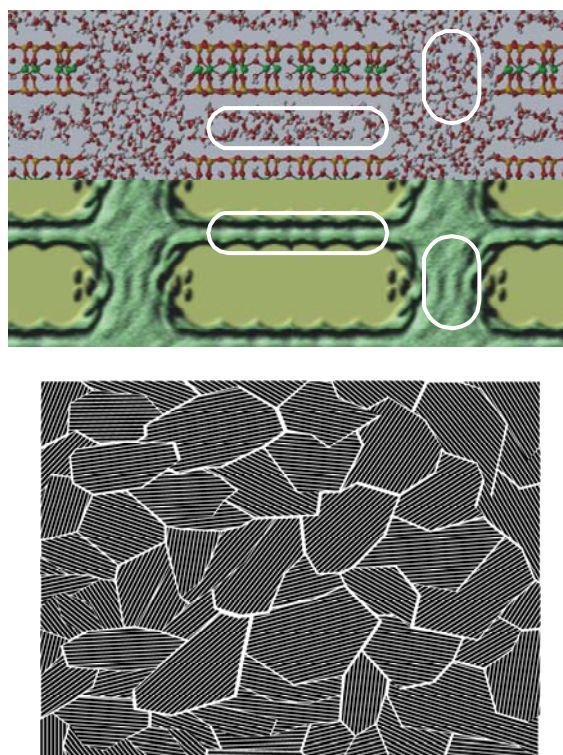
Fig. 3.11: *Top: Local diffusion coefficients are obtained for specified pore regions from MD simulations. Bottom: These local diffusion coefficients are then attributed to corresponding areas in a larger-scale structure consisting of several clay particles with stacks of interlayers. The sample-scale diffusion coefficient is then obtained by random walk simulations.*

The accuracy of the proposed approach has been demonstrated by comparing the results of direct larger-scale molecular simulations for a stack of pyrophyllite nano-particles with the two-step up-scaling approach. Following this, the effect of mineralogical heterogeneities and anion exclusion on the larger-scale diffusion coefficients is being investigated for a model clay structure which resembles a typical clay material. This up-scaling concept is general, and can be used for up-scaling molecular diffusion coefficients for porous materials with arbitrarily complex structures.

3.4.3 Nature of Zn sorption sites on the edges of montmorillonite from atomistic simulations and EXAFS measurements

On the macro-scale, the sorption of divalent transition metals such as Ni and Zn on clay minerals and argillaceous rocks is commonly described using the 2SPNE SC/CE sorption model (BRADBURY & BAEYENS, 1997). Recently, a set of sorption experiments were performed under carefully selected conditions to obtain montmorillonite samples with Zn loadings predominantly on the strong sites or on the weak sites, respectively (DÄHN et al., 2011). These samples were used to obtain the P-EXAFS spectra of Zn adsorbed on montmorillonite on these two sites (see section 4. Clay Sorption Mechanisms).

Density functional theory (DFT) based atomistic calculations has been applied to model the P-EXAFS spectra of Zn^{2+} adsorbed on montmorillonite, and to explain the molecular structure of these Zn^{2+} complexes. Two major sorption mechanisms have been examined: structural incorporation into external cationic sites of the edges and surface complexation on the edges. The structure of incorporated Zn^{2+} complexes was obtained from a set of ab initio lattice optimizations which were performed for different edge surfaces and the structural polymorphs of montmorillonite neglecting water dynamics near the edges. The structure and complexation mechanism of aqueous Zn^{2+} complexes on the edges of montmorillonite were obtained from a set of umbrella sampling ab initio MD simulations in NVT ensemble at 300K, explicitly taking into account the dynamics of water near the interface. Theoretical EXAFS spectra were calculated from ab initio MD trajectories with FEFF 8.40 and were used to model measured EXAFS data for montmorillonite samples with Zn^{2+} in "weak" and "strong" surface complexes.

In contrast to traditional EXAFS data analysis, such as "shell models", the EXAFS spectra simulations were based on 3D molecular structures predicted by atomistic modelling. In this type of analysis, multiple scattering effects and 3D structural relaxation around absorbing and scattering atoms is fully taken into account. The inter-atomic distances are constrained by atomistic simulations, and are not used as fitting parameters. Instead, a weighted sum of EXAFS spectra from different structural complexes, which is the most consistent with measured EXAFS data, is sought. In this way, the contribution from different surface complexes can be discriminated. This can not be achieved with the conventional shell fitting approach (Fig. 3.12).
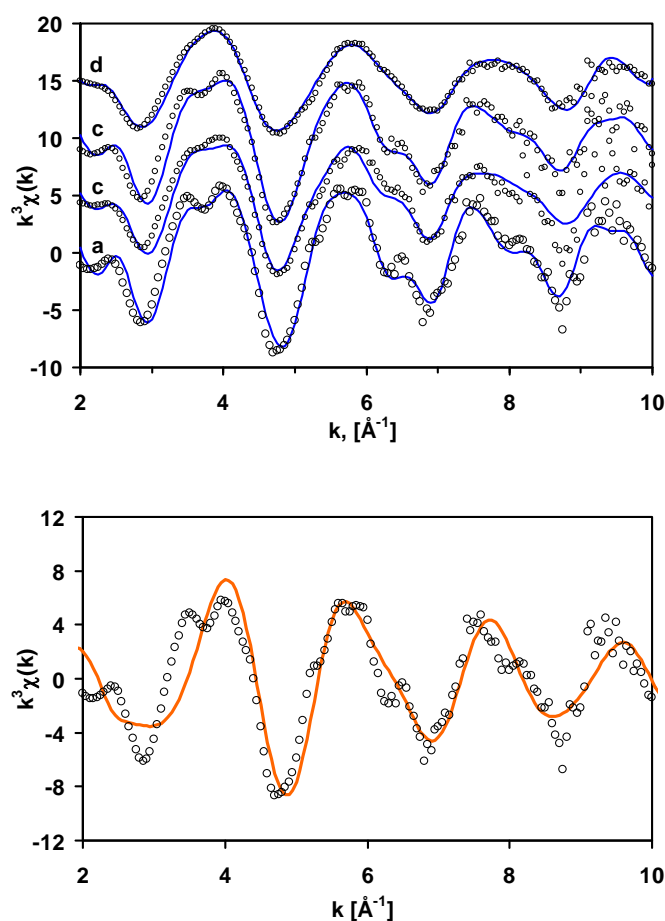
Fig. 3.12: Top: Modelled (blue lines) and measured (black circles) EXAFS spectra of Zn in montmorillonite (DÄHN et. al., 2011). (a) 100 % incorporated; (b) 50 % incorporated 50 % adsorbed on strong sites; (c) 10 % incorporated 90 % adsorbed on strong sites; (d) 7 % adsorbed on strong sites and 93 % adsorbed on weak sites; Bottom: Shell model fit (red line) for the Zn incorporated in montmorillonite, is given for comparison. The conventional shell model fails to reproduce split of the first peak characteristic of multiple scattering.

The results of the molecular simulations are consistent with the former view on the nature of "weak" and "strong" sites inferred from conventional EXAFS modelling and wet chemistry data and a macroscopic sorption model. The measured EXAFS spectra of "weak" surface sites can be explained by mono- and bi-dentate Zn complexes attached to Al-O and Si-O sites on the edge of the TOT sheet. The strong sites can only be explained by cations incorporation in the clay structure. These complexes may form as result of surface defect healing on the clay edges. The analysis of the MD trajectories explains the mechanism of Zn^{2+} absorption on the clays surface and corresponding changes of the surface structure of the clay edges.

3.5   Benchmarking of coupled codes

3.5.1   2D COMEDY benchmark

The PhD project of Haibing Shao, conducted in co-operation with the Department of Environmental Informatics at the Helmholtz Centre for Environmental Research – UFZ Halle-Leipzig, Germany (Prof. O. Kolditz), finished successfully in July 2010. In this project the coupling of the in-house GEMS-PSI code with the transport code OpenGeoSys (http://www.ufz.de/), being developed at the UFZ, was set up.

Benchmarking of the coupled OpenGeoSys-GEMS is an ongoing task. This year this activity concentrated on the COMEDY2D benchmark published by COCHEPIN et al. (2008) which describes a system with strong couplings between hydraulics, transport and chemistry via spatial and temporal changes of the pore space. OpenGeoSys-GEMS was able to successfully reproduce the qualitative behaviour of the defined system (Fig. 3.13). Also, it was seen that different implementations of (chemical) kinetic models strongly influenced the system, in accord with the observations of COCHEPIN et al. (2008).
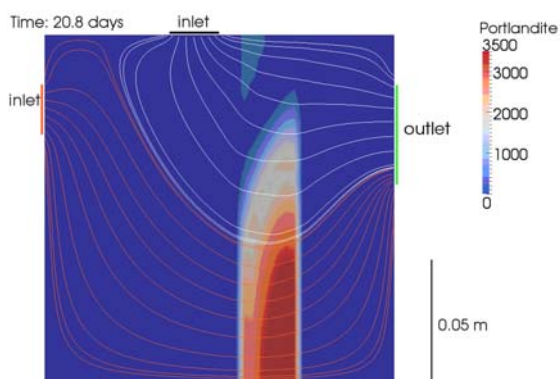
Fig. 3.13: *Comedy 2-D benchmark: Portlandite dissolution at 20.8 days after injection of Na-oxalate in the upper inlet.*

3.5.2   Feedback of porosity change on transport: Analytical solution versus numerical simulations

The transport of a chemically reactive fluid through a porous medium is governed by many kinds of chemical interactions. Heterogeneous reactions such as dissolution/precipitation can modify the aquifer properties (i.e. porosity and hydraulic conductivity). Recently, clogging (i.e. the strong reduction of porosity) has received special attention. There are numerous claims that reactive transport codes have accurately solved the reaction transport problem with feedback on porosity. However, virtually no analytical results are available to test the accuracy of numerical codes. Available analytical and semi-analytical solutions are only applicable in the case of constant hydrodynamic and transport properties, or in the case of small variation in these properties, and thus cannot be used to investigate problems with strong porosity changes (i.e. clogging).

Mohamed Hayek, a postdoc, used the "Simplest Equation Method" to derive analytical solutions for coupled reactive transport problems in which there is feedback of strong porosity changes (HAYEK et al., 2011). For reaction schemes of the form A+B↔M(s), the solutions permit solute concentrations, spatial distributions of a mineral and porosity evolution to be calculated. The solution is valid for initial and boundary conditions defined by a set of arbitrary functions and parameters which offer a framework for adapting closed-form system definition.
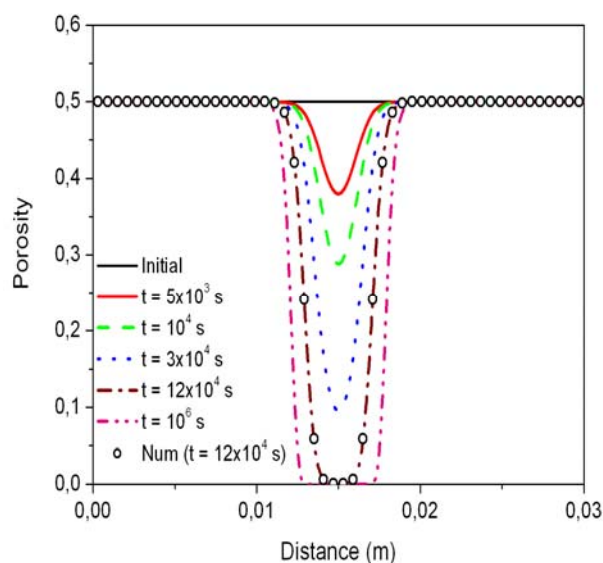
Fig. 3.14: *Porosity evolution for successive time intervals and the numerical solution at $t=12 \times 10^4$ seconds for an example where the precipitation of anhydrite is induced.*

The obtained analytical solutions are exact, explicit in space and time variables, and do not contain any approximations. These analytical solutions can be used for benchmarking numerical codes. In addition, partial differential equations representing conservation of mass using an implicit finite volume technique have been solved. Good agreement has been obtained between the numerical solutions based on a fine discretisation of the domain and the corresponding exact solutions (Fig. 3.14).

3.5.3 Fluid-rock interaction modelling

Several geochemical models have been included into the GEM-Selektor code in the framework of the GEOTHERM project (Ferdinand Hingerl, PhD). These models enable the chemical speciation and the equilibrium assemblage to be modelled in geothermal fluids circulating in an Enhanced Geothermal System. In 2009, two activity models suitable for computations at elevated temperature, high pressure and high salinity, namely the Pitzer and the EUNIQUAC model, were implemented into the GEMS-Selektor code. These models were subsequently subjected to benchmarking studies, in which the "quality of fit" relative to existing model implementations, as well as measured data from different sources, was investigated.

Contrary to expectations, the EUNIQUAC model, chosen as an alternative to the classical Pitzer approach, did not provide results with the necessary accuracy for reactive transport calculations. In order to keep the advantageous structural framework of the EUNIQUAC approach (substantially fewer parameters required and a simple temperature dependency), and, at the same time to enhance the accuracy, a revised version of the EUNIQUAC model named ELVIS was developed. The EUNIQUAC model, which has been in common usage since its re-formulation by Thomsen almost two decades ago (THOMSEN, 1997), consists of three terms. The first one takes into account long-range ion-ion interactions which are screened by the solvent, which is treated as a continuous dielectric. This very simplified Debye-Hückel term was derived for a pure NaCl solution at 25°C, 1 bar and is neither temperature nor pressure corrected. Short-range ion-ion, and explicit ion-solvent interactions, are treated by a temperature dependent residual term, and a temperature independent combinatorial term. Both of the latter terms are based on statistical mechanical considerations and, if used without the Debye-Hückel term, can be directly correlated to physical parameters when applied to solvent-solvent mixtures. Introducing a semi-analytical term which explicitly treats ion-

solvent interactions, as well as applying a more rigorous Debye-Hückel formulation adapted to multi-electrolyte solutions for the ion-ion interactions, significantly resolved the accuracy deficiencies of the EUNIQUAC model (Fig. 3.15). The modified EUNIQUAC model, called ELVIS, has significantly less fitting parameters than the Pitzer approach and is clearly superior to the EUNIQUAC in terms of the quality of the fits (Fig. 3.15).

The new ELVIS activity model was applied to characterise the chemical composition of fluid at the Soultz geothermal site. In a next step the ELVIS model will be benchmarked with the Pitzer and the EUNIQUAC approach in reactive transport simulations. Incorporation of such a robust activity model for highly saline systems in the OpenGeoSys-GEMS reactive transport code opens up the possibility of applications in performance assessment to systems with high porewater salinities (e.g. Effingen Member).
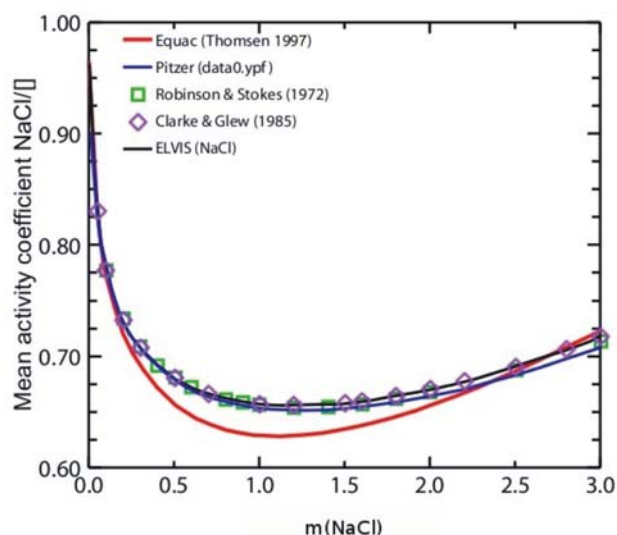
Fig 3.15: *The mean activity coefficient of NaCl in aqueous solution at 25°C, 1 bar as a function of the electrolyte concentration. Red cubes and violet diamonds represent two different sources of reference values for mean activities (ROBINSON & STOKES, 1972 and CLARKE & GLEW, 1985 respectively). The black curve shows the fit of the Pitzer model (database data0.ypf from PHREEQC) and the green curve the values given by EUNIQUAC (parameters from the PhD thesis of THOMSEN, 1997). The blue curve represents the fit of the ELVIS model. Especially in the geochemically highly relevant molality range 0.5 to 1.5 the ELVIS model prevails over the EUNIQUC approach with respect to accuracy.*

3.6   Forthcoming projects

Manav Tyagi, a postdoc fully financed by FK-PSI, joined the group in July 2010. He is working on clay microstructure modelling and pore-scale simulations of ion transport in clays (see. 3.4.2).

In co-operation with EMPA, EPFL and ICB-Dijon a research proposal on "The thermodynamics of amorphous Calcium-Aluminum-Silicate-Hydrate phases", (Project coordinator: B. Lothenbach, EMPA) in the framework of Sinergia SNF program was submitted. The project has received financial support for 3 PhDs in EMPA, EPFL, ICB-Dijon and 1 postdoc shared between ICB-Dijon and PSI. The new postdoc fellow, Luis Pegado, started at PSI on November 2nd, 2010.

3.7   References

BRADBURY M.H., BAEYENS B. (1997)
A mechanistic description of Ni and Zn sorption on Na-montmorillonite. Part II: Modelling. J. Contam. Hydrol. 27, 223-248.

BRADBURY M.H., BAEYENS B. (2005)
Modelling the sorption of Mn(II), Co(II), Ni(II), Zn(II), Cd(II), Eu(III), Am(III), Sn(IV), Th(IV), Np(V) and U(VI) on montmorillonite: linear free energy relationships and estimates of surface binding constants for some selected heavy metals and actinides, Geochim. Cosmochim. Acta 69, 875-892.

CLARKE E. C.W. GLEW D.N. (1985)
Evaluation of the thermodynamic functions for aqueous sodium-chloride from equilibrium and calorimetric measurements below 154-degrees-c. J. Phys. Chem. Ref. Data 14, 489-610.

COCHEPIN B., TROTIGNON L., BILDSTEIN O., STEEFEL C., LAGNEAU V., VAN DER LEE, J. (2009)
Approaches to modelling coupled flow and reaction in a 2D cementation experiment. Adv. Water Resourc. Res. 31, 1540-1551.

DÄHN R., BAEYENS B., BRADBURY M.H. (2011)
Investigation of the different binding edge sites for Zn on montmorillonite using P-EXAFS – the strong/weak site concept in the 2SPNE SC/CE sorption model. Geochem. Cosmochim. Acta (submitted).

HAYEK M., KOSAKOWSKI G., CHURAKOV S. (2011)
Exact analytical solution for coupled reactive transport problem with feedback of porosity change. Water Resourc. Res. (submitted).

JAKOB A., PFINGSTEN W, VAN LOON L.R. (2009)
Effects of sorption competition on caesium diffusion through compacted argillaceous rock. Geochim. Cosmochim. Acta 73, 2441-2456.

NEALL F. (1994)
Modelling of the near-field chemistry of the SMA-repository at the Wellenberg Site: Application of the extended cement degradation model. NTB-94-03, Nagra Wettingen, Switzerland.

ROBINSON R.A., STOKES R.H. (1972)
Electrolyte solutions 2nd edition. Butterworths, London, p. 572.

THOMSEN K. (1997)
Aqueous electrolytes: model parameters and process simulation. PhD Thesis, Department of Chemical Engineering, Technical University of Denmark, p.131.

4 CLAY SORPTION MECHANISMS

B. Baeyens, M.H. Bradbury, R. Dähn, M. Marques-Fernandes, V. Kalbermatter, A. Schaible,
D. Soltermann (PhD), T. Ishidera (guest scientist)

4.1 Overview

A large part of the work performed in the Clay Sorption Mechanisms Group in 2010 was devoted to activities directly related to the Sectoral Plan for Deep Geological Disposal. This work involved the development of sorption data bases (SDBs) to be delivered in Stage 2 of the Sectoral Plan for the selected host rocks, namely, Opalinus Clay, "Brauner Dogger", Effingen Member and Helvetic marls. An experimental programme on the sorption of key radionuclides on Effingen Member has started. The main activities are briefly listed below.

- The methodology to generate SDBs for argillaceous rock systems has been documented in BRADBURY et al. (2010) and this method will be used to compile specific SDBs for the above mentioned host rocks.

- The validity of the approach was tested by comparing and contrasting the sorption values, obtained with this method, with those in already existing SDBs for Opalinus Clay and MX-80 bentonite (BRADBURY & BAEYENS, 2010).

- Sorption measurements of Cs(I), Sr(II), Ni(II), Co(II), Eu(III), Th(IV) and U(VI) have been performed on rock samples of Effingen Member in the "low salinity" reference porewater. The results of the sorption measurements have been compared with blind predictions.

Mechanistic sorption studies on clay minerals are on going activities. The main topics of work in the current year were:

- A combined wet chemistry and polarized extended X-ray absorption fine structure (P-EXAFS) spectroscopy study on Zn(II) uptake on montmorillonite. The aim was to investigate the strong site/weak site hypothesis in the 2SPNE SC/CE sorption model.

- P-EXAFS was used also to obtain a more detailed knowledge of the U(VI) inner sphere surface complexes formed on montmorillonite.

- A modelling study on the reactive transport of Ni(II) through compacted MX-80 bentonite considering competitive sorption from Fe(II) was completed (PFINGSTEN et al., 2010).

Sorption measurements of Cs(I) and Ni(II) have been carried out on MX-80 bentonite originating from the ABM (Alternative Buffer Material from the Äspö Hard Rock Laboratory) experiment and reference MX-80 at 25 ºC and 90 ºC.

A new redox glove box, with an integrated ultracentrifuge, fully financed by Nagra, was commissioned in 2010, and the necessary safety reports were provided and approved by Ensi.

On the 1st August 2010 Daniela Soltermann started her PhD project entitled *"The influence of Fe(II) on clay properties, the sorption of Fe(II) on clays and competitive sorption investigations: a combined macroscopic and microscopic study"*.

LES and the Health and Environmental Physics Department (Hungarian Academy of Sciences, KFKI Atomic Energy Research Institute) have concluded an agreement on a joint programme of work in connection with the Schweizer Erweiterungsbeitrag, DEZA/SECO. The project entitled *"Development of a macro- and microscopic approach to investigate the geochemistry of radioactive waste disposal systems"* started on October 15, 2010 and will last for 3 years.

4.2 Activities in support of the Sectoral Plan

4.2.1 Sorption data bases for argillaceous rocks

In some previous work related to Stage 1 of the Sectoral Plan, sorption data bases (SDBs) were derived for argillaceous, calcareous and crystalline generic rock types (BRADBURY et al., 2008). The main factors influencing sorption on argillaceous rocks were shown to be the phyllosilicate mineral content (particularly 2:1 type clays: illite/smectite/illite-smectite mixed layers) and the porewater chemistry. Based on this work a methodology was developed for producing SDBs for argillaceous rocks which was documented in BRADBURY et al. (2010).

The intention is to use this methodology in Stage 2 of the Sectoral Plan to develop SDBs for MX-80 bentonite and the potential host rock types selected in Stage 1, i.e. Opalinus Clay, "Brauner Dogger", Effingen Member and Helvetic marls. The sorption values selected in the SDBs will take into account the intrinsic background metal concentrations in the various porewaters and the influence of stable isotopes

in the waste which will dissolve simultaneously with the radionuclides (inventory considerations). Further, the findings of the modelling work on the evolution of the near field of a HLW repository (section 3.2.1) will also be taken into consideration. The intention is to complete this work during the early part of 2011, and the SDBs will be used in the so called "Provisional Safety Analyses" for Stage 2 in which at least two sites for each repository type will be proposed.

4.2.2 Validation of the SDB approach for argillaceous rocks

The proposed methodology for generating SDBs for argillaceous rocks is relatively new, and in order to increase the confidence in its application, a verification exercise was carried out. The sorption values obtained using the new approach were compared with those in an already existing SDB for Opalinus Clay used in the Entsorgungsnachweis (NAGRA, 2002).

In order to test the procedure further, a second such study was undertaken with MX-80 bentonite. A SDB for MX-80 bentonite was derived from measurements made on montmorillonite using the same methodology and compared with the values used in the Entsorgungsnachweis (NAGRA, 2002).

The main conclusion drawn from the detailed comparisons made for both Opalinus Clay and MX-80 bentonite (BRADBURY & BAEYENS, 2010) is that very strong evidence has been provided to demonstrate that the same basic approach used in these studies can be applied with confidence to other argillaceous rock systems for which sorption data may be sparse or missing.

4.2.3 Sorption measurements on Effingen Member

Sorption measurements for the radionuclides Cs(I), Sr(II), Ni(II), Co(II), Eu(III), Th(IV) and U(VI) have been made on a rock sample of the Effingen Member in the "low-saline" reference porewater (MÄDER, 2009).

The Effingen Member sample was taken at a depth of -619.45 m. The mineralogical composition of the sample was determined by the University of Bern (MAZUREK, pers. comm.) and its composition is given in Table 4.1. Table 4.2 gives the porewater composition.

Table 4.1: *Mineralogy of Effingen Member (OFT -619.45 m).*

Mineral	wt. %
Calcite	43
Dolomite/Ankerite	3
Siderite	-
Quartz	14
K-Feldspar	1
Pyrite	0.7
Illite	10
Illite/Smectite mixed layers	9
Kaolinite	12
Chlorite	6

Table 4.2: *Composition of the equilibrated synthetic porewater for the Effingen Member sample, pH = 7.70.*

Element	Concentration (M)
Na	3.74×10^{-1}
K	2.0×10^{-3}
Mg	4.5×10^{-2}
Ca	6.0×10^{-2}
Sr	8.1×10^{-4}
Cl	5.66×10^{-1}
S^{VI}	1.2×10^{-2}
C^{IV}	4.3×10^{-4}
Si	1.7×10^{-4}

4.2.4 Blind predictions

For the derivation of SDBs for the different argillaceous rocks under consideration, it is very important to test the sorption values predicted against measured values. In the following, this is illustrated for the above mentioned radionuclides.

Cs(I): In the case of Cs the prediction of the sorption was carried out using the generalised Cs sorption model (BRADBURY & BAEYENS, 2000). In this model the illite content is the only variable parameter for the prediction of the concentration dependent Cs sorption on argillaceous rocks in a well defined porewater. The sorption on pure illite is calculated in the porewater given in Table 4.2 and the results scaled over the illite content in the sample, i.e. 10 wt. %. All other parameters are fixed by the model. The results of this modelling are given by the solid line in Fig. 4.1. As can be seen, the measured data and the predicted values are in good agreement. A slight under-prediction is observed at Cs concentrations around

10^{-6} M and above 10^{-3} M. The latter is due to sorption on the planar sites of other clay minerals present in the Effingen Member sample which was not taken into account.

Sr(II): The Sr concentration in the aqueous phase is defined in the "low salinity" reference porewater, Table 4.2. Single R_d measurements were carried out on the Effingen Member sample by labelling the equilibrated porewater with ^{85}Sr at a high solid to liquid ratio (S:L ratio = 49 g L^{-1}). After 7 days equilibration time, the R_d value from triplicate measurements was determined to be 0.26 ± 0.13 L kg^{-1}. Taking a cation exchange capacity of 80.4 meq kg^{-1}, determined using the ^{134}Cs isotopic dilution method (BAEYENS & BRADBURY, 2004), and using the selectivity coefficients for K-Na, Ca-Na, Mg-Na and Sr-Na equilibria from BRADBURY & BAEYENS (1998), an R_d value of 0.17 L kg^{-1} for Sr was calculated. This R_d value lies within the uncertainty of the measured data. This result shows that the cation exchange model is a valid approach for calculating sorption values for alkaline-earth metals on argillaceous rock systems.

Ni(II), Co(II), Eu(III), Th(IV), U(VI): The sorption results for these elements at low equilibrium concentration ($<10^{-8}$ M) are given in Table 4.3. The predicted sorption values were derived based on the methodology described in BRADBURY et al. (2010). The source sorption data for all these elements were taken from sorption edges on illite (BRADBURY & BAEYENS, 2009a,b). The values selected from the edges were taken at a pH of 7.7, hence no pH conversion factors were required. The total amount of 2:1 clay minerals (illite and illite/smectite mixed layers) in the sample is 19 wt. %, see Table 4.1, and hence the mineralogical conversion factor is 0.19.

Fig. 4.1: *Sorption isotherm of Cs on Effingen Member: the symbols are measured data; the solid line is the model prediction using the generalised Cs sorption model (BRADBURY & BAEYENS, 2000).*

The third modification takes the different speciations into account. These speciation factors were calculated using the updated PSI/Nagra Chemical Thermodynamic Data Base 12/07 (THOENEN, 2011). The speciation was calculated including supplemental thermodynamic data and the aqueous activity corrections were calculated with the SIT approach.

Table 4.3: *Measured and predicted R_d values for Ni(II), Co(II), Eu(III), Th(IV) and U(VI) on Effingen Member at trace concentrations ($< 10^{-8}$ M).*

Radionuclide	Measured R_d (m³ kg^{-1})	Predicted R_d (m³ kg^{-1})	$\dfrac{R_d \text{ predicted}}{R_d \text{ measured}}$	Source illite data (m³ kg^{-1})	Reference
Ni(II)	0.2	0.4	2	4.0	Fig. 3c in [1]
Co(II)	0.4	1.0	2.5	6.3	Fig. 4 in [1]
Eu(III)	63	32	0.5	400	Fig. 5b in [1]
Th(IV)	79	51	0.65	400	Fig. 3b in [2]
U(VI)	1.6×10^{-2}	1.3×10^{-2}	0.8	63	Fig. 4b in [2]

[1] BRADBURY & BAEYENS (2009a); [2] BRADBURY & BAEYENS (2009b)

The results of the "blind" predictions are given in Table 4.3. The table also includes the source data measured on pure illite. The measured and calculated values are in good to very good agreement with each other. This is an important result which supports the methodology to be applied in Stage 2 of the Sectoral Plan for the derivation of SDB for the proposed argillaceous rocks (see section 4.2.1).

4.3 Mechanistic sorption investigations

4.3.1 Zinc uptake by montmorillonite

The 2 site protolysis non electrostatic surface complexation and cation exchange (2SPNE SC/CE) sorption model (BRADBURY & BAEYENS, 1997) has been used over the past decade or so to quantitatively describe sorption edges and isotherms of metals with valences from II to VI on 2:1 clay minerals montmorillonite and illite (BRADBURY & BAEYENS 2005, 2009a,b). One of the main assumptions in this model is that there are two broad categories of edge sorption sites; the so called strong ($\equiv$S^{S}OH) and weak ($\equiv$S^{W1}OH) sites. Because of their different sorption characteristics, it was expected that the coordination environments of the surface complexes on the two site types should be different.

Zn isotherm data on two montmorillonites, Milos and STx-1, were measured and modelled using the 2SPNE SC/CE sorption model. The results were used to define the most favourable experimental conditions under which Zn sorption was either dominated by the strong or by the weak sites. Highly oriented self-supporting films were prepared for P-EXAFS investigations.

Montmorillonites often contain Zn incorporated in the clay matrix. In Milos the structural Zn content is ~ 1 mmol kg^{-1}. The Zn bound in this form was analysed first with P-EXAFS and the structural parameters obtained are shown in Table 4.4. In Fig. 4.2 a visualization of the incorporated Zn (Zn1) is given. The local environment of Zn1 consists of 3 Al at 3.02 Å and 4 Si2 at 3.22 Å neighbouring atoms. P-EXAFS spectra for two samples at low Zn loading ($\equiv$S^{S}OH sites, ~2 mmol/kg) and one at medium Zn loading ($\equiv$S^{W1}OH, ~30 mmol/kg) were analysed taking into account the incorporated Zn species. The Zn spectra on the "strong sites" exhibited a pronounced angular dependency and formed surface complexes in the continuity of the Al-octahedral sheets at the montmorillonite edges (Fig. 4.2, Zn2-Zn5)

In contrast, the Zn "weak site" spectra showed only a weak angular dependency and a significant longer Zn-Si2 bond length. A mixture of Zn surface complexes all of which have bonds to Al and Si at different angles would severely decrease the P-EXAFS angular dependence. It is therefore possible that there is a series of similar complexes in which Zn-polyhedra bridge to the montmorillonite surface in such a manner that the average angle of the Zn–O, Zn-Al and Zn–Si pairs with respect to the c^* direction (β) is close to 54.7°. At this particular β-angle polarized and powder EXAFS spectra are identical and would eliminate any angular dependence in P-EXAFS measurements (DÄHN et al., 2011). The study demonstrated that there is a pronounced difference between the local environment of Zn surfaces complexes at low and medium loadings, providing supporting evidence for the "strong site/weak site" hypothesis in the 2SPNE SC/CE sorption model.

Table 4.4: *Main structural parameters obtained by fitting the P-EXAFS data ($\alpha = 35°$) of different Zn loaded montmorillonite samples.*

| Samples	Zn-O		Zn-Al		Zn-Si1		Zn-Si2	
	CN	*R* (Å)	*CN*	*R* (Å)	*CN*	*R* (Å)	*CN*	*R* (Å)
Milos: incorporated Zn	6.4(4)	2.07(1)	3.3(6)	3.02(2)	-	-	4.0(6)	3.22(2)
Milos: Zn sorbed on strong sites	6.0(3)	2.05(1)	1.5(4)	3.02(2)	1.2(3)	3.10(3)	1.5(3)	3.26(2)
STx-1: Zn sorbed on strong sites	5.1(4)	2.05(1)	1.1(3)	3.02(2)	1.3(2)	3.06(3)	2.1(3)	3.26(2)
STx-1: Zn sorbed on weak sites	5.4(4)	2.05(1)	0.7(4)	3.04(2)			1.0(5)	3.33(3)
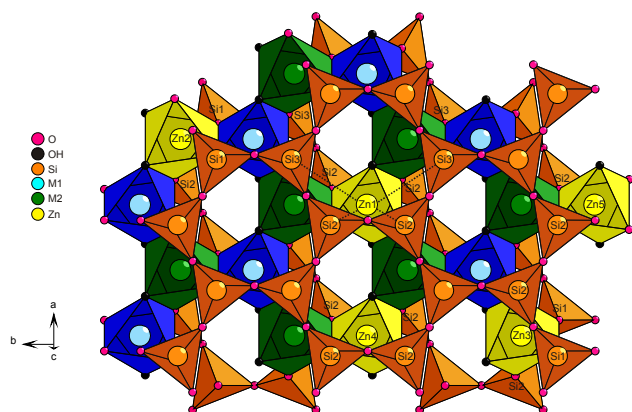
Fig. 4.2: Illustration of Zn incorporated in the structure (Zn1) and Zn located at edge sites (Zn2-Zn5). The dotted lines indicate the next nearest Si2 (~3.22 Å) and Si3 (~4.43 Å) atoms of the Zn1 incorporated species.

In the Transport Mechanisms Group, section 3.4.3, DFT based atomistic calculations have been applied to model the P-EXAFS spectra of Zn^{2+} adsorbed on montmorillonite and to explain the molecular structure of these Zn^{2+} complexes. The results of the molecular simulations are consistent with the nature of "weak" and "strong" sites inferred from conventional EXAFS modelling and wet chemistry data.

4.3.2 U(VI) uptake by montmorillonite

In order to provide information on the sorbed U(VI) species on montmorillite, and support the wet chemistry experiments (MARQUES et al., 2011), P-EXAFS measurements on a sample prepared at pH ~8 with a U(VI) loading of 7.1 mmol kg^{-1} were performed. The P-EXAFS measurements were carried out on a self-supporting clay film at the uranium L_{III} edge at 17166 eV at the Rossendorf Beamline (ESRF, Grenoble).

Fig. 4.3 shows the $k^3\chi(k)$ P-EXAFS spectra and the corresponding radial structure functions (RSFs) of the U(VI) loaded Na-montmorillonite sample measured at beam incidence angles of 10°, 35° and 55° with respect to the self-supporting film. The P-EXAFS spectra were analyzed and fitted using the IFEFFIT software package (NEWVILLE et al., 1995). Back-scattering phases and amplitudes were obtained from FEFF8.2 calculations using the structure of soddyite. The EXAFS parameters obtained by fitting the three angles simultaneously are summarized in Table 4.5.
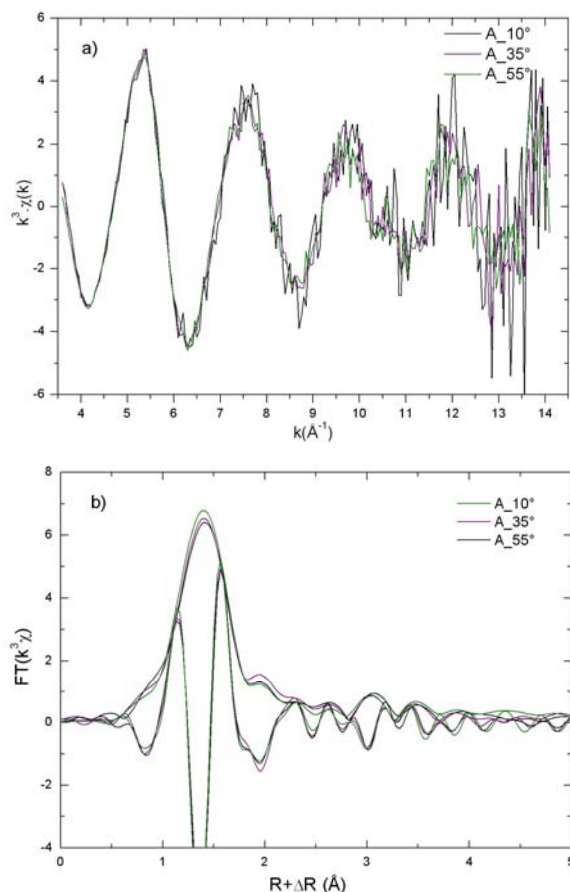
Fig. 4.3: (a) k^3-weighted spectra of the U(VI)-montmorillonite sample at the angles 10°, 35° and 55° and (b) the corresponding Fourier Transforms (FTs).

Data analysis showed the presence of different backscattering pairs (U-Al/Si and U-Fe) and a splitting of the O_{eq} shell in accordance with the formation of inner-sphere complexes at the montmorillonite surface. P-EXAFS was employed to elucidate where on the montmorillonite surface the inner-sphere complexes formed. The P-EXAFS data showed no anisotropy, although the self-supporting films were well oriented. In P-EXAFS, neighboring atoms along the polarization direction of the X-ray beam are preferentially probed, and atoms located in a plane perpendicular to this direction are attenuated (MANCEAU et al., 1998). Therefore, the lack of a P-EXAFS dependency observed in this study indicates that U(VI) is unlikely to be sorbed on the montmorillonite in the continuity of the octahedral sheet as a single surface complex. It is therefore possible that there is a series of similar complexes in which U(VI)-polyhedra bridge to the montmorillonite surface in such a manner that the average angle of the U–O and U–Si pairs with respect to the c^* direction (β) is ~54.7∘. (See above; Zn sorption on weak sites.)

Table 4.5: *Structural information derived from the P-EXAFS analysis of a U(VI) loaded self supporting montmorillonite film.*

	Shell	CN at 10°	CN at 35°	CN at 55°	R (Å)	σ^2 (Å^2)	ΔE_0 (eV)
FT range	U=O$_{ax}$	2.6(3)	2.5(2)	2.4(2)	1.80(1)	0.0036(5)	9
3.6 - 11.4 Å^{-1}	U-O$_{eq1}$	2.3(5)	2.4(4)	2.4(4)	2.27(1)	0.005$^{a,\,b}$(2)	
	U-O$_{eq2}$	1.8(6)	2.2(4)	2.0(3)	2.46(2)	0.005$^{a,\,b}$(2)	
Fit range	U-Si$_1$	0.3(3)	0.4(2)	0.5(2)	3.09(2)	0.003^b	
1 – 4 Å	U-Fe	0.3(2)	0.4(2)	0.5(1)	3.47(2)	0.003^b	
	U-Si$_2$	0.9(9)	1.0(4)	0.8(4)	3.86(2)	0.005^b	

(a) values coupled during the fit (b) value fixed during the fit

4.3.3 Competitive sorption

In close co-operation with the Transport Mechanisms Group, a modelling study on the reactive transport of Ni(II) through compacted MX-80 bentonite taking into account competitive sorption from Fe(II) arising from siderite dissolution has been carried out (PFINGSTEN et al., 2011). The results of this study are fully described in section 3.2.2 and are not treated further here.

4.4 Effect of temperature on sorption

The influence of temperature on the retention properties of radionuclides on clay minerals is still an open question. Cation exchange capacity (CEC) determination and sorption experiments were performed on MX-80 bentonite material originating from the ABM (Alternative Buffer Material) experiment. The ABM field experiment was started at the Äspö Hard Rock Laboratory in 2006 (ENG et al., 2007). The ABM MX-80 material was exposed to temperatures up to 140 °C for 1 year, and this might have altered its sorption properties. Experiments on "undisturbed" reference MX-80 samples were also carried out to compare the sorption properties with those of the ABM MX-80.

Table 4.6: *Log R$_d$ (L kg^{-1}) values obtained from the experiments on undisturbed MX-80 and ABM MX-80 for Cs(I) and Ni(II).*

Element	Reference MX-80		ABM MX-80	
	25 °C	90 °C	25 °C	90 °C
Cs(I)	2.2 ± 0.1	1.8 ± 0.1	2.3 ± 0.1	1.8 ± 0.1
Ni(II)	4.3 ± 0.1	5.0 ± 0.2	4.3 ± 0.1	4.9 ± 0.1

The CEC measurements using the ^{134}Cs isotopic dilution method (BAEYENS & BRADBURY, 2004) for ABM and undisturbed MX-80 were determined to be 731 ± 16 meq kg^{-1} and 741 ± 9 meq kg^{-1}, respectively. Clearly, these results show that the thermal treatment did not influence the cation exchange capacity of the MX-80 bentonite.

Cs(I) and Ni(II) sorption experiments were carried out at 25 °C to check whether the exposure to high temperatures had an influence on the sorption properties of the bentonite material. In addition, sorption experiments were carried out at 90 °C on both materials. The conditions for the experiments were chosen such that the sorption of the radionuclides was pH independent. Thus, small changes in pH would not affect the R$_d$ values and potential effects of temperature on the proton activity were avoided. The results obtained so far are shown in Table 4.6. In the case of Cs the sorption behaviour on both bentonites was the same, but there is a clear trend with temperature. At 90 °C the sorption of Cs decreases by about a factor of 3 compared to room temperature. (This effect was also clearly observed for illite.) On the other hand, the opposite effect was observed for Ni(II). At 90 °C an increase in sorption by a factor of ~4 is seen compared to the measurements at 25 °C.

4.5 PhD project

A PhD proposal entitled "The influence of Fe(II) on clay properties, the sorption of Fe(II) on clays and competitive sorption investigations: a combined macroscopic and microscopic study" has been approved by the Swiss National Science Foundation. The overall objective is to investigate, in a combined macroscopic (wet chemistry) and microscopic (surface analysis) approach, the influence of reducing conditions on the characteristics of representative clay

minerals, particularly with respect to radionuclide retention in the presence of high aqueous Fe(II) concentrations. Fe(II) stability experiments in the absence of clay have been started in the new redox glove box which was commissioned in summer 2010.

4.6 Swiss-Hungarian co-operation project

In connection with the Schweizer Erweiterungsbeitrag DEZA/SECO agreement, a framework agreement between the Swiss Federal Council and the Government of Hungary has been established. A project proposal entitled "Development of a macro- and microscopic approach to investigate the geochemistry of radioactive waste disposal systems" was submitted and has been approved and funded. The main partners within this project are the Hungarian Academy of Sciences (KFKI Atomic Energy Research Institute), Mecsekerc Ltd. and PSI.

The objectives of the project are to make specific contributions to the safety assessment of future radioactive waste repositories through an understanding of relevant retention mechanisms and processes, and to provide the necessary models and databases. In order to investigate sorption mechanisms on molecular and microscopic scales, high-sensitivity X-ray microanalytical measurements are planned. These investigations are strongly linked to macroscopic studies combined with geochemical modelling. The investigations will focus on Opalinus Clay and Boda Clay rock samples.

The 3 years project started on October 15, 2010. The first kick-off meeting took place on 4/5 October 2010 in Budapest, Hungary. A first micro-XRF/XAS beam-time is planned for the beginning of December 2010 at Strahl L HASYLAB/DESY, Hamburg.

4.7 References

BAEYENS B., BRADBURY M.H. (2004)
Cation exchange capacity measurements of illite using the sodium and cesium isotope dilution technique: Effects of the index-cation, electrolyte concentration and competition: Modeling. Clays Clay Miner. 52, 421-431.

BRADBURY M.H., BAEYENS B. (1997)
A mechanistic description of Ni and Zn sorption on Na-montmorillonite. Part II: Modelling. J. Contam. Hydrol. 27, 223-248.

BRADBURY M.H., BAEYENS B. (1998)
A physicochemical characterisation and geochemical modelling approach for determining porewater chemistries in argillaceous rocks. Geochim. Cosmochim. Acta 62, 783-795.

BRADBURY M.H., BAEYENS B. (2000)
A generalised sorption model for the concentration dependent uptake of Cs by argillaceous rock. J. Contam. Hydrol. 42, 141-163.

BRADBURY M.H., BAEYENS B. (2005)
Modelling the sorption of Mn(II), Co(II), Ni(II), Zn(II), Cd(II), Eu(III), Am(III), Sn(IV), Th(IV), Np(V) and U(VI) on montmorillonite: Linear free energy relationships and estimates of surface binding constants for some selected heavy metals and actinides. Geochim. Cosmochim. Acta 69, 875-892.

BRADBURY M.H., BAEYENS B., THOENEN T. (2008)
Sorption data bases for generic Swiss argillaceous, crystalline and calcareous rock systems, NAB 08-50. Nagra, Wettingen, Switzerland.

BRADBURY M.H., BAEYENS B. (2009a)
Sorption modelling on illite. Part I: Titration measurements and the sorption of Ni, Co, Eu and Sn. Geochim. Cosmochim. Acta 73, 990-1003.

BRADBURY M.H., BAEYENS, B. (2009b)
Sorption modelling on illite. Part II: Actinide sorption and linear free energy relationships. Geochim. Cosmochim. Acta 73, 1004-1013.

BRADBURY M.H., BAEYENS B., THOENEN T. (2010)
Sorption data bases for generic Swiss argillaceous rock systems. PSI Bericht 10-03 and NTB 09-03, Nagra, Wettingen, Switzerland.

BRADBURY M.H., BAEYENS, B. (2010)
Comparison of the reference Opalinus Clay and MX-80 bentonite sorption databases used in the Entsorgungsnachweis with sorption databases predicted from sorption measurements on illite and montmorillonite. PSI Bericht 10-09 and NTB 09-07, Nagra, Wettingen, Switzerland.

DÄHN R., BAEYENS B., BRADBURY M.H. (2011)
Investigation of the different binding edge sites for Zn on montmorillonite using P-EXAFS – the strong/weak site concept in the 2SPNE SC/CE sorption model. Geochim. Cosmochim. Acta (in review).

ENG A., NILSSON U, SVENSSON D. (2007)
Äspö Hard Rock Laboratory, Alternative Buffer Material, Installation Report. International Progress Report IPR-07-15. SKB, Stockholm, Sweden.

MÄDER U. (2009)
Reference porewater for the Effingen Member (Standortregion Südjura) for the provisional safety-analysis in the framework of the sectoral plan - interim results (SGT-ZE). NAB 09-13, Nagra, Wettingen, Switzerland.

MANCEAU A., CHATEIGNER D., GATES W.P. (1998)
Polarized EXAFS, distance-valence least-squares modeling (DVLS) and quantitive texture analysis approaches to the structural refinement of Garfield nontronite. Phys. Chem. Miner. 25, 347-365.

MARQUES-FERNANDES M., BAEYENS B., DÄHN R., MACÉ N., BRADBURY M.H. (2011)
U(VI) sorption on montmorillonite: A macroscopic and microscopic study (to be submitted to Geochim. Cosmochim. Acta).

NAGRA (2002)
Project Opalinus Clay: Safety Report. Demonstration of disposal feasibility (Entsorgungsnachweis) for spent fuel, vitrified high-level waste and long-lived intermediate-level waste. NTB 02-05, Nagra, Wettingen, Switzerland.

NEWVILLE M., RAVEL B., HASKEL D., REHR J.J., STERN E.A., YACOBY Y. (1995)
Analysis of multiple-scattering XAFS data using theoretical standards Physica B 208 & 209, 154-155.

PFINGSTEN W., BRADBURY M.H., BAEYENS B. (2011)
The influence of Fe(II) competition on the sorption and migration Ni(II) in MX-80 bentonite. Appl. Geochem. (in review).

THOENEN T. (2011)
Update of the Nagra/PSI TDB 01/01: Compilation of Updated and New Data, PSI TM (in preparation).

5 CEMENT SYSTEMS

E. Wieland, J. Tits, D. Kunz, A. Laube, X. Gaona (guest scientist), B. Dilnesa (Empa)

5.1 Overview

Cementitious materials are foreseen to be used in the planned deep geological repositories for low- and short-lived intermediate-level (L/ILW) and long-lived intermediate-level (ILW) radioactive waste in Switzerland. In performance assessment (PA) studies the source term for radionuclide migration into the host rock is determined by a combination of solubility and sorption constraints in the cementitious near field. The research programme carried out by the group "Cement Systems" is directed towards strengthening the credibility of the sorption values used in PA for predicting radionuclide retention in the cementitious near field and to improving knowledge on the chemical processes in the near field of the planned L/ILW and ILW repositories. The cement used in the experimental studies is a sulfate-resisting Portland cement CEM I 52.5 N HTS (Lafarge, France), which is currently used for the conditioning of radioactive waste in Switzerland. Calcium silicate hydrate (C-S-H) phases are considered to be the most important constituent of hardened cement paste (HCP) for cation and anion binding, which is the reason why complementary studies using C-S-H phases have been carried out.

The main lines of research in 2010 were:

- Literature reviews in conjunction with activities related to the Sectoral Plan;

- Development of an experimental research programme on the speciation of ^{14}C containing small organic molecules formed during the anaerobic corrosion of activated steel;

- Sorption studies with small organic molecules on HCP;

- Wet chemistry experiments, and spectroscopic investigations on the interaction of Np(IV) with C-S-H phases;

- Development of a thermodynamic model of U(VI) uptake by C-S-H and HCP.

The sorption and spectroscopic studies on Np(IV/V) uptake processes by cementitious materials are carried out in the framework of the 7th EU Framework Programme collaborative project "RECOSY" (REdox phenomena COntrolling SYstems).

X. Gaona (guest scientist) left the group in August 2010 to accept a position at the Institute for Nuclear Waste Disposal (INE) at the Karlsruhe Institut of Technology (KIT), Germany. Future collaboration with Dr. Gaona will focus on Np(V/VI) solubility studies under hyperalkaline conditions. The latter study is carried out in the framework of an ACTINET I-3 joint project with KIT-INE (Germany), JRC-ITU (Germany) and MSU (Russia).

5.2 Activities in support of the Sectoral Plan

In the framework of the Sectoral Plan a report on the evolution of the L/ILW repository near-field is currently being prepared in LES. In 2010 chapters on the fate of organic compounds and colloids in the cementitious near field (WIELAND, 2010a; WIELAND, 2010b) were prepared for this report. Both reports include detailed literature surveys.

PA studies carried out within the framework of the Sectoral Plan Stage 2 will require a state-of-the-art cement sorption data-base (SDB). A re-appraisal of the sorption values for all safety relevant radionuclides was made using information from recent in-house sorption studies and measurements published in the open literature after 2002 (WIELAND, 2010c). The latter review is a preliminary step towards a comprehensive up-date of the existing cement SDB (WIELAND & VAN LOON, 2002).

5.3 Dose-determining radionuclides

^{14}C, possibly in the form of small organic compounds resulting from steel corrosion under reducing conditions in a cementitious near field, is a potentially major contributor to the long-term activity release rate (mSv per year) from the cementitious near field into the far field. These compounds may be either inorganic, i.e. ^{14}CO$_3^{2-}$ under hyperalkaline conditions, or organic, i.e. ^{14}C containing oxygenated hydro-carbons, such as alcohols, aldehydes or carboxylic acids, or non-oxygenated hydrocarbons, such as methane, ethane, ethane, etc. At the present time the speciation of carbon under the conditions in a cement-based repository is poorly known. It has been speculated that oxygenated hydrocarbons predominately form under the reducing conditions of a repository (SASOH, 2004). Importantly, the physico-chemical properties are compound-specific. For example, non-oxygenated hydrocarbons are hydrophobic showing a high volatility, which facilitates transport pathways via the gas phase in the unsaturated backfill material (see Fig. 5.1).
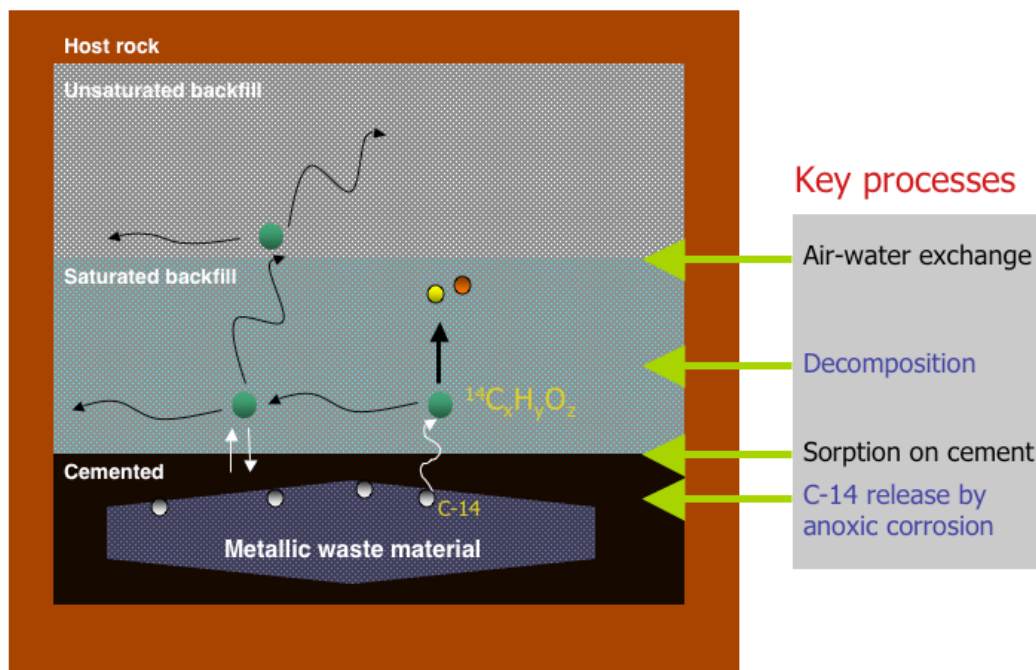
Fig. 5.1: *Schematic presentation of the possible transport pathways of organic compounds in the cementitious near field of a repository and the relevant processes.*

In contrast, oxygenated hydrocarbons have, in general, hydrophilic properties, implying transport pathways and sinks (sorption) in saturated cementitious backfill materials etc. (Fig. 5.1). In 2010 a status report summarising the current knowledge on the speciation of ^{14}C in the cementitious near field, was completed (WIELAND & HUMMEL, 2010). Information on ^{14}C speciation based on experimental studies is very limited and, in many instances, controversial. As an outcome of this study an experimental programme has been proposed with the aim of resolving the currently existing discrepancies concerning the type of organic compounds formed under relevant near field conditions (for details see WIELAND & HUMMEL, 2010). Following on from the latter proposal, a detailed evaluation of the analytical equipment needed was made. Chromatographic separation in combination with suitable detection systems is a common approach applied to detect and identify volatile and non-volatile organic compounds. In this context, the analytical capabilities of High Performance Ion Exclusion Chromatography (HPIEC) coupled with a suitable detection system (Mass Spectrometry, MS) were evaluated and tested in 2010. Furthermore, an experimental set-up was developed which will allow the chemical stability of oxygenated hydrocarbons to be studied under the conditions relevant to the repository system.

Experimental investigations on the uptake of oxygenated hydrocarbons, started in 2008, were continued in 2010 (LES PROGRESS REPORT, 2009). It has been speculated that the latter classes of compounds containing ^{14}C could be present in the cementitious near field (SASOH, 2004). The uptake of selected, small organic molecules (methanol, ethanol, formaldehyde, acetaldehyde, formic acid, acetic acid) by hydrating cement was determined in compact cement samples (0.5 L volume). The latter samples were prepared by mixing un-hydrated cement with methanol, ethanol, formaldehyde, acetaldehyde, formic acid or acetic acid containing solutions. After 28 and 390 days reaction times, cement porewater was squeezed from the hardened samples using the steel die method at pressures up to 530 N mm^{-2}. Total organic carbon was determined in the extracted and filtered pore solutions. Distribution ratios (R_d) were estimated from mass balance considerations. These data can be compared with R_d values after 1 hour reaction time.

Uptake of the above small organic molecules by hydrating cement was found to be very weak (Fig. 5.2), i.e. R_d values typically ranged between 10^{-5} and 10^{-3} m^3 kg^{-1} for all compounds. (Note that the low R_d value determined for ethanol after 390 days reaction is most likely an outlier due to an experimental artefact.) No clear trend with time in the sorption values was observed for the different classes of compounds, and nor did the size of the organic compounds determine the retention sequence.
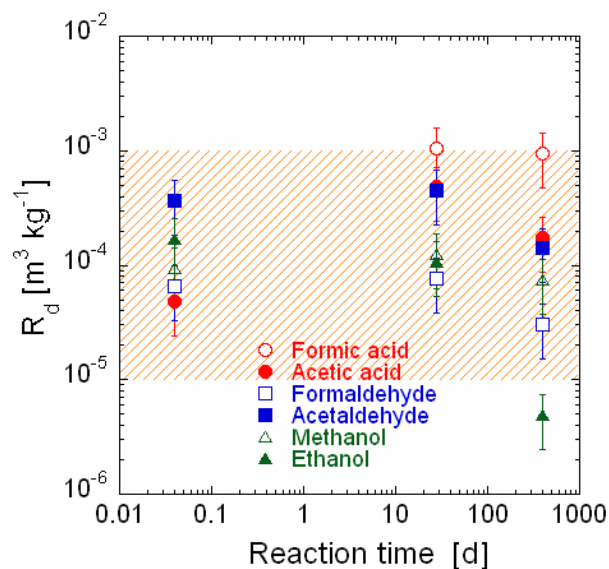
Fig. 5.2: *Uptake of small organic molecules by HCP as a function of reaction time.*

The retention sequence was: formic acid > acetic acid ~ acetaldehyde > formaldehyde ~ methanol ~ ethanol. As the extent of the interaction with HCP is largely independent of the hydration time, it may be further concluded that these organic molecules are not taken up into the structure of any of the cement minerals forming during the course of hydration. Based on the available data sets, a mean R_d value of ~10^{-4} m^3 kg^{-1} was estimated, with lower and upper bounds of 10^{-6} m^3 kg^{-1} and 10^{-3} m^3 kg^{-1}, respectively. It should be noted that uptake by HCP occurs even for the smallest and the least oxidized species, such as methanol, and further, that the interaction with HCP can only be quantified in compact systems.

5.4 Uptake of neptunium under reducing conditions

In the currently existing cement SDB used in PA it is assumed that the sorption behaviour of tetravalent actinides, such as Np(IV) and Pu(IV), is similar to that of Th(IV). To verify this assumption, the uptake of Np(IV) by HCP and C-S-H phases under reducing conditions has been investigated in the framework of the RECOSY project.

5.4.1 Redox measurements

Reliable determination of the redox potential (Eh) of porewaters is important because, together with the pH, this parameter controls the redox speciation, solubility and sorption behaviour of redox-sensitive actinides, such as Np(IV/V). Eh is usually measured using an electrochemical cell (combined Eh electrode) because

the method is easy to apply and allows in situ measurements to be made with little disturbance of the sample. However, several difficulties arise when measuring Eh with combined electrodes; slow and/or erroneous electrode response, the effect of redox couple concentration, the presence of suspended materials, the effect of the "electrode utilisation history" (i.e., previous measurements with the electrode) etc. Therefore, a small project was carried out in 2010 in the framework of a traineeship and in conjunction with the inter-comparison exercise organized by RECOSY. The aim of the project was to assess the reliability of redox measurements in alkaline conditions, and to check whether or not Eh readings can be related to thermodynamic reactions. The experimental programme was finished in 2010. Data analysis is ongoing.

5.4.2 Uptake of Np(IV) by C-S-H

Kinetic studies on the Np(IV) uptake by C-S-H phases with different Ca:Si (C:S) mol ratios and Np(IV) precipitation tests were carried out in alkali-free solutions and in alkali-rich artificial cement porewater (ACW) at pH = 13.3. Note that a C:S ratio of 1.65 corresponds to the Ca-rich environment in fresh HCP, whilst a C:S ratio of 0.65 – 0.75 corresponds to the Si-rich environment observed in a highly degraded cementitious near field. Reducing conditions were established either by adding 5×10^{-3} M Na-dithionite (Na$_2$S$_2$O$_4$) to the suspensions or, in few cases, using a potentiostat. Preliminary C-S-H solubility tests showed that Na-dithionite concentrations up to 5×10^{-3} M had no influence on the Ca and Si concentrations in the equilibrium C-S-H solutions.

Sorption tests with Th(IV) further revealed that the sorption of C-S-H phases was not affected by the presence of 5×10^{-3} M Na-dithionite. Finally, the redox state of aqueous Np(IV) was verified by carrying out an in-house developed sorption test based on differences in the extent of sorption of Np(IV) and Np(V) on Alox at pH = 5.

A series of Np(IV) precipitation tests were carried out in C-S-H solutions at pHs between 10.0 and 13.3 in the presence of 5×10^{-3} M Na-dithionite or under reducing conditions controlled using the potentiostat. Np(IV) precipitation was observed above total concentrations of $(5\pm4) \times 10^{-9}$ M in agreement with the solubility of NpO$_2$·2H$_2$O (HUMMEL et al., 2002). Sorption kinetic tests were carried out using the ^{239}Np isotope at a total Np concentration of 2.5×10^{-11} M. Np(IV) sorption was found to be very rapid and equilibrium was attained within two days (Fig. 5.3).
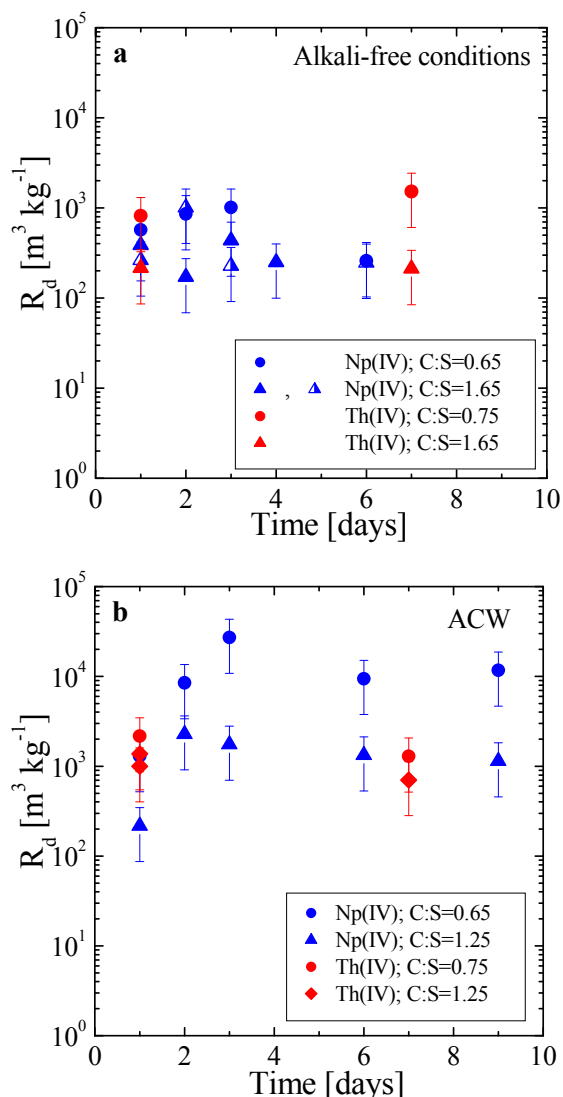
Fig. 5.3: *Np(IV) and Th(IV) sorption kinetics on C-S-H phases with different C:S ratios under (a) alkali-free conditions (C:S mol ratios = 0.65, 0.75 and 1.65) and (b) in alkali-rich ACW at pH = 13.3 (C:S mol ratios = 0.65, 0.75 and 1.25).*

The R_d for Np(IV) was found to range in value between 10^2 and 10^3 m^3 kg^{-1} in alkali-free solutions, and between 10^3 and 10^4 m^3 kg^{-1} in ACW. The latter finding is to be confirmed in further experiments. Fig. 5.3 also shows that the sorption behaviour of Np(IV) and Th(IV) on C-S-H phases is comparable, thus supporting the chemical analogy between the two metals.

5.4.3 EXAFS study on Np(IV) uptake by C-S-H and HCP

Neptunium speciation studies in C-S-H and cementitious systems were carried out with the aim of determining whether or not C-S-H is the uptake-controlling phase in HCP. EXAFS measurements were carried out on the ROBL beamline at the European Synchrotron Radiation Facility (ESRF), Grenoble, France. C-S-H suspensions with C:S mol ratios of 0.75, 1.07 and 1.65 (synthesized in both Milli-Q water and in ACW), and HCP suspensions were doped with Np(IV) to reach a Np loading of ~1000 ppm in the wet paste. Samples were shipped to ESRF under a liquid N$_2$ atmosphere to avoid the oxidation of Np(IV). At the ROBL a cryostat cooled with liquid He was used.

Differences in the k^3-weighted Np L$_{III}$-edge (17610 eV) EXAFS spectra and the corresponding RSFs were observed for the different Np(IV) doped samples (Fig. 5.4). The backscattering contributions from the neighbouring Si shell increased with increasing C:S mol ratio of the C-S-H phases while those from the Ca shell decreased (Fig. 5.4b). Both observations are consistent with the concept that Np(IV) is accommodated in the interlayer of the C-S-H phases (Figs. 5.4c/d). This finding suggests that Np(IV) incorporation into the structure of C-S-H phases is the dominant uptake mechanism at all C:S ratios.

Principal component analysis showed that only two components are needed to model the entire set of Np(IV) EXAFS spectra. These components were identified by iterative target transformation and found to correspond to Np(IV) taken up by C-S-H 0.75 and Np(IV) taken up by C-S-H 1.65. All remaining spectra could be fitted as linear combinations of these two "end members" (Fig. 5.4a; Table 5.1). This showed that, first, Np(IV) uptake by C-S-H phases is only affected by the C:S mol ratio of C-S-H and, secondly, that the local coordination environment of Np(IV) in HCP corresponds to that of Np(IV) in C-S-H phases, i.e. Np(IV) is predominantly taken up by a C-S-H phase with a C:S = 1.65. To the best of our knowledge this is the first study in which successful spectroscopic measurements on Np(IV) loaded cementitious systems have been reported. The measurements clearly prove that the C-S-H phase in HCP is responsible for Np(IV) immobilization by incorporation into the C-S-H structure.

Table 5.1: *Contributions of the Np(IV)(C-S-H 0.75 and the Np(IV)(C-S-H 1.65 EXAFS spectra to the spectra of Np(IV)/C-S-H 1.07, Np(IV)/C-S-H 1.07 (no Na₂S₂O₄), Np(IV)/C-S-H 1.07 in ACW and Np(IV)/HCP determined by linear combination. Calculations were carried out in $k^3\chi(k)$ space in the k range 3 Å⁻¹ – 12 Å⁻¹ using Athena. The R-factor is an indicator of the quality of the fit (%).*

Sample	pH	% C-S-H 0.75	% C-S-H 1.65	R-factor (%)
Np(IV) – C-S-H 1.07	12	42	58	9.6
Np(IV) – C-S-H 1.07 (no Na₂S₂O₄)	12	33	67	7.5
Np(IV) – C-S-H 1.07 ACW	13.3	40	60	11.4
Np(IV) – cement (C:S ~ 1.65)	12.5	11	89	10.7

Experimental data and fits of the EXAFS spectra of Np(IV)-C-S-H 0.75 and Np(IV)-C-S-H 1.65 are shown in Fig. 5.5. The structural parameters are summarized in Table 5.2. Fitting was performed by assuming Np–O, Np–Si, Np-Ca1 and Np-Ca2 back scattering pairs. The high Si-coordination numbers (N_{Si}) obtained for both Np(IV)/C-S-H systems (4.6 ± 1.1 and 2.9 ± 1.1) indicate the incorporation of Np(IV) into the C-S-H structure. If surface complexation were the dominant uptake process, then the number of neighbouring Si atoms would be significantly lower. The number of neighbouring Ca atoms (N_{Ca}) is higher in the Np(IV) loaded C-S-H phase with C:S = 1.65 compared to the Np(IV) loaded C-S-H phase with C:S = 0.75, which is consistent with the larger number of Ca atoms bound in the interlayer in C-S-H with C:S =1.65 (Fig. 5.4d).
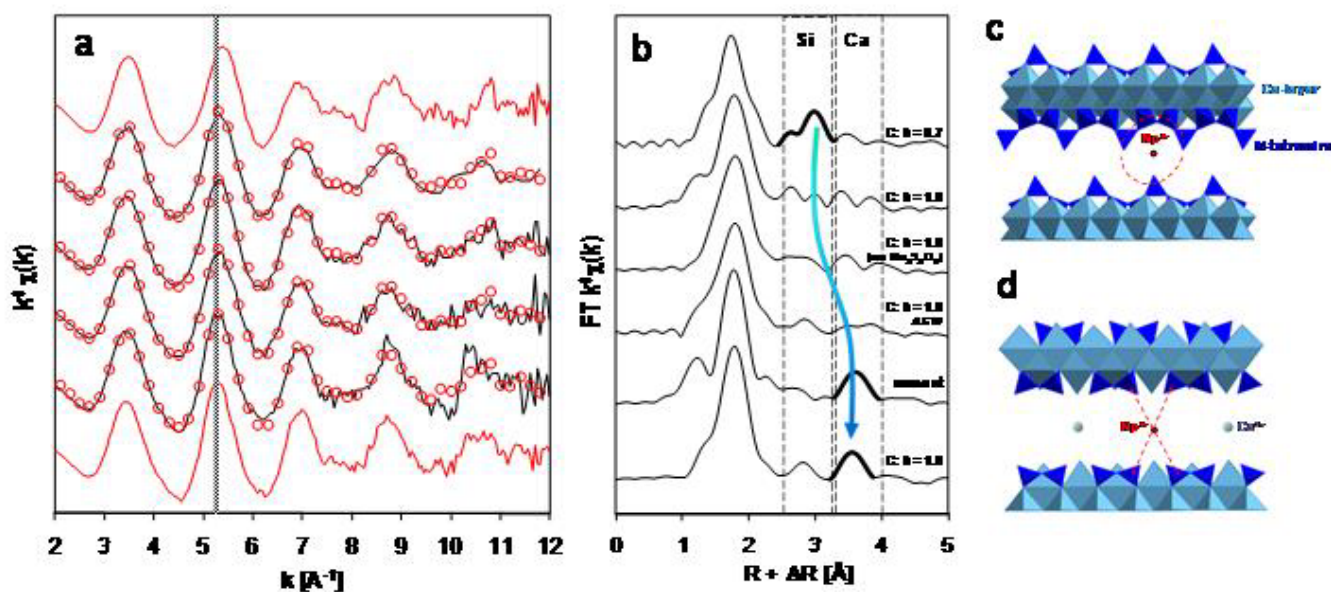
Fig. 5.4: *(a) k^3-weighted Np L_{III}-edge EXAFS spectra (experimental and fit), (b) corresponding RSFs for Np(IV)/C-S-H 0.75, Np(IV)/C-S-H 1.07, Np(IV)/C-S-H 1.07 (no Na₂S₂O₄), Np(IV)/C-S-H 1.07 in ACW, Np(IV)/HCP and Np(IV)/C-S-H 1.65. Fitted data (open circles) of Np(IV)/C-S-H 1.07, Np(IV)/C-S-H 1.07 (no Na₂S₂O₄), Np(IV)/C-S-H 1.07 in ACW and HCP corresponding to linear combinations of the EXAFS spectra of Np(IV)/C-S-H 0.75 and Np(IV)/C-S-H 1.65. Structure of micro-crystalline C-S-H for (c) low and (d) high C:S mol ratios.*

Table 5.2: EXAFS structural parameters determined for Np(IV) taken up by C-S-H 0.75 and C-S-H 1.65.

Sample	Np-O	Np-Si	Np-Ca	Quality of the fit
Np(IV)/C-S-H 0.75	$N_{O1} = 7.7 \pm 1.2$ $r_{O1} = 2.31 \pm 0.01$ Å $\sigma^2 = 0.010 \pm 0.002$	$N_{Si-1} = 4.6 \pm 1.1$ $r_{Np-Si1} = 3.63 \pm 0.02$ Å $\sigma^2 = 0.010 \pm 0.008$	$N_{Ca} = 8.0 \pm 3.0$ $r_{Np-Ca} = 4.19 \pm 0.04$ Å $\sigma^2 = 0.02^*$	$\Delta E = 6.6 \pm 1.1$ eV R-factor = 0.001
Np(IV)/C-S-H 1.65	$N_O = 8.3 \pm 1.2$ $r_O = 2.31 \pm 0.01$ Å $\sigma^2 = 0.010 \pm 0.002$	$N_{Si} = 2.9 \pm 1.1$ $r_{Np-Si} = 3.60 \pm 0.03$ Å $\sigma^2 = 0.010^*$	$N_{Ca} = 12.7 \pm 2.8$ $r_{Np-Ca} = 4.16 \pm 0.04$ Å $\sigma^2 = 0.019 \pm 0.009$	$\Delta E = 4.5 \pm 0.8$ eV R-factor = 0.002

* parameters fixed in the fit
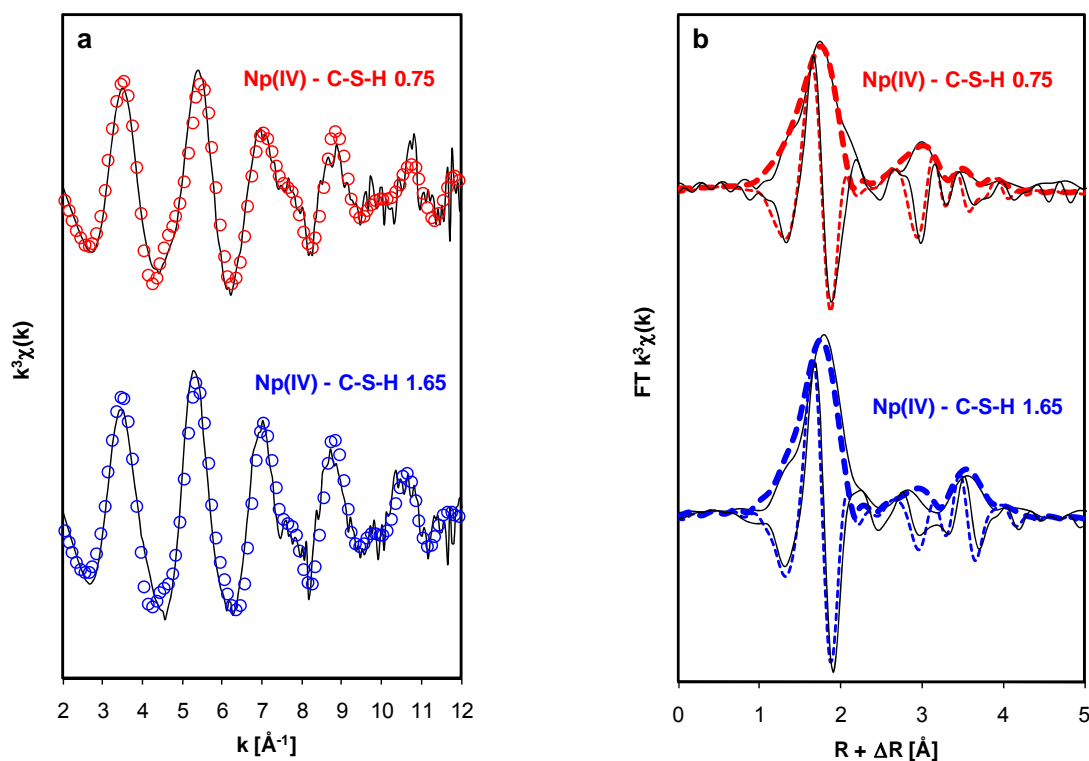
Fig. 5.5: Experimental (solid lines) and fits (circles and dashed lines) of (a) k^3-weighted Np L_{III}-edge EXAFS spectra and (b) the corresponding Fourier transforms (modulus and imaginary parts) for Np(IV) taken up by C-S-H with C:S = 0.75 and 1.65.

5.5 Thermodynamic modelling of U(VI) uptake by cementitious systems

Thermodynamic models of the interaction of radionuclides with cementitious materials are important in connection with long-term predictions of the safe disposal of radioactive waste. A thermo-dynamic model of U(VI) interaction with C-S-H phases was developed based on a solid solution approach (co-operation with the Geochemical Modelling Group). In-house determined wet chemistry data with U(VI) on C-S-H phases with different C:S ratios (TITS et al., 2008) and structural data from recent spectroscopic investigations (MACÉ et al., 2010; TITS et al., 2010) provided the essential information required for model development. The spectroscopic studies showed that U(VI) is neither predominantely bound on the C-S-H surface nor incorporated in the Ca-O octahedral sheets of the C-S-H structure. Rather, U(VI) is predominantely located in the interlayer of C-S-H phases. The latter observation, in connection with the high recrystallization rates observed for the crypto-crystalline 'gel-like' structure of the C-S-H phases (e.g. MANDALIEV et al., 2009), suggests that the U(VI) uptake is controlled by solid solution formation.

The aqueous-solid solution thermodynamic model of U(VI) uptake by C-S-H was developed using the compound energy formalism (CEF) as an extension of the CSH3T model recently developed by KULIK (2010) for 'pure' C-S-H phase solubility. The sub-lattices proposed in the CSH3T model were occupied with U(VI) species in accordance with the spectroscopic findings, which suggested interlayer occupancy. Parametrization of the extended CSH3T model was done using the GEMS code and experimental sorption isotherms determined with U(VI) on C-S-H phases (Fig. 5.6). This allowed the end members reported in Table 5.3 to be identified (for details see GAONA et al., 2010). The resulting CSH3T-U model successfully predicted trends in U(VI) uptake by cementitious materials for varying conditions, such as pH dependence (Fig. 5.7) and varying carbonate concentrations (GAONA et al., 2010). The calculations were made for two different U(VI) initial concentrations (10^{-7} M and 3×10^{-4} M). The strong influence of the initial U(VI) concentration, $[U]_0$, on sorption above pH 11, as predicted by the model, is a direct consequence of the non-linear sorption of U(VI) on C-S-H phases. To the best of our knowledge this is the first thermodynamic model which allows the predictive modelling of U(VI) immobilization in a degrading cementitious near field of a repository over the pH range ~ 13.5 to ~10 (Fig. 5.7).

Table 5.3: *Final selection of U(VI) end members and their corresponding G^0_{298} values included in the CSH3T-U model.*

| End member	Bulk formula	G^0_{298} (kJ·mol^{-1})
TobH	$(CaO)_2(SiO_2)_3(H_2O)_5$	-5121.92
T5C	$(CaO)_{2.5}(SiO_2)_{2.5}(H_2O)_5$	-5036.18
T2C	$(CaO)_3(SiO_2)_2(H_2O)_5$	-4931.88
T5U	$(CaO)_2(UO_3)_1(SiO_2)_{2.5}(H_2O)_5$	-5867.00
T2U	$(CaO)_2(UO_3)_{1.5}(SiO_2)_2(H_2O)_5$	-6011.30
TCU	$(CaO)_3(UO_3)_{1.5}(SiO_2)_2(H_2O)_{5.5}$	-6806.42
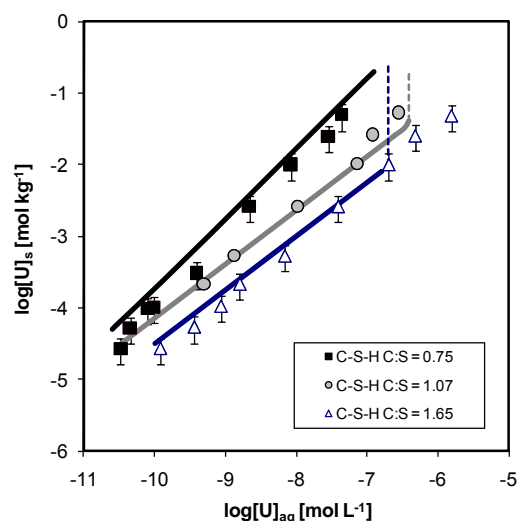
Fig. 5.6: *Experimental (symbols) and modelled (solid lines) of U(VI) sorption isotherm on C-S-H phases with C:S = 0.75, 1.07 and 1.65 in alkali-free porewaters. Dashed lines indicate the calculated solubility of CaUO$_4$(s). Experimental data were taken from TITS et al. (2008). End members of the CSH3T-U model are given in Table 5.3.*
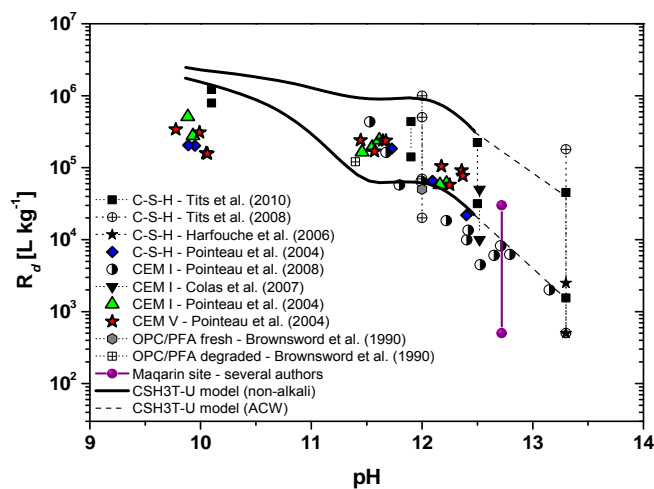
Fig. 5.7: *Comparison of the experimental R_d values for U(VI) on C-S-H phases, cement and the "cemented zone" of the Maqarin site with data predicted using the CSH3T-U model in the pH range 10 – 13.3. Model calculations were carried out for $[U]_0 = 10^{-7}$ M (upper bound) and 3×10^{-4} M (lower bound) and S/L = 5 g L^{-1}. Note that $[U]_0$ and the S/L ratio are the only parameters which can be varied in the modelling. The experimental data for the cementitious systems were taken from various sources (see legend). The measurements from the Maqarin site were reported in SMELLIE (1998) and LINKLATER et al. (1996).*

5.6   References

BROWNSWORD M., BUCHAN A.B., EWART F.T., MCCROHON R., ORMEROD G.J., SMITH-BRIGGS J.L., THOMASON H.P. (1990)
The solubility and sorption of uranium (VI) in a cementitious repository. Mat. Res. Soc. Symp. Proc. 176, 577-582.

COLÀS E., GRIVÉ M., GAONA X., DURO L., ROJO I., ROVIRA M., MARTI V., DE PABLO J. (2007)
Uptake of U(VI) by hydrated and degraded cement. Geochim. Cosmochim. Acta 71, A181.

HARFOUCHE M., WIELAND E., DÄHN R., FUJITA T., TITS J., KUNZ D., TSUKAMOTO M. (2006)
EXAFS study of U(VI) uptake by calcium silicate hydrates. J. Colloid Interface Sci. 303, 195-204.

GAONA X., KULIK D.A., MACÉ N., WIELAND E. (2010)
Aqueous-solid solution thermodynamic model of U(VI) uptake in C-S-H phases. Geochim. Cosmochim. Acta (submitted).

HUMMEL W., BERNER U., CURTI E., PEARSON F.J., THOENEN T. (2002)
Nagra/PSI chemical thermodynamic data base 01/01. Universal Publishers, Florida, USA.

KULIK D.A. (2010)
Improving the structural consistency of C-S-H solid solution thermodynamic models. Cem. Concr. Res. (submitted).

LINKLATER C.M., ALBINSSON Y., ALEXANDER W.R., CASAS I., MCKINLEY I.G., SELLIN P. (1996)
A natural analogue of high-pH cement porewaters from the Maqarin area of northern Jordan: Comparison of predicted and observed trace-element chemistry of uranium and selenium. J. Contam. Hydrol. 21, 59-69.

MACÉ N., DÄHN R., TITS J., SCHEINOST A., WIELAND E. (2010)
U(VI) sorption on hardened cement paste controlled by calcium silicate hydrates: Evidence from EXAFS. Environ. Sci. Technol. (submitted).

MANDALIEV P., WIELAND E., DÄHN R., TITS J., CHURAKOV S.V., ZAHARKO O. (2010)
Nd(III) uptake mechanisms by 11 Å tobermorite and xonotlite. Appl. Geochemistry 25, 763-777.

POINTEAU I., LANDESMAN C., GIFFAULT E., REILLER P. (2004)
Reproducibility of the uptake of U(VI) onto degraded cement pastes and calcium silicate hydrate phases. Radiochim. Acta 92, 645-650.

POINTEAU I., COREAU N., REILLER P.E. (2008)
Uptake of anionic radionuclides onto degraded cement pastes and competing effect of organic ligands. Radiochim. Acta 96, 367–374.

SASOH M. (2004)
The study for the chemical forms of C-14 released from activated metals. In: L.H. JOHNSON & B. SCHWYN (eds), Proceedings of a workshop on the release and transport of C-14 in repository environments. Nagra unpublished internal report, Nagra, Wettingen, Switzerland, 2004.

SMELLIE J.A.T. (1998)
MAQARIN natural analogue study: Phase III, SKB Technical Report TR-98-01, Vol. 1 and 2, SKB, Stockholm, Sweden.

TITS J., FUJITA T., TSUKAMOTO M., WIELAND E. (2008)
Uranium(VI) uptake by synthetic calcium silicate hydrates. Mater. Res. Soc. Symp. Proc. 1107, 467-474.

TITS J., GEIPEL G., MACÉ N., EILZER M., WIELAND E. (2010)
Incorporation of uranyl into calcium silicate hydrates: A wet chemistry and time-resolved laser fluorescence spectroscopy study. J. Colloid Interface Sci. (submitted).

WIELAND E., VAN LOON L.R. (2002)
Cementitious near-field sorption database for performance assessment of an ILW repository in Opalinus clay. PSI Bericht 03-06, NTB 02-20, Nagra Wettingen, Switzerland.

WIELAND E., HUMMEL W. (2010)
The speciation of ^{14}C in the cementitious near field of a repository for radioactive waste, PSI Internal Report, TM 44-10-01.

WIELAND E. (2010a)
Degradation of organic materials in the near field of a L/ILW repository and impact on hydrated cement, PSI Internal Report, AN 44-10-07.

WIELAND E. (2010b)
Colloids in the cementitious near field of a L/ILW repository: A literature survey, PSI Internal Report, AN 44-10-08.

WIELAND E. (2010c)
Retardation of radionuclides in the cementitious near field: Preliminary evaluation of sorption values, PSI Internal Report, AN 44-10-02.

6 COLLOID CHEMISTRY

C. Degueldre, S. Frick, N. Albarran (guest scientist)

6.1 Introduction

The aim of the colloid sub-program is to understand the role of colloids in the migration of radionuclides in the geosphere. The colloid properties studied are their concentration, size distribution and behaviour under safety relevant conditions. The activities carried out in 2010 in the framework of the Grimsel colloid project: "Colloid Formation and Migration" (CFM), are reported. The focus remained on colloid property investigations using single particle counting (SPC) techniques. The colloid generation investigations were continued. Labeling colloids with Ge was a new activity carried out in collaboration with CIEMAT.

The status of the report on colloid properties in the new sedimentary rock formations written in support of the Sectoral Plan is also given.

6.2 Activities in support of the Sectoral Plan

The focus of the work was to evaluate the colloid properties in the porewaters of Opalinus Clay and Effingen Member, "Brauner Dogger", and Helvetic marls identified as potential host rocks for L/ILW repository. In this work colloid concentrations were characterised on the basis of their size distribution, either quantified experimentally using single particle counting techniques or estimated on the basis of a model. The colloid properties are estimated from systems analogous to the hydrogeochemical systems encountered in the new sedimentary formation considered in the study.

The study includes hydrogeochemical systems ranging from crystalline to sedimentary formations and a summary of the results from previous field studies. The colloid concentrations were analysed as a function of the alkali and alkali earth element concentration in the water. Extrapolations to the salt concentrations in the groundwaters in the new formations were based on the properties of the attachment factor of the clay colloids.

Experimental work is described in which the generation of clay colloids from a compacted pellet in quasi-stagnant water is compared to the sedimentation of the suspension. The results indicate that the size distribution of a colloidal suspension evolves toward a common particle size distribution for both extremes of initial conditions: starting from an almost colloid-free liquid phase on top of a pellet, or starting from a very concentrated colloidal suspension. The size distribution and the morphology of the colloids or aggregates at pseudo-equilibrium have been studied experimentally, for example using scanning transmission x-ray microscopy, and a model has been developed to understand their behaviour. The understanding of the generation of colloids at a clay bed/water interface under quasi-stagnant conditions is crucial in environmental science not only for the development of the formation (sedimentology), but also for the study of the transport of contaminants in aquifers. Included in the report is a discussion on colloid generation and attachment/sedimentation rates explaining why colloid properties are system size dependent under in situ conditions.

The colloid mobility in the Opalinus Clay was evaluated and colloids were found to be of minor relevance. In contrast to the homogeneous Opalinus Clay, the "new" host rocks (Effingen Member, "Brauner Dogger", and Helvetic marls) might contain fracture systems where hydraulic flow governs fluid transport. Based on the science of ground water colloids, and especially the experience gained at Wellenberg and Mont Terri, the colloid mobility in fractured clay rocks with regard to colloid borne radionuclide transport was reviewed. The report gives an expert view on the aspects relevant for the long-term safety of a repository.

6.3 Activities in the CFM project

The CFM project is conducted in the framework of Phase VI (2004 to 2013) of the research program of the Grimsel Test Site (GTS). The main participants are: JAEA, INE/KIT, KAERI, SKB, CRIEPI, POSIVA and NAGRA. LES/PSI and CIEMAT collaborate in this work.

The main aim of the LES contribution is to understand the generation of colloids at a bentonite block/groundwater flow interface with quasi-stagnant water. Experiments are performed, amongst others, to investigate colloid generation rates and mechanisms at the engineered barrier system – host rock boundary under in-situ conditions.

The studied clay is the FEBEX bentonite whose formula is:

$[Si_{7.66}Al_{0.34}][Al_{2.68}Fe_{0.34}Mg_{0.91}]X_{0.8}1O_{20}(OH)_4$ with X = (OH,F,Cl) and has a molecular weight M = 745.03 g mol^{-1}. The Al in the bentonite colloids, 81.49 g per mol of clay, was analysed and used as a quasi "natural" tracer to measure the breakthrough curves

The breakthrough curve recorded in February 2010 (homologue test run 10 - 01) for the clay colloids in a 6.08 m long dipole flow field did not yield any valuable data. This was due to the too slow flow rate which resulted in a large dilution and consequently in a too low colloid maximum peak concentration: 30'000 ml^{-1} nm^{-1} compared to a background level of 10'000 ml^{-1} nm^{-1} in the Grimsel groundwater.

In contrast, the breakthrough curve recorded in October 2010 (homologue test run 10 - 03) for the clay colloids in the same set up was very successful, see Fig. 6.1. The injection volume of the clay suspension was 2 L. The analysis of the source clay suspension cocktail was carried out for Al: 9.60±0.05 mg L^{-1} (105 mg L^{-1} bentonite colloids) as well as for the homologue tracers: Eu, Tb, Hf and Th. The colloid analysis via LIBD revealed that the bentonite concentration was 120±10 mg L^{-1}, with an average colloid size of 110±10 nm (back calculated from 1:1000 dilution). For the run 10-03, the clay colloids reached a maximum after about 5790±45 min and came after uranine (4500±45 min). There was no significant colloid size effect for all sizes between 50 and 1000 nm (see Fig. 6.1). LES found a maximum colloid size range of 100 - 150 nm (before injection and after breakthrough) and INE/KIT a colloid size range of 110±10 nm (before injection and after breakthrough). The Al peak (indicator element for clay colloids) was recorded after 5790±45 min. The Th and Hf (homologue elements absorbed on the clay) peaks were also recorded after 5790±45 min after the injection in the dipole.

In the laboratory, both generation and sedimentation processes of bentonite colloids in water were examined using the SPC technique. These activities were published.
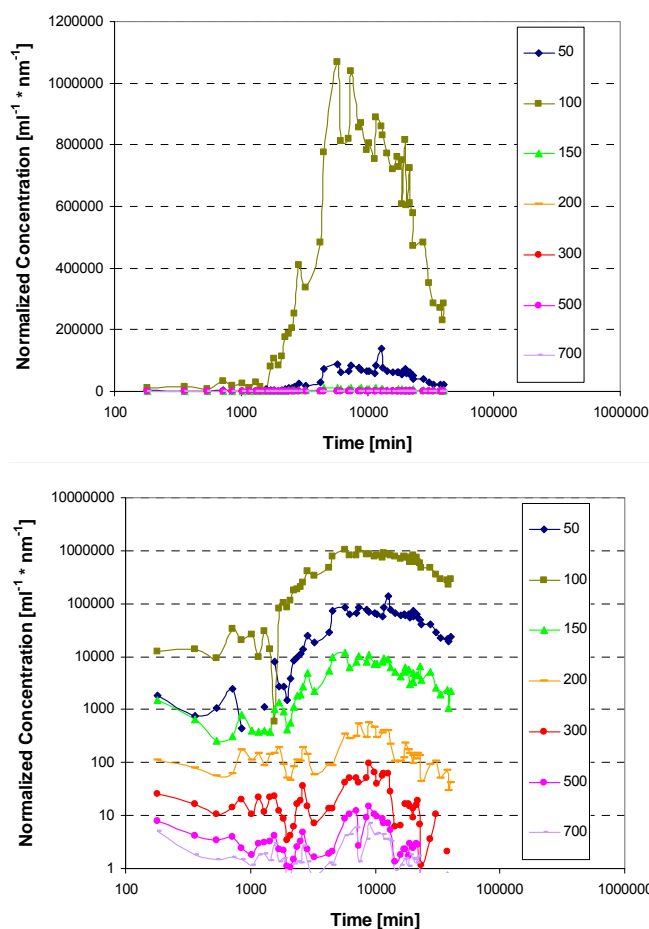

Fig. 6.1: LES SPC breakthrough data of the colloids from the October 2010 homologue test run 10-03. Size analysis shows no apparent chromatographic effects for the larger size fraction (50 – 1000 nm) of the clay colloids.

Other strategies are currently being studied, including labeling the FEBEX clay particles with Ge. FEBEX clay doped with GeCl$_4$ (evaporation) and/or doped with ^{68}Ge can be analysed by ICP-MS and/or detected by scintillation counting (samples extracted from breakthrough test) or by Positron Emission Tomography (imaging during breakthrough). Ge bentonite studies included TEM/EDS/EELS, XSTM, XAFS, SPC and the dialysis of suspensions. These tests were carried out in co-operation with CIEMAT. The EXAFS spectrum of Ge labeled bentonite produced by GeCl$_4$ evaporation (Fig. 6.2) shows that the bentonite was covered by a monolayer of Ge, and not by multilayers.

a)

b)
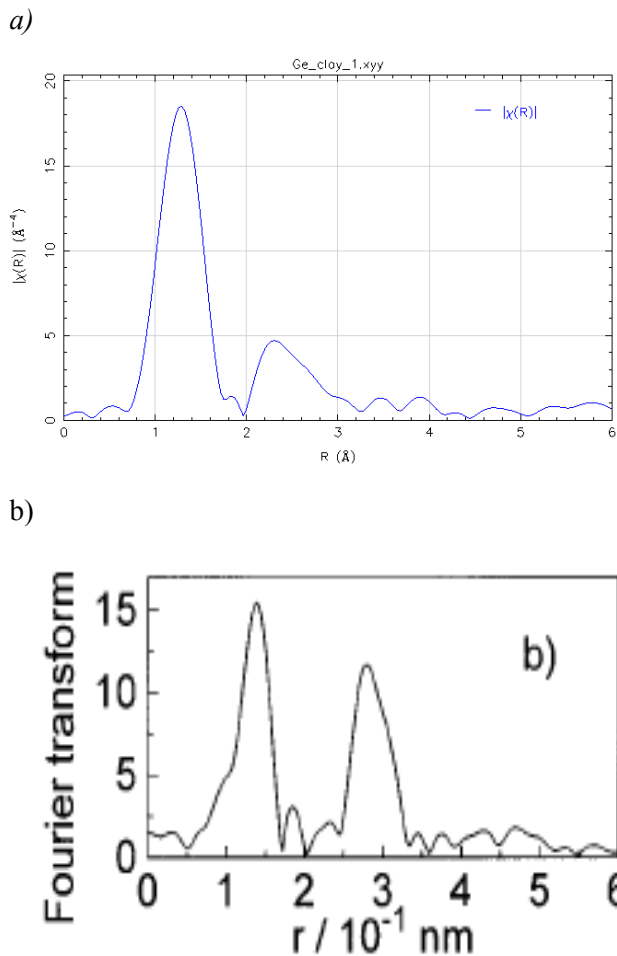
Fig. 6.2: *Fourier transform of k^3 weighted Ge K-edge EXAFS data for (a) data from OKUMURA et al. (1998). Ge doped clay (after analytical washing with water) data recorded at the SNBL@ESRF and (b) GeO$_2$, conditions: transform performed from k = 2 to 10 Å^{-1}.*

6.4   Future work

New homologue tests are foreseen in 2011, and PCS will be used together with other techniques for characterizing colloids during breakthrough. The intention is to vary the flow rate from one experiment to another. For the CFM project, the generation of colloids at a bentonite block/groundwater flow interface with quasi-stagnant water is being studied from a mechanistic point of view. The existing "in house" model will be used to describe colloid generation during the main experiment (BESSHO & DEGUELDRE, 2009).

6.5   References

BESSHO K., DEGUELDRE C. (2009)
Generation and sedimentation of colloidal bentonite particles in water. Appl. Clay Sci. 43, 253-259.

OKUMURA K., ASAKURA K., IWASAWA Y. (1998)
Reversible structure change of one-atomic layer GeO$_2$ on SiO$_2$ surface under the interaction with Rh particles by in situ XAFS studies. Catalysis Today 39, 343-350.

7 DIFFUSION PROCESSES

L.R. Van Loon, M.A. Glaus, W. Müller, S. Frick, N. Diaz (postdoc)

7.1 Overview

The focus of the activities in the Diffusion Processes Group lie in i) understanding the diffusion mechanism(s) of radionuclides in compacted argillaceous materials and ii) measuring diffusion parameters (effective diffusion coefficients and rock capacity values) which can be used in PA studies.

Within the framework of the Sectoral Plan diffusion measurements with HTO, $^{36}Cl^-$ and $^{22}Na^+$ on the potential host rocks, Helvetic marls, "Brauner Dogger" and Effingen Member were performed. The measurements were used to check the validity of the extended Archie's relation for estimating effective diffusion coefficients. On June 1st, 2010 the new EU 7th Framework project CatClay officially started. The project focuses on the diffusion of strongly sorbing radionuclides in argillaceous rocks.

The 2 PhD students, whose projects are mainly based at the large facilities of PSI (SINQ and SLS), made good progress in 2010 and the first publications are in preparation.

The work on pure clay minerals (TRAPHICCS) was continued. The work focused on diffusion measurements of bivalent anions ($^{75}SeO_4^{2-}$ and $^{35}SO_4^{2-}$) and on $^{134}Cs^+$. Unlike $^{36}Cl^-$, both anions showed significant retention in the compacted clay. The effective diffusion coefficients for bivalent anions are lower than for the monovalent anions. The diffusion results for $^{134}Cs^+$ showed a larger retention than estimated from batch sorption experiments.

7.2 Activities in support of the Sectoral Plan

Diffusion experiments with HTO, $^{36}Cl^-$ and $^{22}Na^+$ on potential host rocks such as Effingen Member, Helvetic marls and "Brauner Dogger" were performed. The main aim of the measurements was to check the validity of the extended Archie's relation for estimating effective diffusion coefficients. The only parameter required for this estimation is the accessible porosity. Fig. 7.1 shows some experimental data for Effingen Member and Helvetic marls together with the plotted extended Archie's relation (VAN LOON et al., 2011). Within the uncertainty range indicated (dashed lines), the experimental data can be described by the relation:
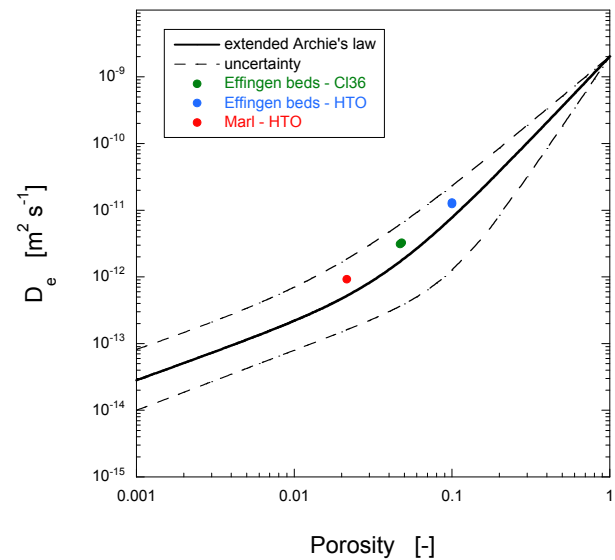

Fig. 7.1: Extended Archie's relation (solid line) describing the relationship between the diffusion accessible porosity and the effective diffusion coefficients together with experimental data for Effingen Member and Helvetic marls.

$$D_e = D_w \cdot \varepsilon^m + A \cdot \varepsilon^n \qquad (1)$$

where:

D_w = diffusion coefficient in bulk water

m = 2.5 (min. value = 2; max. value = 3.5)

A = 1 x 10^{-11} m^2 s^{-1} (min. value = 5 x 10^{-12} m^2 s^{-1}; max. value = 2 x 10^{-11} m^2 s^{-1})

n = 0.85 (min. value = 0.8; max. value = 0.9)

7.3 CatClay

A new EU 7th Framework project CatClay started on June 1st, 2010. The project focuses on the diffusive behaviour of strongly sorbing tracers, i.e. tracers that sorb via surface complexation. The outcome of the previous EU 6th Framework project FUNMIG clearly indicated that there was a lack of understanding on the diffusive behaviour of such radiotracers. The project is subdivided in 3 Work Packages (WP1: modelling; WP2: studies on illite; WP3: studies on host rocks). LES is mainly involved in WP2 and WP3. In the framework of WP2, a large batch of illite du Puy was purified and conditioned and distributed to different participants in CatClay, i.e. BRGM, SCK-CEN and

KIT. A thorough characterisation of the conditioned illite will be carried out by BRGM. After this, diffusion and sorption studies on illite will be started.

In the framework of WP3, some preliminary in-diffusion experiments with ^{60}Co(II) in OPA were performed. Small drill cores embedded in an epoxy resin were used (Fig. 7.2). After in-diffusion, the tracer profile in the samples was analysed using a modified version of the abrasive peeling technique.
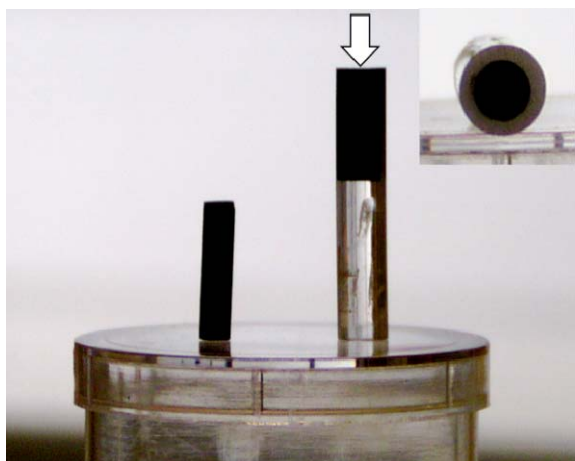

Fig. 7.2: *Small OPA bore cores embedded in epoxy resin were used for the ^{60}Co(II) diffusion experiments. The white arrow indicates the diffusion direction into the sample.*
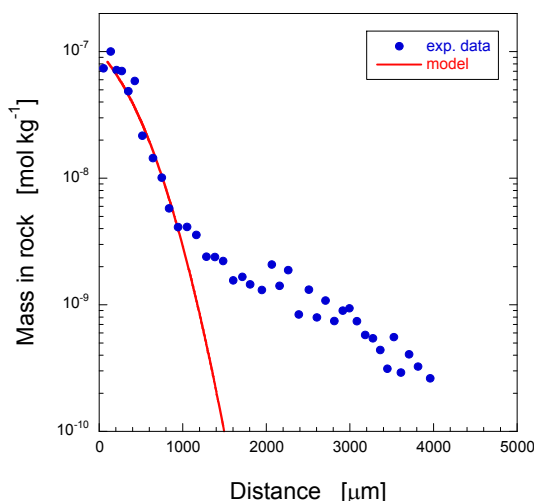

Fig. 7.3: *Diffusion of ^{60}Co(II) in OPA. The profile shows that Co(II) diffuses deeper into OPA than calculated using a sorption value taken from batch measurements ($D_e = 4 \times 10^{-11}$ m^2 s^{-1}; $K_d = 230$ ml g^{-1}). The source concentration in the solution was 3×10^{-10} M. At this low concentration the sorption can be assumed to be linear.*

The experiment clearly shows that Co(II) diffuses faster than expected (Fig. 7.3). This may be due to the presence of Fe(II) in the porewater competing with Co(II) for the sorption sites (see PFINGSTEN et al., 2010), resulting in a higher apparent diffusion coefficient (Fe(II) arises from the siderite in OPA). Modelling with the reactive transport code MCOTAC-sorb and PHREEQC are ongoing. First results indeed indicate that the presence of Fe(II) has a significant effect on the diffusion rate of Co(II) in OPA.

7.4 Assessment of heterogeneities (Amicam)

This project is performed in close co-operation with the Transport Modelling Group. Details on the project can be found in Chapter 3 of this report.

7.5 Dynamics of water in compacted montmorillonite (PhD project M. Bestel)

In highly compacted Na-montmorillonite the water is located mainly in the interlayer, or close to the external surfaces of the clay platelets. A previous study performed in LES indicated that 2-D diffusion could probably be measured with neutron scattering (GONZALEZ, 2007). New neutron scattering measurements performed on Na-montmorillonite at the TOFTOF time-of-flight spectrometer at FRM-II in Germany confirmed that diffusion in highly compacted Na-montmorillonite ($\rho = 1800$ kg m^{-3}) is indeed 2-D.

Quantification of different types of water, i.e. interlayer water and water in macropores, was done on the neutron backscattering spectrometer, Spheres (FRM-II, Germany). The intensity of elastically scattered neutrons measured as a function of the temperature provides a good approximation of the amount of "static" hydrogen, i.e. hydrogen present in a solid phase such as "ice" (Fig. 7.4). The jump in intensity for Na-montmorillonite ($\rho = 1300$ kg m^{-3}) below 270 K is due to the freezing of bulk-like water in the macropores. Water in the interlayer is confined, and can be significantly undercooled, resulting in a further intensity increase below 255 K. The difference in intensity between the two plateaus at the highest and lowest temperature is proportional to the total amount of water. For the Na-montmorillonite with a bulk dry density of 1800 kg m^{-3}, no sudden increase in intensity can be observed below 270 K. This indicates that at 1800 kg m^{-3} there is essentially no free bulk-like water present, and all of the water is in the interlayer.
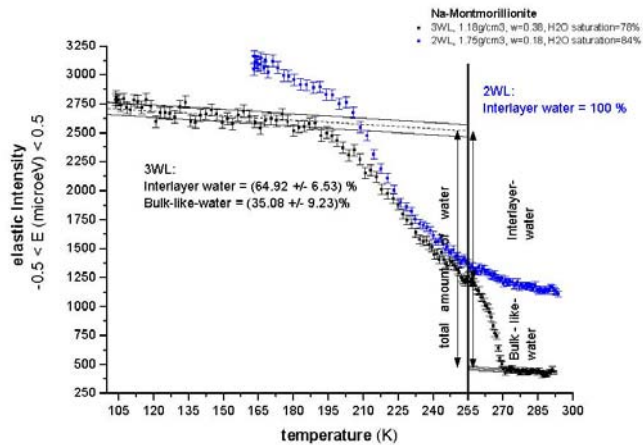
Fig. 7.4: *Amount of "immobile" hydrogen in Na-montmorillonite as a function of temperature. The intensity of the elastically scattered neutrons is proportional to the amount of immobile hydrogen, i.e. hydrogen present in "ice". Black symbols represent Na-montmorillonite with a bulk dry density of 1300 kg m⁻³, and the blue symbols represent Na-montmorillonite with a bulk dry density of 1800 kg m⁻³.*

Complementary neutron diffraction studies showed the presence of hexagonal ice (ice Ih) below 270 K at low dry densities. At higher bulk dry densities, only amorphous ice could be detected. The formation of hexagonal ice is typical for freezing of bulk water (FLETCHER, 1970) and indicates the presence of bulk-like-water in macro pores. This is consistent with the results of the neutron scattering studies.

7.6　Micro-heterogeneous systems (PhD project H. Wang)

Micro-heterogeneity is an inherent and highly relevant characteristic of most natural and engineered (geo-) materials. Obtaining – with high spatial resolution – quantitative chemical and molecular information on such materials is scientifically important and challenging. A project has been started on the use of Laser Ablation Inductively Coupled Plasma Mass Spectrometry (LA ICP-MS) and Micro X-ray fluorescence (microXRF) for measuring shallow diffusion profiles in heterogeneous materials such as Opalinus Clay.

Calibration of microbeam techniques with appropriate standards is very important for quantitative analysis.

Different standard materials for Cs-analysis by LA ICP-MS and microXRF were prepared. A standard addition approach based on mill-mixing of homogenised geo-material and additions of known Cs-bearing minerals turned out to have its limitations due to considerable spatial heterogeneity (in the range of few μm) of the resulting material. The dilution (distribution) of Cs-containing mineral grains in the Cs-free geo-materials resulted in pronounced hot spots. As an optimisation measure, a wet chemical preparation method based on the adsorption of aqueous Cs cations onto the surface of geo-material powder obtained by ball milling was tried. A significant improvement in standard homogeneity was established. However, inherent in any standard material based on powder particles, is grain-to-grain heterogeneity and the corresponding grain size distribution. This limits the applicability of such standard materials for calibrations of micro-beam techniques. A commonly used standard preparation method is to produce a melt based on reference material diluted in a $Li_2B_4O_7$ matrix. The homogeneity of such melts on the micrometer-scale, as well as potential matrix effects due to the dilution, are currently under investigation.

A novel cross-calibration approach, combining complementary measurements done by independent techniques, was studied and applied to heterogeneous OPA samples (WANG et al., 2010). By mapping an $800 \times 800 \ \mu m^2$ area, chemical micro-images were produced for the elements Cs, Ca, Fe, and Ti (Figs. 7.5a-h). The images obtained by microXRF show higher spatial resolution, but the quantification accuracy is limited due to the lack of appropriate matrix-matched calibration standards. In contrast, the images taken by LA-ICP-MS have a coarser spatial resolution, but the application of a 100% mass normalization results in an enhanced quantitative robustness. A comparison of the corresponding elemental images obtained by the two independent techniques yielded a high level of agreement. Characteristic spatial distribution patterns were readily apparent in either one of the two images. Consequently, by combining the complementary information content of the two images, a chemical image with high spatial resolution image and improved quantitative reliability could be obtained.
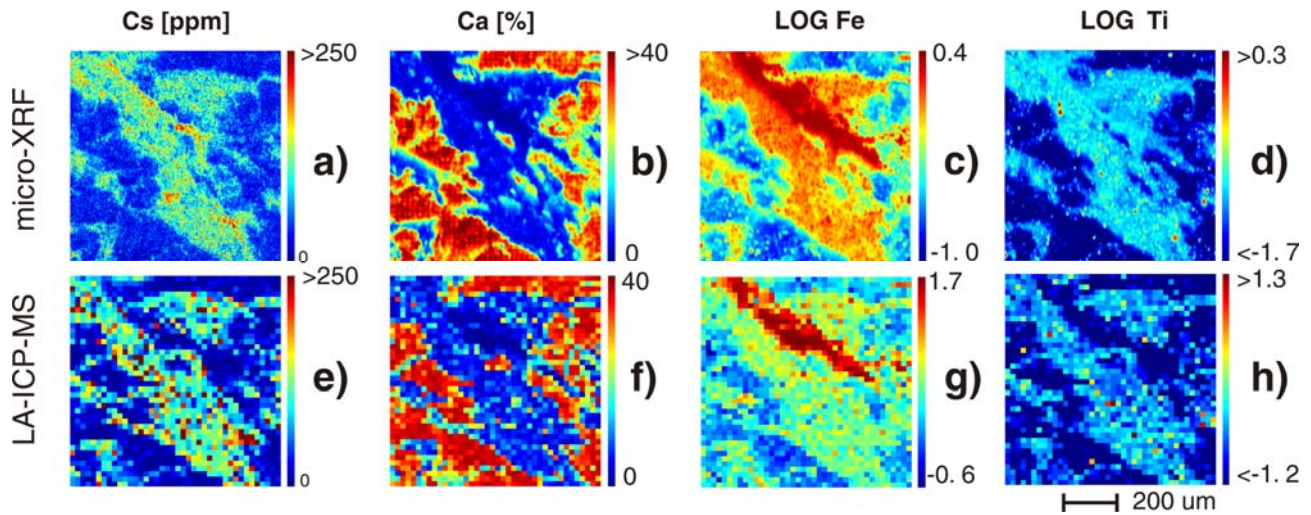
Fig. 7.5: Comparison of elemental images obtained from LA-ICP-MS and microXRF (WANG et al., 2010).

7.7 Transport phenomena in compacted clay systems (TRAPHICCS)

The diffusion experiments using SO_4^{2-} and SeO_4^{2-} in compacted Na-montmorillonite were completed by out-diffusion experiments. The diffusion experiments were carried out at a high compaction (bulk dry density of ~1900 kg m^{-3}) and with different external solution salinities (0.1 M, 0.5 M and 1.0 M NaClO$_4$). These experiments served two purposes; on the one hand to investigate the diffusive behaviour of bivalent anions, on the other hand to obtain diffusion data on the safety-relevant radionuclide SeO_4^{2-} species. Owing to the expected strong exclusion of these anions from the interlayer porosity, and the relatively fast decay of the radioactive tracers used (half lives of ~87 d for $^{35}SO_4^{2-}$ and 119 d for $^{75}SeO_4^{2-}$), long experimental times and measurements near the detection limits had to be expected, and inevitably generated larger experimental uncertainties than is typically encountered with "simple" tracers.

The diffusion parameters (effective diffusion coefficients, D_e, and rock capacity factors, α) obtained from the through-diffusion experiments are summarised in Table 7.1. A clear trend of increasing D_e and α values with increasing salinity is apparent. The experimentally determined flux curves are shown in Fig. 7.6. As already observed for monovalent anions such as Cl$^-$ or I$^-$, the results of the out-diffusion experiments (not shown) deviated from the expected behaviour in that the flux at the original tracer reservoir side was much higher than expected from a steady-state distribution of the tracer across the clay sample. This behaviour can partly be explained by the

heterogeneous distribution of porosity (GLAUS et al., 2011). However, in the case of the bivalent anions investigated here, additional reasons are needed to explain the deviations in the behaviour in the out-diffusion tests. A possible explanation could be found in the accumulation of the tracer in the solid, either by isotopic exchange with a trace mineral impurity or by incorporation in a solid solution. Such a hypothesis is supported by the disproportionate increase in α, particularly for the SO_4^{2-} data (cf. Table 7.1). For non-sorbing tracers, for which the equality $\alpha = \varepsilon_{acc}$ (accessible porosity) applies, a functional dependence between D_e and ε_{acc} exists according to the Archie's relation (cf. section 7.3):

$$\varepsilon_{acc} = \sqrt[m]{\frac{D_e}{A}} \qquad (2)$$

Using the parameter values for m and A published for compacted Na-montmorillonite (GLAUS et al., 2010), hypothetical values for $\alpha = \varepsilon_{acc}$ were obtained for the non-sorbing case. A comparison with the measured values (Table 7.1) shows that the latter are much larger than the predicted values, particularly at high salinities.

Another unexplained feature of the experiments with SO_4^{2-} and SeO_4^{2-} are the differences in D_e values. The diffusion coefficients for diffusion in bulk water of these two anions are almost identical (VLAEV et al., 2005; LI & GREGORY, 1974). A possible explanation for the differences could be the formation of ion pairs, which may be favoured to form at the low water activities in the interlayers of the clay.

Table 7.1: *Overview of diffusive properties of sulphate and selenate obtained from through-diffusion experiments. The results for chloride are shown for the purpose of comparison with a monovalent anion.*

Tracer	Salinity [M]	D_e [m^2 s^{-1}]	α [-]	ε_{acc} [a]
$^{35}SO_4^{2-}$	0.1	$(6 \pm 2) \times 10^{-15}$	0.006 ± 0.002	0.005
	0.5	$(7 \pm 2) \times 10^{-14}$	0.4 [b]	0.018
	1.0	$(1.2 \pm 0.3) \times 10^{-13}$	0.6 ± 0.3	0.025
$^{75}SeO_4^{2-}$	0.1	$(2.3 \pm 0.4) \times 10^{-14}$	0.03 ± 0.01	0.010
	0.5	$(3.6 \pm 0.6) \times 10^{-14}$	0.06 ± 0.02	0.013
	1.0	$(5.8 \pm 0.7) \times 10^{-14}$	0.07 ± 0.02	0.016
$^{36}Cl^-$ [c]	0.1	$(7.2 \pm 0.8) \times 10^{-14}$	0.019 ± 0.002	0.019
	0.5	$(2.5 \pm 0.4) \times 10^{-13}$	0.036 ± 0.001	0.037
	1.0	$(4.7 \pm 0.5) \times 10^{-13}$	0.051 ± 0.007	0.052

[a] Calculated under the assumption of no interaction between the tracer and the solid from D_e using equation 2.
[b] Uncertainty not determined because of deviant flux curve.
[c] GLAUS et al., 2010
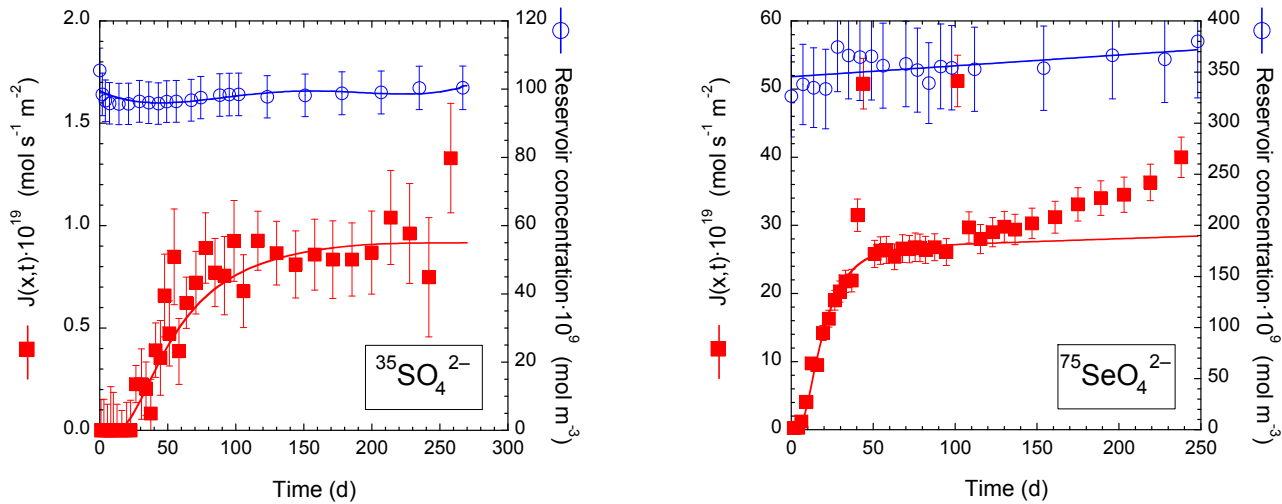
Fig. 7.6: *Breakthrough curves and reservoir concentrations for the through-diffusion of sulfate and selenate in Na-montmorillonite (dry bulk density of ~1900 kg m^{-3}) measured in 0.1 M NaClO$_4$ as the external solution*

Although the tendency to form ion pairs for SO$_4^{2-}$ and SeO$_4^{2-}$ are relatively similar (PARKER et al., 1997), small differences could be amplified because the formation of ion pairs alters the electrostatic attraction or repulsion of these ions, which would have direct consequences on the accessible porosity. Although no mechanistic explanations for the differences in behaviour between SO$_4^{2-}$ and SeO$_4^{2-}$ can be given, two conclusions can be drawn from the experiments: (i) bivalent anions have lower diffusion coefficients in swelling clays than mono-valent anions and (ii) their interaction with even trace levels of some of the mineral phases present may lead to a retarded break-through.

The evaluation of the in-diffusion experiments of ^{134}Cs$^+$ in Na-montmorillonite compacted to a bulk dry density of 1600 kg m^{-3} were also finished during the current year. These experiments were carried out at different external solution salinities and three different initial input concentrations of Cs (~10^{-7}, ~10^{-4} and ~10^{-2} M). Only the results obtained at "trace concentrations" (~0.1 μM) of Cs$^+$ gave a consistent picture between the measured diffusion front in the solid and the decrease of tracer concentration in the liquid reservoir. An example for 1.0 M NaClO$_4$ is shown in Fig. 7.7
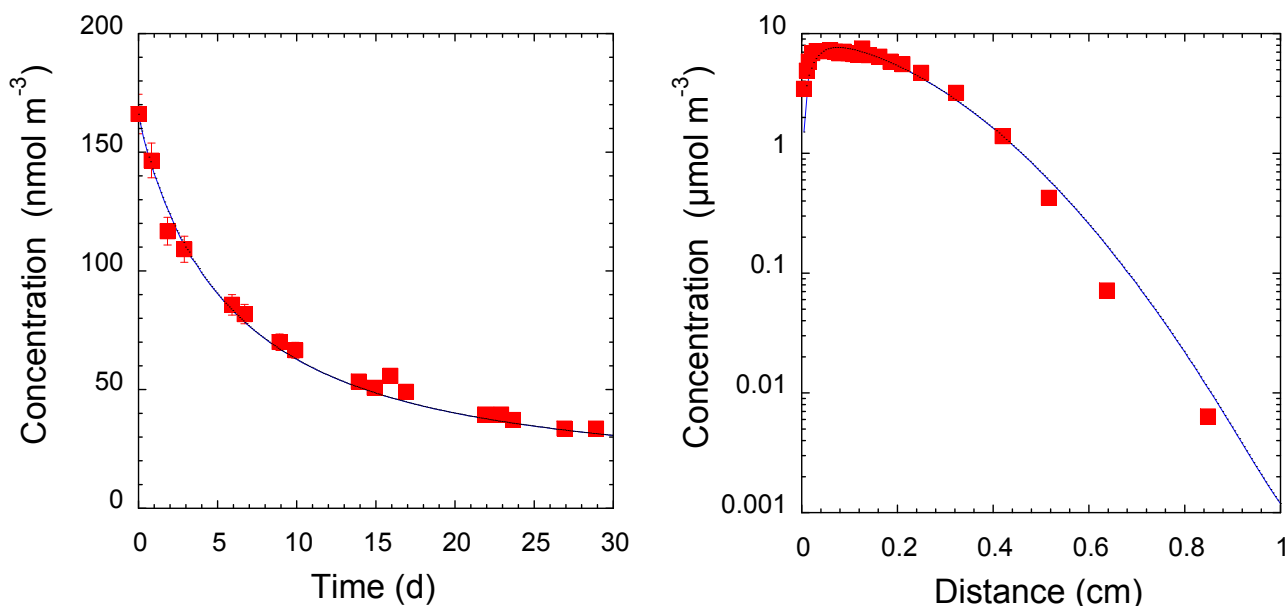
Fig. 7.7: *In-diffusion of $^{134}Cs^+$ in Na-montmorillonite (1600 kg m^{-3}) in a 1.0 M NaClO$_4$ external solution. No stable Cs was added to the system. The concentration in the reservoir solution was governed by the content of stable Cs in the stock solution of the radioactive tracer. The left-hand plot shows the concentration in the reservoir solution, the right-hand plot the concentration in the clay sample (mass per volume of clay).*

As expected from the experiments with other cations (Na$^+$ or Sr^{2+}), the D$_e$ values for the diffusion of $^{134}Cs^+$ were higher than those of HTO measured under comparable conditions (GLAUS et al., 2007). The mobility of Cs$^+$ ions in the interlayer porosity of the clay, and the quantity sorbed as the driving force for diffusion, are the presently favoured explanations for the large D$_e$ values. The experiments at higher levels of stable Cs could not be modelled with a simple single-species diffusion model. The slices of clay sampled were not only analysed for $^{134}Cs^+$, but also for Na$^+$, K$^+$, Ca^{2+}, Mg^{2+} and Cs$^+$ by cation chromatography. The analyses revealed that these cations were inhomogeneously distributed in the clay samples in the direction of diffusion. A homogeneous distribution is, however, required for an evaluation of the experiments with a single-species model. One important unknown in such experiments is the functional dependence of sorption distribution ratios on the degree of compaction (cf. VAN LOON & GLAUS, 2007). Unfortunately a series of batch sorption experiments using compacted clay samples at dry bulk densities between 1300 and 2100 kg m^{-3} were unsuccessful (the reason is not clear.) Repeating these experiments and continuing the in-diffusion experiments are activities foreseen for the coming years. Similar experiments are also planned for Na-illite as a model system for the evaluation of the more complex diffusion experiments with $^{134}Cs^+$ in OPA.

7.8 References

FLETCHER N.H. (1970)
The chemical physics of ice. Cambridge University Press, 271 pp.

GLAUS M.A., BAEYENS B., BRADBURY M.H., JAKOB A., VAN LOON, L.R., YAROSCHCHUK, A. (2007)
Diffusion of ^{22}Na and ^{85}Sr in montmorillonite: evidence of interlayer diffusion being the dominant pathway at high compaction. Environ. Sci. Technol. 41, 478-485.

GLAUS M.A., FRICK S., ROSSÉ R., VAN LOON L.R. (2010)
Comparative study of tracer diffusion of HTO, ^{22}Na$^+$ and ^{36}Cl$^-$ in compacted kaolinite, illite and montmorillonite. Geochim. Cosmochim. Acta 74, 1999-2010.

GLAUS M.A., FRICK S., ROSSÉ R., VAN LOON L.R. (2011)
Consistent interpretation of the results of through-, outdiffusion and tracer profile analysis for tracer diffusion of chloride in compacted montmorillonite. Submitted to J. Contam. Hydrol.

VLAEV L.T., NIKOLOVA M.M., GOSPODINOV G.G. (2005)
Electrotransport properties of ions in aqueous solutions of H$_2$SeO$_4$ and Na$_2$SeO$_4$. J. Struct. Chem. 46, 633–640.

GONZÁLEZ F. (2007)
Water diffusion through compacted clays analyzed by neutron scattering and tracer experiments. PhD. Thesis, University of Bern, Bern, Switzerland.

LI Y.H., GREGORY S. (2007)
Diffusion of ions in sea water and in deep-sea sediments. Geochim. Cosmochim. Acta 38, 703–714.

PARKER D.R., TICE K.R., THOMASON D.N. (1997)
Effects of ion pairing with calcium and magnesium on selenate availability to higher plants. Environ. Toxicol. Chem. 16, 565–571.

PFINGSTEN W., BRADBURY M.H., BAEYENS B. (2010)
The influence of Fe(II) competition on the sorption and migration of Ni(II) in MX-80 bentonite. Appl. Geochem. (submitted).

VAN LOON L.R., MIBUS J., MÜLLER W. (2011)
The use of an extended version of Archie's law for estimating effective diffusion coefficients of radionuclides in argillaceous rocks. Appl. Geochem. (in preparation).

VAN LOON L.R., GLAUS M.A. (2007)
Mechanical compaction of smectite clays increases ion exchange selectivity for cesium. Environ. Sci. Technol. 42, 1600–1604.

WANG H.A.O., GROLIMUND D., GÜNTHER D., VAN LOON L.R., BARMETTLER K., BORCA C.N., AESCHLIMANN B. (2010)
Chemical imaging of element diffusion into heterogeneous media using synchrotron micro-XRF, LA-ICP-MS, and EXAFS spectroscopy. Environ. Sci. Technol. (in preparation)

8 PUBLICATIONS

8.1 Peer reviewed journals

ABOLHASSANI S., BART G., JAKOB A. (2010)
Examination of the chemical composition of irradiated zirconium based fuel claddings at the metal/oxide interface by TEM. J. Nucl. Mat. 399, 1-12

APPELO C.A.J.[1], VAN LOON L.R., WERSIN P.[2] (2010)
Multicomponent diffusion of a suite of tracers (HTO, Cl, Br, I, Na, Sr, Cs) in a single sample of Opalinus Clay. Geochim. Cosmochim. Acta. 74, 1201-1219
[1] Hydrochemical Consultant, Amsterdam, The Netherlands
[2] Gruner AG, Basel, Switzerland

CHURAKOV S.V., KOSAKOWSKI G. (2010)
An ab initio molecular dynamics study of hydronium complexation in Na-Montmorillonite. Philos. Mag. 90, 2459-2474

CURTI E., FUJIWARA K.[1], IIJIMA K.[1], TITS J., CUESTA C., KITAMURA A.[1], GLAUS M.A., MÜLLER W. (2010)
Radium uptake during barite recrystallization as a function of solution composition at 23±2°C: An experimental ^{133}Ba and ^{226}Ra tracer study. Geochim. Cosmochim. Acta 74, 3553-3570
[1] JAEA, Tokai, Japan

FILELLA M.[1], HUMMEL W. (2010)
Trace element complexation by humic substances: issues related to quality assurance. Accred. Qual. Assur. Published online: 23 October 2010, DOI 10.1007/s00769-010-0716-3
[1] University of Geneva, Switzerland

GLAUS M.A., FRICK S., ROSSÉ R., VAN LOON L.R. (2010)
Comparative study of tracer diffusion of HTO, ^{22}Na$^+$ and ^{36}Cl$^-$ in compacted kaolinite, illite and montmorillonite. Geochim. Cosmochim. Acta 74, 1999-2010

KULIK D.A., VINOGRAD V.L.[1], PAULSEN N.[1], WINKLER B.[1] (2010)
(Ca,Sr)CO$_3$ aqueous- solid solution systems: From atomistic simulations to thermodynamic modeling. Phys. Chem. Earth 35, 217-232
[1] University of Frankfurt, Frankfurt-am-Main, Germany

MANDALIEV P., DÄHN R., TITS J., WEHRLI B.[1], WIELAND E. (2010)
EXAFS study of Nd(III) uptake by amorphous calcium silicate hydrates (C-S-H). J. Colloid Interface Sci. 342, 1-7
[1] ETH, Zürich, Switzerland

MANDALIEV P., WIELAND E., DÄHN R., TITS J., CHURAKOV S.V., ZAHARKO O. (2010)
Nd(III) uptake mechanisms by 11 Å tobermorite and xonotlite. Appl. Geochem. 25, 763-777

MARQUES FERNANDES M, STUMPF T.[1], BAEYENS B., WALTHER C.[1], BRADBURY M.H. (2010)
Spectroscopic identification of ternary Cm-carbonate surface complexes. Environ. Sci. Technol. 44, 921–927
[1] KIT INE Karlsruhe, Germany

PURANEN A.[1], JONSSON M.[1], DÄHN R., CUI D.[2] (2010)
Reduction of selenite and selenate on anoxically corroded iron and the synergistic effect of uranyl reduction. J. Nucl. Mater. 406, 230-237
[1] KTH, Stockholm, Sweden
[2] Studsvik Nucl AB, Nykoping, Sweden

ROZOV K., BERNER U., TAVIOT-GUÉHO C.[1], LEROUX F.[1], RENAUDIN G.[1], KULIK D.A., DIAMOND L.W.[2] (2010)
Synthesis and characterization of the LDH hydrotalcite–pyroaurite solid-solution series. Cem. Concr. Res. 40, 1248-1254
[1] Université Blaise Pascal, Aubière, France
[2] University of Bern, Bern, Switzerland

WIELAND E., MACÉ N., DÄHN R., KUNZ D., TITS J. (2010)
Macro- and micro-scale studies on U(VI) immobilization in hardened cement paste. J. Radioanal. Nucl. Chem. 286, 793-800

WIELAND E., DÄHN R., VESPA M.[1], LOTHENBACH B.[2] (2010)
Micro-spectroscopic investigations of Al and S speciation in hardened cement paste hydrated at 50° C. Cem. Concr. Res. 40, 885-891
[1] ITU, Karlsruhe, Germany
[2] Empa, Dübendorf, Switzerland

8.2 Publications in books

KULIK D.A. (2010)
Geochemical thermodynamic modelling of ion partitioning. In: Ion-partitioning in ambient temperature aqueous systems (Eds. M. Prieto, H. Stoll), EMU Notes in Mineralogy, Vol. 10, Chapter 3, 65-138

8.3 PSI and Nagra NTB reports

BRADBURY M.H., BAEYENS B., THOENEN T. (2010)
Sorption data bases for generic Swiss argillaceous, crystalline and calcareous rock systems, PSI Bericht 10-03

BRADBURY M.H., BAEYENS B., THOENEN T. (2010)
Sorption data bases for generic Swiss argillaceous rock systems, Nagra NTB 09-03 Nagra, Wettingen, Switzerland

BRADBURY, M.H., BAEYENS, B. (2010)
Comparison of the reference Opalinus Clay and MX-80 bentonite sorption databases used in the Entsorgungsnachweis with sorption databases predicted from sorption measurements on illite and montmorillonite. PSI Bericht 10-09 and NTB 09-07, Nagra, Wettingen, Switzerland

8.4 Conference proceedings

HINGERL F.F., WAGNER T.[1], KULIK D.A., DRIESNER T.[1], KOSAKOWSKI G., THOMSEN K.[2] (2010)
Enhanced geothermal systems: influence of thermodynamic data and activity models on predicted mineral precipitation-dissolution reactions. Geochim. Cosmochim. Acta 74, p. A406. Goldschmidt 2010, Knoxville Tennessee, USA, 13-18 June 2010
[1] ETH, Zürich, Switzerland
[2] Technical University of Denmark, Lyngby, Denmark

HINGERL F.F., WAGNER T.[1], KULIK D.A., DRIESNER T.[1], KOSAKOWSKI G., THOMSEN K.[2] (2010)
Sensitivity of predicted scaling and permeability in enhanced geothermal systems to thermodynamic data and activity models. Geophysical Research Abstracts 12, EGU 2010-14657-1, EGU General Assembly 2010, Vienna, Austria, 2-7 May 2010
[1] ETH, Zürich, Switzerland
[2] Technical University of Denmark, Lyngby, Denmark

KULIK D.A., LÜTZENKIRCHEN J.[1], PAYNE T.E.[2] (2010)
Consistent treatment of 'denticity' in surface complexation models. Geochim. Cosmochim. Acta 74, p. A544. Goldschmidt 2010, Knoxville Tennessee, USA, 13-18 June 2010
[1] KIT INE, Karlsruhe, Germany
[2] ANSTO, Menai, Australia

ORLOV A., KULIK D.A., DEGUELDRE C., BART G., KAUFMANN W.[1], VALIZADEH S.[2] (2010)
Corrosion Product Deposits on BWR Cladding: A Comparison of Thermodynamic Modelling Predictions with Experimental Analytical Results. CD Proceedings, p. 8. Nuclear Plant Chemistry Conference 2010, Quebec City, Canada, 3-7 October 2010
[1] Kernkraftwerk Leibstadt AG, Leibstadt, Switzerland
[2] Westinghouse Electric Sweden AB, Wasteras, Sweden

8.5 Conference/Workshop Presentations

AIMOZ L., TAVIOT-GUÉHO C.[1], VESPA M.[2], DÄHN R., LEROUX F.[3], MAEDER U.[4], CURTI E.
Iodine Uptake by Layered Double Hydroxides. 20th General Meeting of the International Mineralogical Association, Budapest, Hungary, 21-27 August 2010
[1] Clermont Université, Aubière, France
[2] KIT INE, Karlsruhe, Germany
[3] K.U. Leuven, Heverlee, ESRF, Grenoble, France
[4] University of Bern, Bern, Switzerland

BERNER U., KOSAKOWSKI G., KULIK D.A.
Reactive transport calculations on the geochemical evolution of cement/clay interfaces. 4th International Meeting on Clays in Natural & Engineered Barriers for Radioactive Waste Confinement, Nantes, France, 29 March–1 April 2010

BRADBURY M.H., BAEYENS B.
Application of the "Bottom Up" approach for the predictive modelling of sorption isotherms for Ni(II), Co(II), Eu(III), Th(IV) and U(VI) on MX-80 bentonite and Opalinus Clay. 4th International Meeting on Clays in Natural & Engineered Barriers for Radioactive Waste Confinement, Nantes, France, 29 March–1 April 2010

CHURAKOV S.V., DÄHN R.
Mechanism of Zn(II) sorption on the edges of montmorillonite. CECAM Workshop "Aqueous Solvation of Ions". ETH Zurich, 22-24 February 2010

CHURAKOV S.V., GIMMI T.
Multi-scale modelling of transport in clays: from ab-initio atomistic to continuum scale. International Symposium Transpore 2010, Villigen PSI, Switzerland, 19/20 August 2010

CURTI E., FUJIWARA K., IIJIMA K., TITS J., CUESTA C., KITAMURA A., GLAUS M.A., MUELLER W.
Ra-barite solid solution formation during recrystallization in aqueous solutions. 20th General Meeting of the International Mineralogical Association, Budapest, Hungary, 21-27 August 2010

DÄHN R., POPOV D., PATTISON P., MÄDER U., WIELAND E.
Application of micro-diffraction to characterise newly formed minerals at interfaces. 20th General Meeting of the International Mineralogical Association, Budapest, Hungary, 21-27 August 2010

DÄHN R., POPOV D., GAONA X., WIELAND E.
Micro-XRF/XAS/XRD investigations on actinide containg waste materials. Plutonium Futures – The Science 2010, Keystone Co, USA, 19-23 September 2010

DIAZ N., VAN LOON L.R., JAKOB A., GROLIMUND D.
Modeling the cesium diffusion front in argillaceous rock: effects of the 3D microstructure. 4th International Meeting on Clays in Natural & Engineered Barriers for Radioactive Waste Confinement, Nantes, France, 29 March–1 April 2010

DIAZ N., CHURAKOV S.V., JAKOB A., VAN LOON L.R., GROLIMUND D.
Cesium diffusion front in argillaceous rock: effects of the 3D microstructure. International Symposium Transpore 2010, Villigen PSI, Switzerland, 19/20 August 2010

DILNESA B.Z.[1,2], LOTHENBACH B.[1], WIELAND E., DÄHN R., WICHSER A.[1], SCRIVENER K.L.[2] (2010)
Preliminary investigation on the fate of iron during cement hydration. CONMOD 2010, Symposium on Concrete Modelling, Lausanne, Switzerland, 22–25 June, 2010
[1] Empa, Dübendorf, Switzerland
[2] EPFL, Lausanne, Switzerland

GAONA X., ALTMAIER M.[1], PETROV V.[2], FELLHAUER D.[1,3], TITS J., WIELAND E., KALMYKOV S.[2], FANGHAENEL T.[3]
Aqueous speciation and solubility of Np(V/VI) in hyperalkaline systems: a KIT-INE / PSI-LES / JRC-ITU/MSU joint project. RECOSY 2nd Annual Workshop, Larnaca, Cyprus, 16-19 March 2010
[1] KIT INE, Karlsruhe, Germany
[2] Lomonosov Moscow State University, Russia
[3] ITU, Karlsruhe, Germany

GAONA X., TITS J., KIRSCH R.[1], FELLHAUER D.[2], WIELAND E.
RECOSY ICE: Comparison of experimental, reference and thermodynamic Eh values. RECOSY 2nd Annual Workshop, Larnaca, Cyprus, 16-19 March 2010
[1] FZD, Dresden, Germany; ROBL/ESRF, France; LGIT, Grenoble, France
[2] KIT INE, Karlsruhe, Germany

GAONA X., KULIK D.A., MACÉ N.[1], WIELAND E.
Aqueous-solid solution model of U(VI) uptake in C-S-H phases. NEA Symposium – from Thermodynamics to the Safety Case, Karlsruhe, Germany, 17-19 May 2010
[1] CEA Saclay, Gif-Sur-Yvette, France

GIMMI T., KOSAKOWSKI G., GLAUS M.A.
On the mobility of exchangeable cations on clay surfaces. 4th International Meeting on Clays in Natural & Engineered Barriers for Radioactive Waste Confinement, Nantes, France, 29 March–1 April 2010

GIMMI T., KOSAKOWSKI G., GLAUS M.A.
Predicting cation diffusion coefficients in clays and clay rocks. EGU General Assembly, Vienna, 2-7 May, 2010

GIMMI T., SOLER J.M.[1], SAMPER J.[2], NAVES A.[2], YI S.[2], LEUPIN O.X.[3], WERSIN P.[4], VAN LOON L.R., EIKENBERG J., DEWONCK S.[5], WITTEBROODT CH.[6]
Insights from modelling the diffusion and retention experiment at the Mont Terri. 4th International Meeting on Clays in Natural & Engineered Barriers for Radioactive Waste Confinement, Nantes, France, 29 March–1 April 2010
[1] IDAEA-CSIC, Barcelona, Spain
[2] Universtiy of La Coruña, La Coruña, Spain
[3] Nagra, Wettingen, Switzerland
[4] Gruner AG, Basel, Switzerland
[5] Andra, Châtenay-Malabry, France
[6] IRSN, Fontenay aux Roses, France

GLAUS M.A., GIMMI T., JAKOB A., VAN LOON L.R.
On the usefulness of various types of diffusion coefficients in the assessment of the mobility of cations in swelling clays. 4th International Meeting on Clays in Natural & Engineered Barriers for Radioactive Waste Confinement, Nantes, France, 29 March–1 April 2010

GROLIMUND D., GUENTHER D.[1], BORCA C.N., WANG H.A.O., VAN LOON L.R., STAMPANONI M., MARONE F., MOKSO R., DIAZ N., JAKOB A., BARMETTLER K.[1], AESCHLIMANN B.[1], WERSIN P.[2]
Evolution of reactive transport plumes: decipher physico-chemical micro-complexity using chemical micro-imaging and micro-tomography. International Symposium Transpore 2010, Villigen PSI, Switzerland, 19/20 August 2010
[1] ETH, Zürich, Switzerland
[2] Gruner AG, Basel, Switzerland

HINGERL F.F., WAGNER T.[1], KULIK D.A., DRIESNER T.[1], KOSAKOWSKI G., THOMSEN K.[2], HEINRICH CH.[1] (2010)
Influence of thermodynamic data and activity models on predicted scaling and permeability in enhanced geothermal systems. European Geothermal PhD Day 2010, GFZ-Potsdam, Germany 11/12 February 2010
[1] ETH, Zürich, Switzerland
[2] Technical University of Denmark, Lyngby, Denmark

HINGERL F.F., FOWLER S.F.[1], DRIESNER T.[1], WAGNER T.[1], KULIK D.A., KOSAKOWSKI G., THOMSEN K.[2] (2010)
Accurate models for geothermal fluid-rock interaction and scale formation. CCES Latsis Symposium 2010, ETH Zürich, Switzerland, 15-17 November 2010
[1] ETH, Zürich, Switzerland
[2] Technical University of Denmark, Lyngby, Denmark

KOSAKOWSKI G.
OpenGeoSys-GEMS: Status, applications and future. 1. OGS User Meeting, Leipzig, Germany, 18 March 2010

KOSAKOWSKI G., BERNER U., KULIK D.A.
Reactive transport simulations of the evolution of a cementitious repository in clay-rich host rocks. EGU General Assembly, Vienna, 2-7 May 2010

KOSAKOWSKI G., GOUEBAULT E.[1], SHAO H.[2]
The COMEDY2D benchmark: reactive transport simulations of strong chemistry – transport couplings. 2. OGS User Meeting, Leipzig, 30. September 2010
[1] University Nantes, France
[2] Helmholtz Centre for Environmental Research – UFZ, Leipzig, Germany

LEUPIN O.X.[1], WERSIN P.[2], GIMMI T., SOLER J.M.[3], DEWONCK S.[4], SAVOYE S.[5], WITTEBROODT C.[6], VAN LOON L.R., EIKENBERG J., BAEYENS B., SAMPER J.[7]
Diffusion and retention experiment at the Mont Terri Underground Rock Laboratory in St. Ursanne. 4th International Meeting on Clays in Natural & Engineered Barriers for Radioactive Waste Confinement, Nantes, France, 29 March – 1 April 2010
[1] Nagra, Wettingen, Switzerland
[2] Gruner AG, Basel, Switzerland
[3] IDAEA-CSIC, Barcelona, Spain
[4] Andra, Châtenay-Malabry, France
[5] CEA Saclay, Gif-Sur-Yvette, France
[6] IRSN, Fontenay aux Roses, France
[7] University of La Coruña, La Coruña, Spain

PFINGSTEN W., BAEYENS B., BRADBURY M.H.
Modelling Ni diffusion in bentonite using different sorption models. 4th International Meeting on Clays in Natural & Engineered Barriers for Radioactive Waste Confinement, Nantes, France, 29 March – 1 April 2010

SHCHERBINA N.S., SVEDKAUSKAITE-LE GORE J., KIVEL N., GUENTHER-LEOPOLD I., KULIK D.A. (2010)
Thermodynamic modeling of fission product release during thermal treatment of spent oxide fuel. EMRS, Strasbourg, 2010 N: Nuclear materials IV, 7-11 June 2010

SOLER J.M.[1], LEUPIN O.X.[2], GIMMI T., HIRSCHORN S.[3]
Planning of a new tracer and reactive diffusive transport experiment in the Opalinus Clay at the Mont Terri Underground Rock Laboratory. EGU General Assembly, Vienna, 2-7 May 2010
[1] IDAEA-CSIC, Barcelona, Spain
[2] Nagra, Wettingen, Switzerland
[3] NWMO, Toronto, Canada

TITS J., GAONA X., DÄHN R., WIELAND E.
Actinide sorption by cementitious materials: The case of neptunium. Plutonium Futures - The Science 2010, Keystone Co, USA, 19-23 September 2010

TITS J., GAONA X., WIELAND E.
Influence of the oxidation state on neptunium uptake by calcium-silicate-hydrates and cement. RECOSY 2nd Annual Workshop, Larnaca, Cyprus, 16-19 March 2010

VAN LOON L.R., MUELLER W.
Diffusion of ^{60}Co(II), ^{154}Eu(III) and ^{134}Cs(I) in Opalinus Clay: Results from in-diffusion measurements combined with a high-resolution abrasive method. 4th International Meeting on Clays in Natural & Engineered Barriers for Radioactive Waste Confinement, Nantes, France, 29 March–1 April 2010

VAN LOON L.R., APPELO C.A.J.[1], LEUPIN O.X.[2]
Multicomponent diffusion of cations, anions and neutral species in Opalinus Clay: effect of porewater composition. 4th International Meeting on Clays in Natural & Engineered Barriers for Radioactive Waste Confinement, Nantes, France, 29 March–1 April 2010
[1] Hydrochemical Consultant, Amsterdam, The Netherlands
[2] Nagra, Wettingen, Switzerland

VINOGRAD V.L.[1], KULIK D.A., RAITERI P.[2], GALE J.D.[2], WINKLER B.[1] (2010)
Computer simulations of $CaCO_3$-$MgCO_3$-$CdCO_3$ system and calculations of solid solution – aqueous solution equilibria. Abstract S10-T01, Jahrestagung der Deutschen Mineralogischen Gesellschaft, Münster, 19-22 September 2010
[1] University of Frankfurt, Frankfurt-am-Main, Germany
[2] Curtin University, Perth, Australia

WIELAND E., MACÉ N.[1], DÄHN R., GAONA X., POPOV D., TITS J.
Micro-scale investigations of U(VI) immobilization by cementitious materials. 16th Radiochemical Conference, Marianske Lazne, Czech Republic, 18-23 April 2010
[1] CEA Saclay, Gif-Sur-Yvette, France

WIELAND E., MACÉ N.[1], DÄHN R., GAONA X., TITS J.
Micro-scale investigation of U(VI) speciation in hardened cement paste. 11th International Symposium on Environmental Radiochemical Analysis, Chester, UK, 15-17 September 2010
[1] CEA Saclay, Gif-Sur-Yvette, France

WANG H.A.O., GROLIMUND D., GUENTHER D.[1], VAN LOON L.R, BORCA C.N., AESCHLIMANN B.[1], BARMETTLER K.[1]
Quantitative imaging of elemental diffusion into heterogeneous media using LA-ICP-MS and synchrotron microXRF. 10th European Workshop on Laser-Ablation, Kiel, Germany, 29 June-1 July 2010
[1] ETH, Zürich, Switzerland

8.6 Invited talks

CHURAKOV S.V.
Dynamics of water and ions confined in clay minerals and cement phases. Swiss Association of Computational Chemistry. Annual Spring Meeting, Bern, 19 February 2010

CHURAKOV S.V.
Atomistic modelling: application to cement phases. Invited plenary lecture at a symposium on concrete modelling, CONMOD, Lausanne, 23-25 July 2010

CHURAKOV S.V.
Molecular simulations of Zn^{2+} sorption on edges of montmorillonite. UPMC Paris, 29 October 2010

CHURAKOV S.V.
Up-scaling molecular diffusion coefficients in clay rich materials. Institute Seminar, Institute of Physical Chemistry, University of Zurich, 9 December 2010

GIMMI T.
Drying of Opalinus Clay – preliminary investigations. Seminar at Soil and Terrestrial Environmental Physics, Institute for Terrrestrial Ecosystems (ITES-STEP), ETH Zürich, 17 November 2010

KOSAKOWSKI G.
Coupled reactive transport modeling in the framework of the sectoral plan for deep geological disposal. Taiheiyo Cement Group, Sakura, Japan, 19 October 2010

KULIK D.A.
Thermodynamic modelling of solid-aqueous geochemical speciation. GeoSpec2010 Conference "Geochemical Speciation & Bioavailability of Trace Elements: Progress, Challenges and Future Trends", Lancaster, UK, 7-8 September 2010

PFINGSTEN W.
Neue analytische Forschungsmethoden am PSI für die sichere Tiefenlagerung radioaktiver Abfälle. SGK, Baden, Schweiz, 7 September 2010

TITS J., GAONA X., MACÉ N.[1], KULIK D.A., STUMPF T.[2], WALTHER C.[2], WIELAND E.
Experimental sorption studies on cement systems. International Workshop on Actinide and Brine Chemistry in a Salt-based Repository (ABC-SALT), Carlsbad NM, USA, 15-17 September 2010
[1] CEA Saclay, Gif-Sur-Yvette, France
[2] KIT INE, Karlsruhe, Germany

8.7 Internal presentations

BERNER U.
Ein "Solid Solution" Modell für Montmorillonit

DIAZ N.
Modelling the Cs diffusion front in Opalinus Clay considering the 3D spatial mineral heterogeneities

GAONA X.
Chemistry of neptunium in hyperalkaline systems

8.8 Others/teachings

BAEYENS B.
Modelling of sorption processes and Sorption databases. ITC Course on "Transport and Retention of Radionuclides in Argillaceous and Fractured Media", Villigen PSI, 30 November–7 December 2010

GIMMI T.
Upscaling from lab to field; Part I: Field experiments and Upscaling from lab to field; Part II: natural tracer profiles. ITC Course on "Transport and Retention of Radionuclides in Argillaceous and Fractured Media", Villigen PSI, 30 November–7 December 2010

GIMMI T.
Lecture and examinations 'Fluids in the Crust' within frame of Master of Environmental and Resource Geochemistry, University of Bern, Fall Semester 2010

GLAUS M.A.
Diffusion of radionuclides in clays: experimental aspects. ITC Course on "Transport and Retention of Radionuclides in Argillaceous and Fractured Media", Villigen PSI, 30 November–7 December 2010

HINGERL F.F., WAGNER TH.[1], KULIK D.A., KOSAKOWSKI G., DRIESNER TH.[1], THOMSEN K.[2], HEINRICH CH.[1]
Geochemical models for fluid-rock interaction in enhanced geothermal systems, ETH Zürich IGP, 6 Oktober 2010
[1] ETH, Zürich, Switzerland
[2] Technical University of Denmark, Lyngby, Denmark

JOHNSON C.A., HUMMEL W., PLÖTZE L.M.
Landfilling, nuclear repositories and contaminated sites. Course for Major in Biogeochemistry and Pollutant Dynamics (Master of Environmental Sciences) and for Major in Ecological Systems Design and Waste Management (Master of Environmental Engineering), ETH Zurich, Autumn Semester 2010

KOSAKOWSKI G.
Statistics in Earth Sciences. University of Tübingen, Germany, Summer Semester, 2010

KOSAKOWSKI G.
Introduction to the reactive transport modeling with OGS-GEMS. Special lecture for Bachelor and Master students, Gunma University, Japan, 21-22 October 2010

KULIK D.A.
GEMS teaching (PhD/postdoc level) at the joint DMG-DGK-Helmholtz-Virtual-Institute workshop "From atomistic calculations to thermodynamic modelling", University of Frankfurt, Germany, 1-6 March 2010

KULIK D.A.
GEMS teaching (PhD/postdoc level) at the EMU-School 2010 "Ion-partitioning in ambient temperature aqueous systems", Oviedo, Spain, 27-30 June 2010

KULIK D.A.
GEMS teaching (PhD/postdoc level) at the GeoSpec2010 Conference "Geochemical Speciation & Bioavailability of Trace Elements: Progress, Challenges and Future Trends", University of Lancaster, UK, 7-8 September 2010

PFINGSTEN W.
Modelling of Processes in Soils and Aquifers: 701-1334-00L, Department for Environmental Sciences, ETH Zurich, Spring Semester 2010

PFINGSTEN W.
Transport processes and coupling of transport and chemistry. ITC Course on "Transport and Retention of Radionuclides in Argillaceous and Fractured Media", Villigen PSI, 30 November–7 December 2010

PRASSER H.M., GÜNTHER-LEOPOLD I., HIRSCHBERG S., HUMMEL W., WILLIAMS T., ZUIDEMA P.K.
Nuclear Energy Systems. Lecture course with exercises, ETH Zurich, Spring Semester 2010

VAN LOON L.R.
Diffusion and sorption of radionuclides in argillaceous materials: practical aspects and Diffusion of radionuclides in argillaceous materials. ITC Course on "Transport and Retention of Radionuclides in Argillaceous and Fractured Media", Villigen PSI, 30 November–7 December 2010

8.9   PhD thesis

ROZOV K. (2010)
Stability and solubility of hydrotalcite-pyroaurite solid solutions: synthesis, characterization and thermodynamic modeling. Inauguraldissertation der Philosophisch-naturwissenschaftlichen Fakultät der Universität Bern, angenommen den 28 Oktober 2010, 140 p.